AD-A036 539 NAVAL UNDERSEA CENTER SAN DIEGO CALIF F/G 17/1
LORA: A MODEL FOR PREDICTING THE PERFORMANCE OF LONG-RANGE ACTI--ETC(U)
DEC 76 D W HOFFMAN
UNCLASSIFIED NUC-TP-541 NL

1 OF 2
AD A036539

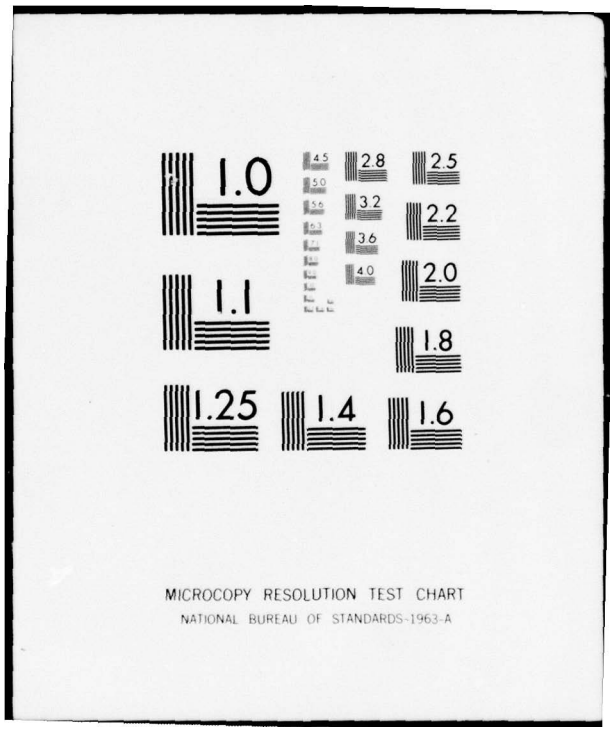
1.0
1.1
1.25
1.4
1.6
1.8
2.0
2.2
2.5
2.8
3.2
3.6
4.0
4.5
5.0
5.6
6.3
7.1
8.0
9.0
MICROCOPY RESOLUTION TEST CHART
NATIONAL BUREAU OF STANDARDS-1963-A

(13)

NUC TP 541

# LORA: A MODEL FOR PREDICTING THE PERFORMANCE OF LONG-RANGE ACTIVE SONAR SYSTEMS

by

D.W. HOFFMAN

Undersea Surveillance Department

December 1976

NAVAL UNDERSEA CENTER, SAN DIEGO, CA. 92132

AN ACTIVITY OF THE NAVAL MATERIAL COMMAND

R. B. GILCHRIST, CAPT, USN
Commander

HOWARD L. BLOOD, PhD
Technical Director

## ADMINISTRATIVE STATEMENT

Initial model development (NEWACT) was sponsored by A. Franceschetti of NAVSHIPS 902, under the Acoustic Modeling Program, Subproject SF52-552-601, task 16409. Subsequent specialized model development was carried out until December 1973 in compliance with task and software requirements specified by B. A. Levin, Naval Intelligence Support Center.

In 1974 and 1975 extensive software modifications produced a general-purpose performance-prediction program. This effort, culminating in the present paper, was made possible by the interest and support of C. D. Smith, NAVSEA 06H1, under the Environmental Acoustic Data Bank and Modeling Program, Subproject SF52-552-601, task 19324.

The author is indebted to R. W. McGirr, who initiated the work with the NEWACT computer program. The skeleton of LORA is essentially the same as NEWACT, although 95% of the original computer coding has changed. R. W. McGirr also provided extensive notes which were used in preparing this paper. Credit belongs to many others who gave direct aid, either in model development or programming: L. K. Arndt and J. L. Teeter developed the probability of detection models; E. D. Chaika implemented an early version of curvilinear ray tracing by using C. L. Bartberger's curve-fitting subroutines to fit the sound-speed profile; J. C. Hall wrote encoding and decoding subroutines for ease of input–output with different computers; G. P. Schumacher provided extensive support in program checkout and debugging; and M. Schulkin gave valuable suggestions relating to surface backscattering strength.

This report was reviewed for technical accuracy by M. A. Pedersen and G. Martin.

Released by
**M. R. AKERS, Head**
System Concepts and Analysis Division

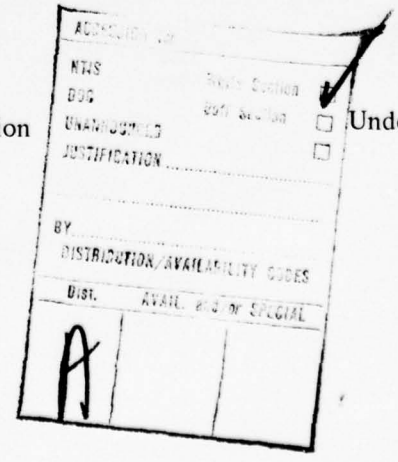


Authorized by
**H. A. SCHENCK, Head**
Undersea Surveillance Dept.

UNCLASSIFIED

SECURITY CLASSIFICATION OF THIS PAGE (When Data Entered)

## REPORT DOCUMENTATION PAGE

READ INSTRUCTIONS BEFORE COMPLETING FORM

| | |
|---|---|
| 1. REPORT NUMBER: NUC TP 541 | 2. GOVT ACCESSION NO. |
| 3. RECIPIENT'S CATALOG NUMBER | |
| 4. TITLE (and Subtitle): LORA: A MODEL FOR PREDICTING THE PERFORMANCE OF LONG-RANGE ACTIVE SONAR SYSTEMS | 5. TYPE OF REPORT & PERIOD COVERED: Final Report, 1972-1976 |
| 6. PERFORMING ORG. REPORT NUMBER | |
| 7. AUTHOR(s): D. W. Hoffman | 8. CONTRACT OR GRANT NUMBER(s) |
| 9. PERFORMING ORGANIZATION NAME AND ADDRESS: Naval Undersea Center, San Diego, CA 92132 | 10. PROGRAM ELEMENT, PROJECT, TASK AREA & WORK UNIT NUMBERS: NAVSEA Subproject SF52-552-601, Task 16409, Task 19324 |
| 11. CONTROLLING OFFICE NAME AND ADDRESS: Commander, Naval Sea Systems Command, Attn: C. D. Smith, Code 06H1, Washington, D.C. 20362 | 12. REPORT DATE: December 1976 |
| | 13. NUMBER OF PAGES: 126 |
| 14. MONITORING AGENCY NAME & ADDRESS (if different from Controlling Office): 125p. | 15. SECURITY CLASS. (of this report): Unclassified |
| | 15a. DECLASSIFICATION/DOWNGRADING SCHEDULE |

16. DISTRIBUTION STATEMENT (of this Report)

Approved for public release; distribution unlimited.

F52552 SF52552601

17. DISTRIBUTION STATEMENT (of the abstract entered in Block 20, if different from Report)

18. SUPPLEMENTARY NOTES

19. KEY WORDS (Continue on reverse side if necessary and identify by block number)

| | | | |
|---|---|---|---|
| Sonar | Reverberation | Noise | Beam pattern |
| Active sonar | Ray paths | Ambient noise | Directivity index |
| Performance prediction | Ray tracing | Probability of detection | |
| Propagation loss | Echo level | Masking background | |

20. ABSTRACT (Continue on reverse side if necessary and identify by block number)

LORA is a model developed to predict the performance of long-range active sonar systems. The supporting computer program uses 3-8 cpu seconds per run on the UNIVAC 1110 computer and requires 38,000 words of core storage. The performance prediction model comprises models that estimate propagation loss, reverberation level, and probability of detection. The propagation loss models are (1) empirical equations (modified AMOS) for near-surface ducts and (2) ray theory (Pedersen and Gordon) for direct-path, bottom-bounce,

OVER

DD FORM 1 JAN 73 1473 EDITION OF 1 NOV 65 IS OBSOLETE

UNCLASSIFIED

SECURITY CLASSIFICATION OF THIS PAGE (When Data Entered)

390 458

and convergence-zone sound propagation. The sound-speed profile is corrected for earth curvature, but is otherwise constant with range. Models for estimating reverberation use ray tracing to the centers of backscattering areas and volumes. The surface backscattering strength is obtained by using the Chapman–Harris equations, Eckart's equations, and Richter's data. The bottom backscattering strength uses equations derived from Lambert's Law and Schmidt's data. The volume backscattering strength is represented as column backscattering strength. Five probability-of-detection models are derived for various assumptions for signal distortion and detector characteristics.

LORA features target doppler corrections for reverberation levels; multi-ping reverberation calculations; optional passive coherent and incoherent propagation loss outputs; and multiple bottom-bounce and multiple convergence-zone calculations.

## SUMMARY

### OBJECTIVE

Develop a computer model for predicting the performance of active sonar systems for long horizontal ranges, that is, for multiple convergence zones and bottom bounces.

### COMPUTER PROGRAM CAPABILITIES

The model and supporting computer program have been developed and embrace the following capabilities:

1. Active sonar performance predictions are available for up to five convergence zones or bottom bounces.
2. The target and active-sonar source may be situated at any ocean depth.
3. Optional passive coherent and incoherent propagation losses are available for up to 30 convergence zones or bottom bounces.
4. Curvilinear techniques are used with the sound-speed profile to reduce false caustics.
5. Multi-ping reverberation is available, as well as doppler shifting of the signal caused by target motion.
6. Five probability-of-detection models for different assumptions of signal degradation and type of detector are available.
7. The computer program is able to perform many successive runs without failure.
8. Computer costs are low, approximately $2 for a complete set of performance predictions using an average commercial computer.
9. Core storage required is about 38,000 words.

### RECOMMENDATIONS

The development of an adequate subsurface duct model is needed, perhaps using normal mode theory. Propagation loss in the duct should be related to duct width, duct strength, source and target positions, and the frequency of the propagating sound.

Volume reverberation calculations could be improved by averaging propagation losses from transmitter to scatterers over the whole scattering volume. Nonspecular scattering could be included.

The input package of the computer program could be modified to include a curve of recognition differential versus signal-to-noise ratio to render the program more sensitive to certain active sonars.

## CONTENTS

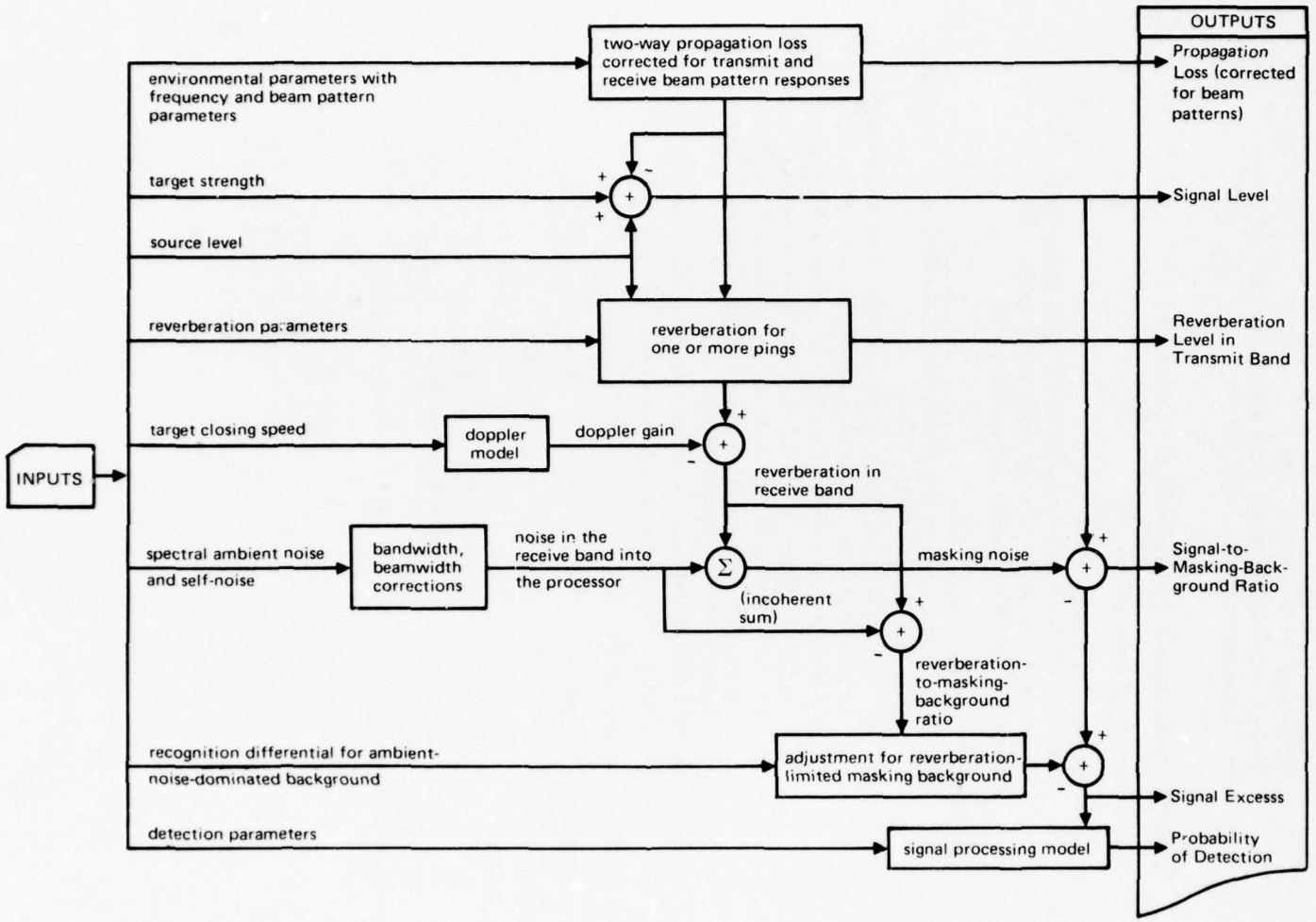


Frontispiece. Block diagram of the computational structure of the LORA computer program.

## INTRODUCTION

In order to assess the effectiveness of long-range weapon systems, an active sonar model known as LORA has been developed. LORA is, essentially, an extension of FAST NISSM,[1] the utility version of the Navy Interim Surface Ship Model (NISSM).[2] LORA was the next logical iteration in a series of models developed to predict active sonar performance. Its supporting computer program is a high-speed, user-oriented program, with a flexible input routine. Program execution is rapid and inexpensive, costing less than $2 (4 cpu seconds plus input–output charges) for a full set of near-surface (direct-path), multi-bottom-bounce, and multi-convergence-zone performance predictions.

The LORA model affords analysts the opportunity to evaluate the long-range detection capabilities of operational and future active sonar systems. Specifically, LORA can be used to –

- Compare the performance of candidate sonar systems under identical environmental conditions.
- Evalute the performance of a given sonar system under various environmental conditions.
- Analyze the sensitivity of performance to changes in selected environmental and system parameters.
- Estimate the improvements in performance resulting from proposed changes in system components.
- Establish a set of performance reference data, which would make possible the comparison of performance measurements made in different environments.

The body of this report contains the total model description. First, the active sonar equation is presented to illustrate the procedure used to determine signal excess. Next, models are given for the various kinds of losses which degrade transmit signal and target echo. Then noise and reverberation models are given. Finally, several models for probability-of-detection are presented for various assumptions of signal distortion and detector characteristics.

The appendixes contain information about the LORA computer program. Appendix A discusses the logical structure of the program; Appendix B defines the input parameters; Appendix C describes the input format; and Appendix D contains sample runs.

## MODEL DESCRIPTION

The model considered here is capable of predicting the performance of monostatic, active sonar systems, hull-mounted or towed. Some of the salient features of the model include:

- No limitation to source and target depths within the ocean.
- Automatic curve fitting for the sound-speed profile to reduce the effect of false caustics caused by the digitizing of the sound-speed data.
- Multiple convergence-zone predictions (maximum of five).
- Multiple bottom-bounce predictions (maximum of five).
- Multiple-ping time histories for reverberation (maximum of nine pings).
- Choice of five probability-of-detection models.
- Optional passive coherent and incoherent propagation losses for a maximum of 30 bottom bounces or convergence zones.

Model inputs are basic descriptive variables defining the ocean medium, the transmitting and receiving system, and the signal processor. Predictions are restricted to active sonar systems which operate at frequencies between 0.5 and 25 kHz. Two restrictions have been imposed on environmental representations to facilitate the application of high-speed ray-tracing techniques. First, horizontal homogeneity of the water column is assumed; that is, a single sound-speed profile is specified along any range track of interest. Second, both surface and bottom boundaries are assumed locally flat with a constant bottom depth, although corrections are made to account for earth curvature.

Model output is probability-of-detection for those ranges from the active sonar which can be irradiated at a specific target depth. Intermediate quantities such as propagation loss, reverberation level, signal level, and signal excess are supplementary calculations and are useful outputs in their own right. Model implementation is effected by a FORTRAN computer program which requires about 38,000 36-bit words on the UNIVAC 1110.

Probability-of-detection is used as the measure of sonar system performance and is calculated as a function of horizontal range between source (own ship) and target. A useful measure of acceptable performance can be defined as those range intervals where the probability-of-detection exceeds some predetermined probability level.

Single-ping detection probability is a function of signal excess, which is the amount by which the target echo level exceeds the masking background level.

The signal differential, $L_{SN}$, often referred to as the signal-to-noise level, is the difference within a designated frequency band between the echo level, $E$, and the masking background level, $M$; that is

$$L_{SN} = E - M \text{ (dB)} \tag{1}$$

The minimum recognizable value of echo level, $E_M$, is that portion of the masking background, $M$, such that

$$E_M = M + R_D \text{ (dB)} \tag{2}$$

where

$R_D$ is the recognition differential

The recognition differential provides a measure of sonar operator performance. It is a psycho-acoustic measure of a sonar operator's ability to recognize a target echo 50% of the time given a specified probability of false alarm. In terms of $E_M$, any echo level can be expressed as

$$E = E_M + S_{EX} \tag{3}$$

where

$S_{EX}$ is referred to as signal excess

If a signal is transmitted, then for a given target strength, $S_T$, the echo level is given by

$$E = L_0 + S_T - H_2 \tag{4}$$

where

$L_0$ is the signal level 1 yard from the source

and

$H_2$ is the two-way propagation loss plus the degradation accrued from the transmit and receive beam patterns

Signal excess, $S_{EX}$, is obtained by combining Eq. 2, 3, and 4:

$$S_{EX} = L_0 + S_T - H_2 - M - R_D \tag{5}$$

This is the active sonar equation for echo ranging.

## PROPAGATION LOSS

Sound pressure is the root-mean-square increase in pressure over hydrostatic pressure due to the propagation of harmonic acoustic energy through the position of measurement. Propagation loss is a measure of the reduction of far-field sound pressure from that of a reference sound pressure at a specified distance from the sound source. The expression for propagation loss is

$$H = -10 \log (p^2/p_0^2) \text{ in dB} \tag{6}$$

where

$p$ is the sound pressure at some range of interest

and

$p_0$ is the reference sound pressure level at a reference range

This model assumes that four physical processes in which the propagating acoustic energy interacts with the ocean environment contribute to a reduction (in some refractive cases an increase) in sound pressure and therefore an increase in propagation loss. These processes are refraction–spreading, absorption, surface reflection, and bottom reflection of the acoustic pressure waves. These four processes are assumed to contribute independently to the total propagation loss:

$$H_T = H_R + H_A + H_S + H_B \text{ in dB} \tag{7}$$

where

$H_R$ is refraction–spreading loss

$H_A$ is absorption loss

$H_S$ is surface–reflection loss

and

$H_B$ is bottom–reflection loss

Each of these four processes has the following characteristics in common. Let $p_1$ be the sound pressure at the start of the process and $p_2$ be the sound pressure at the end of the process; then the ratio $p_1/p_2$ is independent of $p_1$. This characteristic results directly in the associativity of the terms on the right side of Eq. 7, since $p_1$ can be identified with $p_0$ and $p_2$ with $p$ in Eq. 6. Thus, the components of propagation loss can be calculated independently and assembled in any order.

Several techniques for determining propagation loss are used in this model, depending on the sound speed and the source and target depths. The empirical Acoustic, Meteorological, and Oceanographic Survey (AMOS) equations[3] are used when surface-duct calculations are warranted. Simple subsurface-duct equations are

used if both source and target are in the duct. Otherwise, direct-path calculations are performed using ray-tracing techniques based on a sound-speed profile fitted with continuous-gradient curvilinear segments. Bottom-bounce, convergence-zone, surface-bounce, and reliable-acoustic-path calculations are performed by using curvilinear ray-tracing techniques. For active sonar predictions, only the path yielding the minimum propagation loss at each range is used for determining propagation loss versus range. Average losses for boundary reflections are obtained as a function of frequency and angle of incidence. The number of surface and bottom reflections are counted, and boundary loss is calculated and added into the total loss for a path. The result is the total propagation loss caused by the environment, which is represented by Eq. 7. Beam pattern responses (transmit and receive) also degrade the intensity for a ray path. Beam pattern responses in dB, $H_\phi$, are added to $H_T$ of Eq. 7 to give the propagation loss used in comparing paths competing to give minimum propagation loss to the target.

Table 1 gives a summary of the components needed to compute propagation loss for several modes of acoustic propagation.

Table 1. Applicability of propagation-loss terms to various propagation modes.

| Propagation Mode | Propagation Loss Equation |
|---|---|
| Surface Duct (SD) | $H = H_R + H_A + H_S$ |
| Subsurface Duct (SSD) | $H = H_R + H_A$ |
| Direct Path (DP) | $H = H_R + H_A + H_S + H_\phi$ |
| Bottom Bounce (BB) | $H = H_R + H_A + H_S + H_B + H_\phi$ |
| Convergence Zone (CZ) | $H = H_R + H_A + H_S + H_\phi$ |
| Surface Bounce (SB) | $H = H_R + H_A + H_S + H_\phi$ |
| Reliable Acoustic Path (RAP) | $H = H_R + H_A + H_\phi$ |

Passive one-way propagation-loss outputs are also available. The options are:

1. Coherent summation over all the paths contributing to acoustic pressure at the target.

2. Incoherent summation over all the paths contributing to acoustic pressure at the target.

3. Fading coherent summation of all the paths contributing to acoustic pressure at the target. (This option is simply a linear decrease of coherence with range until incoherence is obtained at 50 kyd. It is admitted that this is not a realistic fading coherence model.)

4. Passive simulation in which the receive beam pattern is included in the pressure calculation for each ray path before summation.

5. Communications simulation in which the transmit beam pattern response (evaluated for the ray angle at the transmitter) and the receive beam pattern

response (evaluated for the ray angle at the target) are included in the pressure calculation for each ray path before summation. This model is not complete in that time histories of the signals, with appropriate summation over the phase-distorted, time-displaced signal waveforms, are not calculated.

These models have nothing to do with active sonar modeling but are useful byproducts of the calculations needed for active sonar performance predictions. It must be noted that one-way passive propagation losses are not in general one-half of the two-way active propagation losses. This is because summation over several paths connecting source and target can produce, say, a 10 dB increase over the single-path, minimum propagation loss used for active sonar performance prediction. When propagation loss is calculated for active sonars, it is assumed that the pulse length is short enough in time to be resolved in every multipath occurrence. The assumption for passive sonars is that the signal is CW and constant over the maximum time interval between any two paths in the summation.

**Absorption Loss**

The expression for absorption loss is

$$H_A = \alpha S$$

where

$S$ is the curvilinear path length (kyd)

and

$\alpha$ is the absorption coefficient (dB/kyd)

Values of $\alpha$ are obtained from an equation developed by Hall and Watson[4] that combines the low-frequency predictions of Thorp[5] with the high-frequency predictions of Schulkin and Marsh.[6] The resulting expression is

$$\alpha = \frac{1.776f^{1.5}}{32768 + f^3} + \frac{1 - 6.54 \times 10^{-4}P}{1 + 32768f^3}\left(\frac{0.65053f_T f^2}{f^2 + f_T^2} + \frac{0.026847f^2}{f_T}\right) \qquad (8)$$

where

$f$ is frequency in kHz

$P$ is pressure in atmospheres

and

$f_T$ is the relaxation frequency in kHz

Pressure is a function of depth in feet, $z$, so that

$$P = 1.04 + 0.031244z \text{ atm}$$

The relaxation frequency is determined by

$$f_T = 21.9 \times 10^{(30T+102)/(5T+2297)} \text{ kHz}$$

where

$T$ is temperature in Fahrenheit

Figure 1 shows $\alpha$ as a function of frequency for several average ocean temperatures computed by Eq. 8. A curve showing Thorp's deep ocean prediction is presented for comparison.

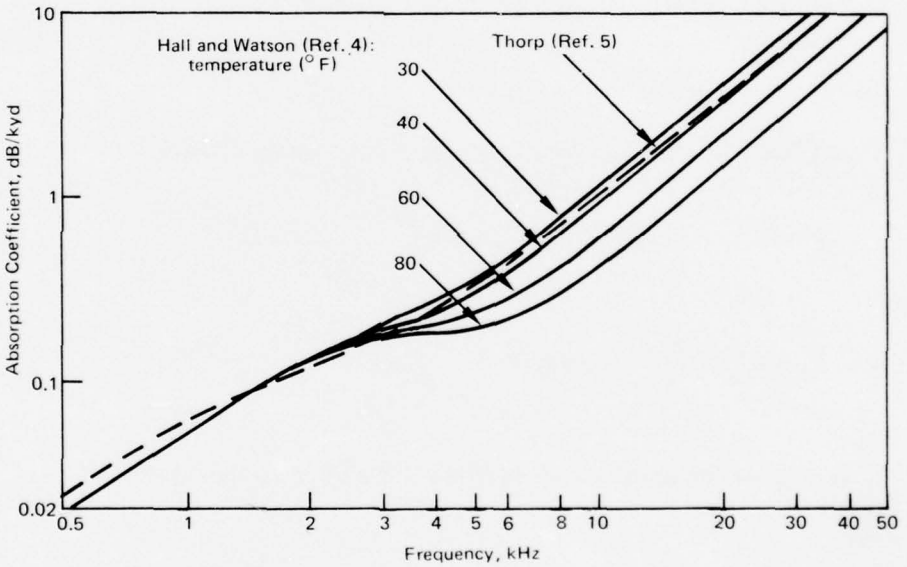


Figure 1. Absorption coefficient vs frequency.

## Propagation Loss in the Near-Surface Ducts

The near-surface empirical propagation-loss equations were obtained by Marsh and Schulkin from the AMOS transmission-loss measurements for frequencies between 2 and 25 kHz.[3] For completeness the equations applicable to surface-duct propagation loss will be presented here, even though they have been reproduced in numerous reports. Certain limits to their applicability have been imposed, and new subsurface duct equations are used. The equations for the scattering loss coefficient

will be shown first; then expressions for scaling range and depth; then four propagation-loss equations from the AMOS study, as well as a table which describes their application with respect to the scaled ranges and depths; then the normal mode cutoff term for lower frequencies, which is to be added to the chosen propagation-loss expression; and lastly, the subsurface-duct equations.

**Surface-Scattering-Loss Coefficient**. For energy propagating in a surface duct, the surface-scattering loss per bounce, $\Gamma$, is obtained from an analytic expression developed by Schulkin and Marsh:[7]

$$\begin{aligned} \Gamma &= 10 \log [1+(fh/4.14)^4], \quad fh \leq 4.2691 \\ &= 1.59(fh)^{1/2}, \quad fh > 4.2691 \end{aligned} \tag{9}$$

where

$f$ is frequency in kHz

and

$h$ is waveheight in feet

The surface-scattering-loss coefficient, $\alpha_s$, is obtained by dividing $\Gamma$ by the bounce distance, $R_B$, that is

$$\alpha_s = \Gamma / R_B \text{ dB/kyd} \tag{10}$$

where

$$R_B = (C_L^2 - C_S^2)^{1/2} / 1500 g_0 \text{ kyd}$$

where

$C_L$ and $C_S$ are the sound speeds in ft/sec at the layer depth and the surface, respectively

and

$g_0$ is the sound-speed gradient in $\text{sec}^{-1}$ in the surface duct

The surface reflection loss is

$$\begin{aligned} H_S &= \alpha_s (R - R') \text{ for } R > R' \\ &= 0 \qquad \text{for } R \leq R' \end{aligned}$$

where

$R$ is the horizontal range between source and target, in kyd

$$R' = Z_L^{1/2}(r_1 + 0.5) \text{ in kyd}$$

where

$Z_L$ is the layer depth in feet

and

$r_1$ is a scaled range defined in the next section

A curve of surface loss versus the product of frequency and wave height is illustrated in Fig. 2.

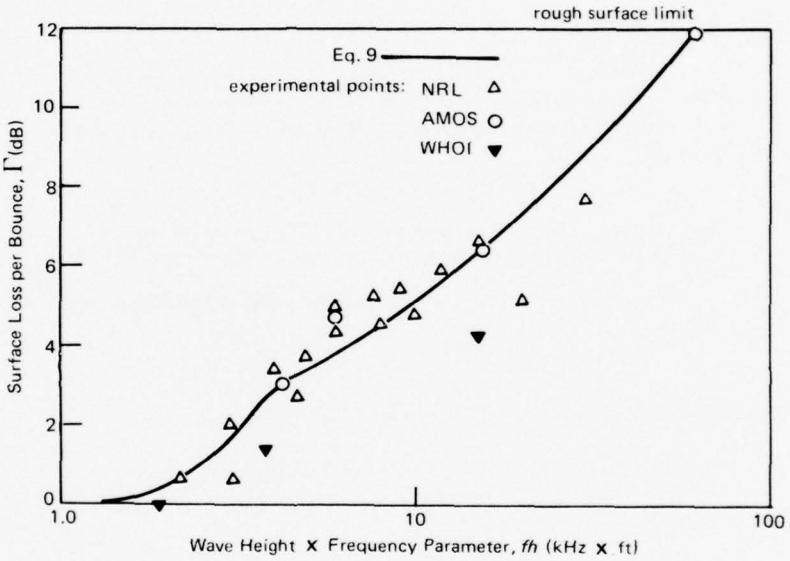


Figure 2. Surface-reflection-loss curve (from Ref. 7).

**AMOS Scaling Relationships and Propagation-Loss Equations.** The AMOS equations[3] may be expressed in terms of the following variables:

$R$: horizontal range between source and target (kyd)

$Z_L$: surface layer depth (feet)

$Z_X$: source depth (feet)

$Z_T$: target depth (feet)

$f$: frequency (kHz)

The variables $R$, $Z_L$, $Z_X$, and $Z_T$ are used to define scaled variables which in turn are used in four surface-duct propagation-loss equations. The selection of the appropriate propagation-loss equation is determined by scaled zones and the scaled source and

target depths. Three propagation zones are distinguished: a zone of direct radiation, a zone of single-surface-bounce scattering, and a zone of multiple-surface-bounce scattering, as defined in Table 2.

Table 2. Selection of the proper AMOS propagation-loss equation.

| Insonification Zone (Scaled Range) | Source-Target Positions (Scaled Depths) | Propagation-Loss Equation Used |
|---|---|---|
| $0 \leqslant r \leqslant r_1$ | $z_X \leqslant 1$ and $z_T \leqslant 1$ | $H = H_1$ |
| | $z_X > 1$ and/or $z_T > 1$* | $H = \text{Min}(H_1, H_2)$** |
| $r_1 < r \leqslant r_1 + 1/2$ | $z_X$, $z_T$ any value* | $H = \text{Min}(H_1, H_3)$** |
| $r_1 + 1/2 < r$ | $z_X$, $z_T$ any value* | $H = \text{Min}(H_2, H_4)$** |

*The AMOS equations are used in this model only if $Z_L \leqslant 1000$ feet and if

$$Z_X \text{ and } Z_T < 32\sqrt{Z_L}$$

Thus, the source or target may be located at $30\sqrt{Z_L}$, the traditional best depth to avoid detection, but not much deeper for the AMOS equations to be used.

**The minimum of the quantities contained within the parentheses is retained.

The scaled variables are

$$r = R\sqrt{Z_L}$$

$$z_X = \sqrt{Z_X/Z_L}$$

$$z_T = \sqrt{Z_T/Z_L}$$

and

$$r_1 = (1-z_X)/4 + (1-z_T)/4,\ z_X \leqslant 1,\ z_T \leqslant 1$$

$$= (1-z_X)/4 + (\sqrt{z_T^2-1})/5,\ z_X \leqslant 1,\ z_T > 1$$

$$= (\sqrt{z_X^2-1})/5 + (1-z_T)/4,\ z_X > 1,\ z_T \leqslant 1$$

The four propagation loss equations are

$$H_1 = 20 \log (R/R_0) + \alpha R + (r/r_1)G(z_X, z_T) + 60$$

$$H_2 = 20 \log (R/R_0) + \alpha R + (25 - \sqrt{|Z_X - Z_L|} - \sqrt{|Z_T - Z_L|} + 5R)(f/25)^{1/3} + 60$$

$$H_3 = 20 \log (R/R_0) + \alpha R + 2(r - r_1)F(z_X, z_T) + [1 - 2(r - r_1)]\, G(z_X, z_T) + 60$$

$$H_4 = 10 \log (R/R_0) + (\alpha + \alpha_s)R + F(z_X, z_T)$$
$$- \alpha_s Z_L (r + 0.5) + 10 \log [\sqrt{Z_L}\,(r + 0.5)] + 60$$

where

$R_0$ is a reference range of 1 yard

$\alpha$ is the absorption coefficient given by Eq. 8

$\alpha_s$ is the surface reflection-loss coefficient given by Eq. 9 and 10

$$G(z_X, z_T) = 0.1 \times 10^{2.3|z_X - z_T|}\,(f/25)^{1/3}, \quad |z_X - z_T| < 1$$
$$= 20(f/25)^{1/3}, \quad |z_X - z_T| \geq 1$$

and

$$F(z_X, z_T) = 0.4 C_f (10^{z_X} + 10^{z_T} + 10^{|z_X - z_T|})$$

with

$$C_f = 1, \quad f \leq 8$$
$$= 0.5 f^{1/3}, \quad f > 8$$

One of the equations $H_1$, $H_2$, $H_3$, or $H_4$ will be used for $H$ in Table 1, depending on the relationships between the scaled parameters $r$, $r_1$, $z_X$, and $z_T$. Table 2 shows the selection of the proper equation.

**Modification of the AMOS Equations for Lower Frequencies.** The AMOS surface-duct propagation-loss model discussed above is empirical and not valid for frequencies less than 2.2 kHz. Predictions based on the AMOS model for frequencies below 2.2 kHz typically do not show good agreement with Fleet operational data. This disagreement with low-frequency data can be explained in part by the low-frequency cutoff phenomenon as described by Arase[8] and Clay.[9] In the paper by Arase, experimental attenuation rate is studied as a function of frequency. For frequencies less than cutoff, the attenuation rate increases as a function of decreasing frequency. Arase found good agreement between experimental attenuation rate and theoretical first-mode attenuation rates based on a normal-mode propagation model.

To extend the applicability of the AMOS surface-duct propagation model to lower frequencies, an additive cutoff loss term has been incorporated. It is based on an approximation to the normal-mode surface duct model of Pedersen and Gordon.[10,11] The normal-mode cutoff term is

$$H_{co} = 8686\tau_1 R$$

where

$R$ is the horizontal range in kyd

and

$\tau_1$ is the first-mode damping factor, which is given by

$$\tau_1 = (\pi f g_0^2)^{1/3}\ Im(MX_1)/C_S$$

where

$f$ is frequency in kHz

$g_0$ is the sound-speed gradient in the duct in $sec^{-1}$

$Im(MX_1)$ is the imaginary component of the first eigenvalue

**Propagation Loss in the Subsurface Duct.** A subsurface duct is formed when the sound-speed profile has a concavity to the right, as illustrated in Fig. 3a. The dotted lines in Fig. 3a extend from the upper to the lower boundaries of the several ducts pictured. If both the source and the target depths are between these boundary depths, then the subsurface-duct equations are used, except for two special cases: (1) when the subsurface duct is part of a surface duct (Fig. 3b), and (2) when the axis of the duct is the deep minimum (deep axis) of the sound-speed profile (Fig. 3c). In case (1) the AMOS surface-duct equations are used, and in case (2) ray tracing is used.

Since the equation for subsurface-duct propagation loss derived from the AMOS data gives losses consistently greater than spherical spreading loss, and since a duct in the ocean is expected to trap sound energy and give losses on the order of cylindrical spreading, the subsurface-duct equation given in Ref. 3 was modified. The new equations are

$$\begin{aligned} H_D &= 20 \log R + \alpha R + H_Z + 60, \qquad R \leqslant R_v \\ &= 10 \log RR_v + \alpha R + H_Z + 60, \qquad R > R_v \end{aligned} \tag{11}$$

where

$H_D$ is propagation loss in the subsurface duct

$R$ is range in kyd

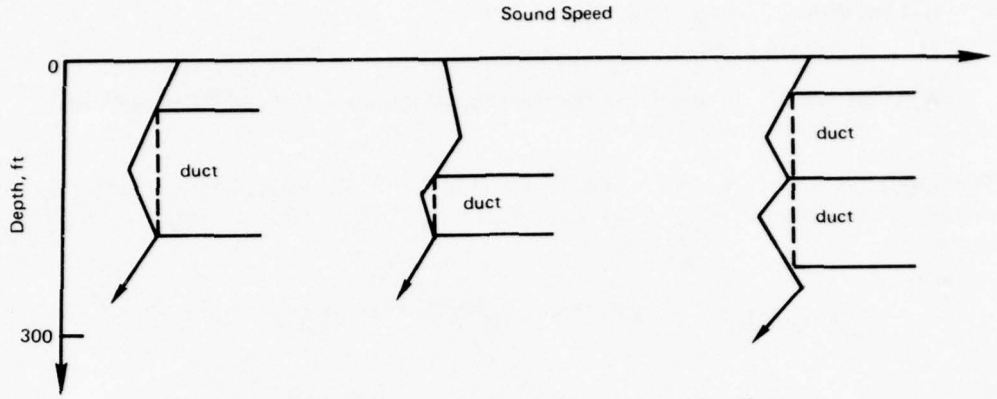


(a) Subsurface ducts to which the subsurface duct model applies.

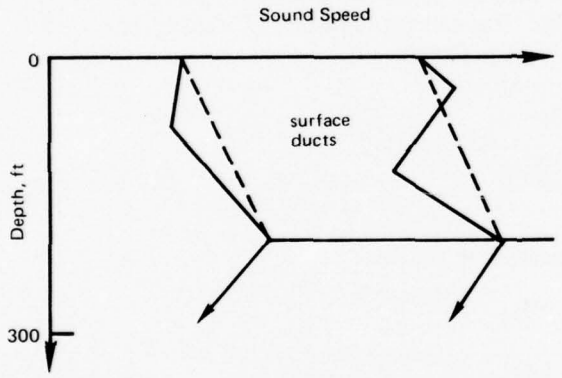


(b) Subsurface duct that is part of a surface duct. Subsurface duct model does not apply.

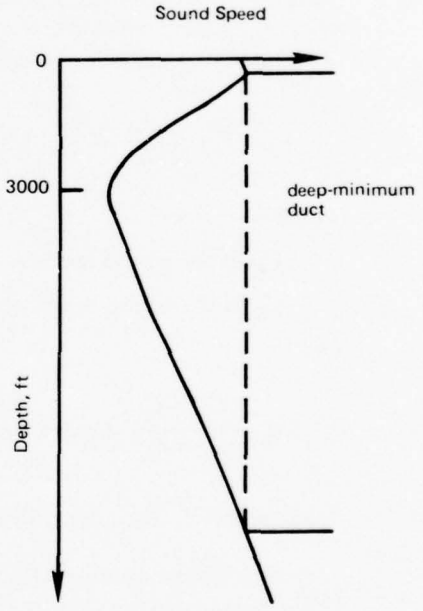


(c) Subsurface duct that is the *deep minimum duct*. Subsurface duct model does not apply.

Figure 3. Examples of subsurface ducts.

$\alpha$ is the absorption coefficient in dB/kyd

$H_Z$ is the depth loss factor (see below)

$R_v$ is the maximum distance a ray starting on the duct axis can travel without vertexing (derived below)

The depth loss factor, $H_Z$, is a function of source depth, $Z_X$, in feet, target depth, $Z_T$, in feet, duct axis depth, $Z_D$, in feet, duct width, $Z_W$, in feet, and frequency, $f$, in kHz, and is given by

$$H_Z = 0.4(f/8)^{1/3}(10^{|Z_X - Z_T|/Z_W} + 10^{|Z_X - Z_D|/Z_W} + 10^{|Z_T - Z_D|/Z_W}) \qquad (12)$$

where

$(f/8)^{1/3}$ is set to unity for $f<8$ kHz

The quantity $R_v$ in Eq. 11 is derived in the following manner. Figure 4 depicts two paths which have vertices (become horizontal) at the edges of the duct, an upward path and a downward path. In this case the downward path is used to determine $R_v$, since it produces the larger value. Ray theory for a constant-gradient sound-speed profile segment yields the following equation for $R_v$:

$$R_v = \frac{1}{|\gamma_b|} \sqrt{C_M^2 - C_D^2}$$

where

$C_M$ is the sound speed at the boundaries of the duct

$C_D$ is the sound speed at the duct axis

and

$\gamma_b = \dfrac{C_M - C_D}{Z_b - Z_D}$ is the sound-speed gradient in the lower branch of the duct

**Propagation by Ray Acoustics**

**The Wave Equation.** The propagation of acoustic energy through the ocean medium is approximated by the wave equation:[12]

$$\nabla^2 p = \frac{1}{C^2} \frac{\delta^2 p}{\delta t^2}$$

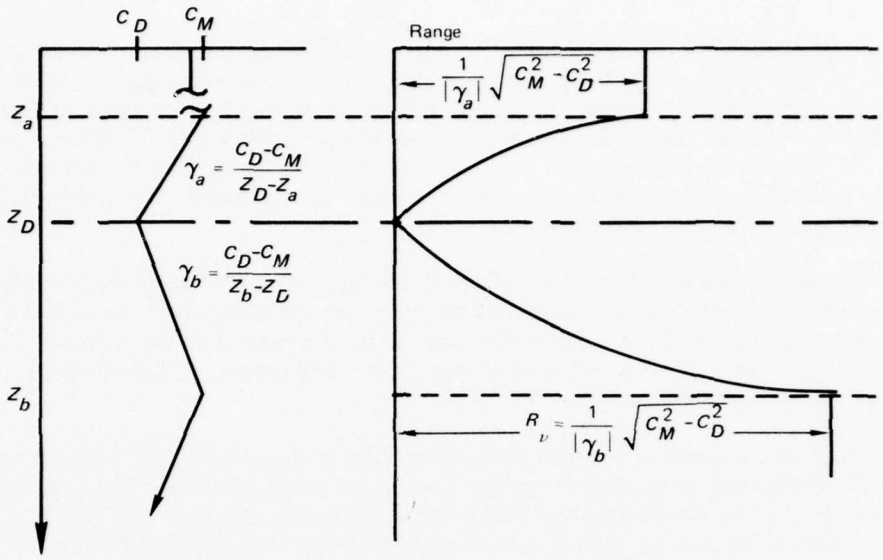


Figure 4. Ray vertexing ranges in a subsurface duct.

where

$p$ is the excess pressure at some constant phase on the wave front

and

$C$ is the sound speed; both $p$ and $C$ are functions of the spatial and time dimensions

**The Eikonal Equation.** Wave fronts of harmonic waves which are defined by

$$W(x,y,z) = C_0\ (t - t_0) \tag{14}$$

can represent a time-independent solution to the wave equation called the eikonal equation, which is

$$\left(\frac{\delta W}{\delta x}\right)^2 + \left(\frac{\delta W}{\delta y}\right)^2 + \left(\frac{\delta W}{\delta z}\right)^2 = \left(\frac{C_0}{C}\right)^2 \tag{15}$$

The eikonal equation can be derived by relating the pressure wave front to $W$ and by directly substituting into Eq. 13 or by using Eq. 14 to apply Huygens' principle for constructing successive wave fronts normal to preceding wave fronts.[12]

The eikonal equation is a special case of the wave equation, valid only if the wavelength of the propagating sound is much less than the radius of curvature of any portion of the ray path.

**Applicability for Sonar Systems.** All current active sonar systems operate at frequencies large enough (wavelengths small enough) for the eikonal equation to be valid. Passive sonar systems, however, are designed for detection at low frequencies. At 500 Hz the wavelength is about 10 feet, which does not preclude use of the eikonal equation. At 100 Hz the wavelength is about 50 feet, which suggests that the applicability of the eikonal equation and the ray acoustics which spring from it may not be valid for realistic sound-speed changes in the ocean.

**Definition of a Ray Path.** Normals to the wave surface (constant phase) in space at a given time can be constructed using Huygens' principle or can be computed using the eikonal equation, Eq. 15. The continuous path of a normal to the wave surface obtained by varying time is called a ray path. It is along ray paths that acoustic energy theoretically propagates.

Since sound speed is assumed to be a function of depth only, ray paths are restricted to the vertical plane through the source and target positions. Thus, ray tracing is accomplished in two dimensions which are (horizontal) range, $R$, and depth, $Z$. The origin is at the ocean surface vertically above the source, and $Z$ is positive downward, as in Fig. 5. Positive angles are measured downward from the horizontal.

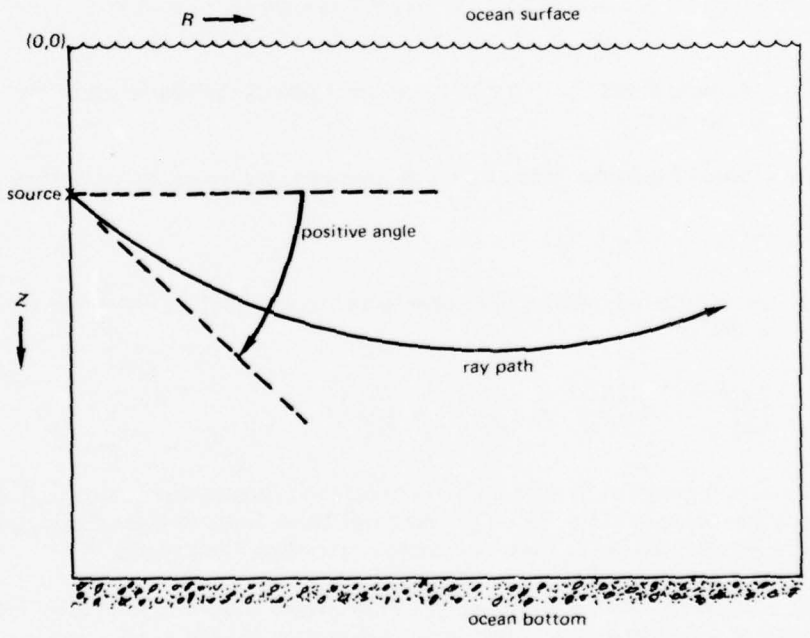


Figure 5. Coordinate geometry for ray tracing.

**Propagation Loss in Ray Theory**. Propagation loss is defined as the ratio of the source strength to the sound-field intensity in decibels.[12]

$$H \equiv 10 \log \frac{F}{I} \tag{16}$$

where

$F$ is the source strength in energy units per unit solid angle per second

and

$I$ is the intensity in units of energy crossing an elemental area $dA$ perpendicular to the ray path and bounded by an elemental solid angle $d\Omega$

The ratio $F/I$ is easily obtained using the concept of solid angle:[12]

$$\frac{I}{F} = \frac{d\Omega}{dA} = \left| \frac{\cos \phi_X}{R \left( \frac{\delta R}{\delta \phi_X} \right)_Z \sin \phi_T} \right|$$

with the absolute value sign used, since neither $F$ nor $I$ can ever be negative. With $\cos \phi_X = C_X/C_v$, Eq. 16 becomes

$$H = 10 \log \left| R \left( \frac{\delta R}{\delta \phi_X} \right) \sin \phi_T (C_v/C_X) \right| + 60 \text{ in dB re 1 yd} \tag{17}$$

where

$H$ is propagation loss in decibels re 0 dB at 1 yard slant range from the source along the ray path

$R$ is range in kyd

$\phi_T$ is the angle of the ray at the ending (target) depth

$C_X$ is the sound speed at the source depth

$C_v$ is the sound speed at the vertex depth

and

60 represents the conversion in units from yards to kiloyards in the range and range-derivative factors

$\phi_X$ is the starting angle of the ray at the source depth

$\left( \frac{\delta R}{\delta \phi_X} \right)_Z$ is the constant-depth derivative of the range with respect to the starting angle

Except for the units, Eq. 17 is general, independent of algorithms for determining $R$ and $\left(\frac{\delta R}{\delta \phi_X}\right)_Z$, for which expressions will be given in Eq. 20, 21, 23, and 24.

**Curvilinear Sound-Speed Profile.** The adjectives "straight-line" and "curvilinear," used as descriptors of sound-speed profile, signify the functional representation of the sound speed from the surface to the bottom of the ocean when sound speeds are known only for discrete depths. "Straight-line" refers to a sound-speed profile constructed of straight-line segments connecting the points. "Curvilinear" refers to fitting the sound-speed profile to within a given tolerance with quadratic equations of the form

$$C = C_a^2 [1-K_a(Z-Z_a)^2]^{-1} \tag{18}$$

where

$Z$ is depth

$C_a$, $Z_a$, and $K_a$ are three curve parameters evaluated for each curve segment

The curve parameters between successive segments are dynamically adjusted so that successive curves and their derivatives are continuous at the sound-speed profile points.

Pedersen[13] has shown that a straight-line sound-speed profile produces undefined propagation losses for certain ranges calculated using ray theory. This problem is a direct result of having discontinuities in the first derivative anywhere on the sound-speed profile. Introducing more points compounds the problem, since more discontinuities in the first derivative are added.

Pedersen and Gordon[14] introduced the curvilinear approximation to the sound-speed profile, Eq. 18, and required that the curve-fitting segments and their derivatives be everywhere continuous over the profile. Numerical examples given by Pedersen and Gordon show that a curvilinear approximation to the sound-speed profile eliminates the false caustics (false regions of infinite intensity) characteristic of the straight-line approximation.

The major obstacle to implementing the curvilinear method is developing a computer program which can reliably fit the sound-speed profile within an adequate tolerance. Some computer programs were written and are still being used which require trial and error on the part of the user to adjust and add points to the sound-speed profile in order to get an adequate fit. This kind of software is unacceptable for support of an active sonar performance prediction program which must run to completion without idiosyncracies. Fortunately, a set of subroutines does exist which performs the task adequately. These subroutines were developed by Charles Bartberger[15] of NADC. He used Pedersen's and Gordon's equations and applied varying tolerance versus depth. The subroutines used in the LORA program are essentially

Bartberger's, with changes in one of the tolerance equations to obtain a closer fit. The new tolerance equations, in the form of Bartberger's equations, are

$$T = T_d(y_{av}) + T_g(g) \text{ ft/sec}$$

where

$y_{av}$ is the average depth of all the points being fitted

and

$g$ is the smallest of the absolute straight-line gradients connecting adjacent points of the set, with the functions

$$T_d(y_{av}) = 2.9 - 2.5 \exp(-0.00000272\, y_{av})$$

and

$$T_g(g) = \frac{3}{2} [1 + \tanh 4.8(g - 0.35)]$$

In a numerical evaluation with a typical surface-duct sound-speed profile which extends to 10,000 feet, the curve-fitted profile differs from the linear profile by less than 0.2 ft/sec at the duct maximum, less than 0.5 ft/sec down to 1,000 feet, and less than 0.01 ft/sec between 4,000 and 10,000 feet. The standard deviation is less than 0.2 ft/sec over the whole profile (110 points in the sample).

Equation 18 can manifest three types of curves, depending on the signs of the curve parameters. These are shown in Fig. 6. The sound-speed profile will be constructed from segments which appear in these forms. Curves of Types I and II occur most frequently, Type III seldom. Even though a curve of Type I or II may fit a minimum or maximum adequately, an extra layer is introduced at that point. Reference 15 gives both a complete description of the mathematical technique for curve-fitting the sound-speed profile and a listing of the computer software.

**Earth Curvature Correction.** Bartberger[15] gives a derivation for the first-order spherical earth curvature correction to the sound-speed profile. With slight changes in nomenclature his equations are

$$C_i = C_i'(1 + Z_i'/R_e)$$

$$Z_i = Z_i'(1 + Z_i'/2R_e)$$

where

$C_i'$ is input sound speed

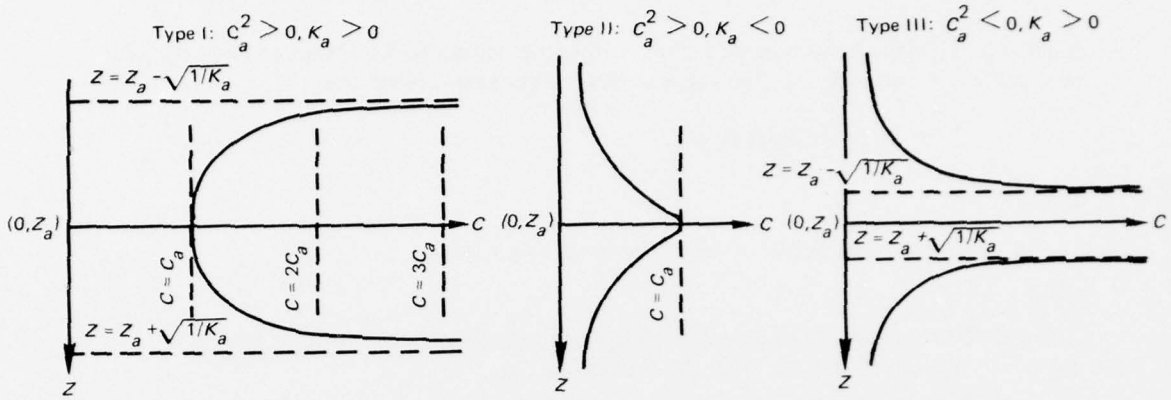


Figure 6. Schematic plots of the three types of curves used to fit the sound-speed profile with curvilinear segments (from Ref. 14).

$Z_i'$ is corresponding input depth

$C_i$ and $Z_i$ are the corrected sound speeds and depths

and

$R_e$ is the radius of the earth in corresponding units

**Snell's Law.** *This model assumes that the* sound speed varies in only one spatial dimension, depth. Snell's law is therefore

$$\frac{\cos \phi}{\cos \phi_0} = \frac{C}{C_0} \tag{19}$$

where

$\phi$ and $\phi_0$ are angles that a ray path makes with respect to the horizontal

and

$C$ and $C_0$ are sound speeds that correspond to the depths at which the angles are measured

Snell's law applied to the sound-speed profile can yield the following information:

1. The starting angle for a ray to get to a given depth.
2. The angle of the ray at any depth, given the starting angle and depth.
3. Determination of whether it is possible for a ray to vertex at a given depth, given the starting angle and depth.
4. The depths that a ray cannot reach, given the starting angle and depth.

Snell's law is an important concept that has been used extensively in this model, both for the selection of rays to be traced and in the interpretation of the outputs in anticipating modes of propagation, shadow zones, and the like. Frequently users' questions about the interpretation of the LORA program outputs are answered through some application of Snell's law.

**Curvilinear Ray Tracing.** Curvilinear ray tracing means calculating the locus of points in range and depth of a ray governed by a sound-speed profile which is defined by curvilinear segments of the form of Eq. 18. Four important quantities are obtained from ray tracing between specified depths: range, $R$, time, $T$, range derivative with respect to starting angle, $D$, and absorption loss, $H_A$.

A layer is defined as the depth region over which one given curvilinear segment is valid. An interface is defined as the depth at which one curvilinear segment makes transposition to another. Figure 7 shows a typical layer. In ray tracing, two depths are specified and the ray parameters $R$, $T$, $D$, and $H_A$ are calculated and summed as the tracing proceeds through the layers. $H_A$ will be described in the next section.

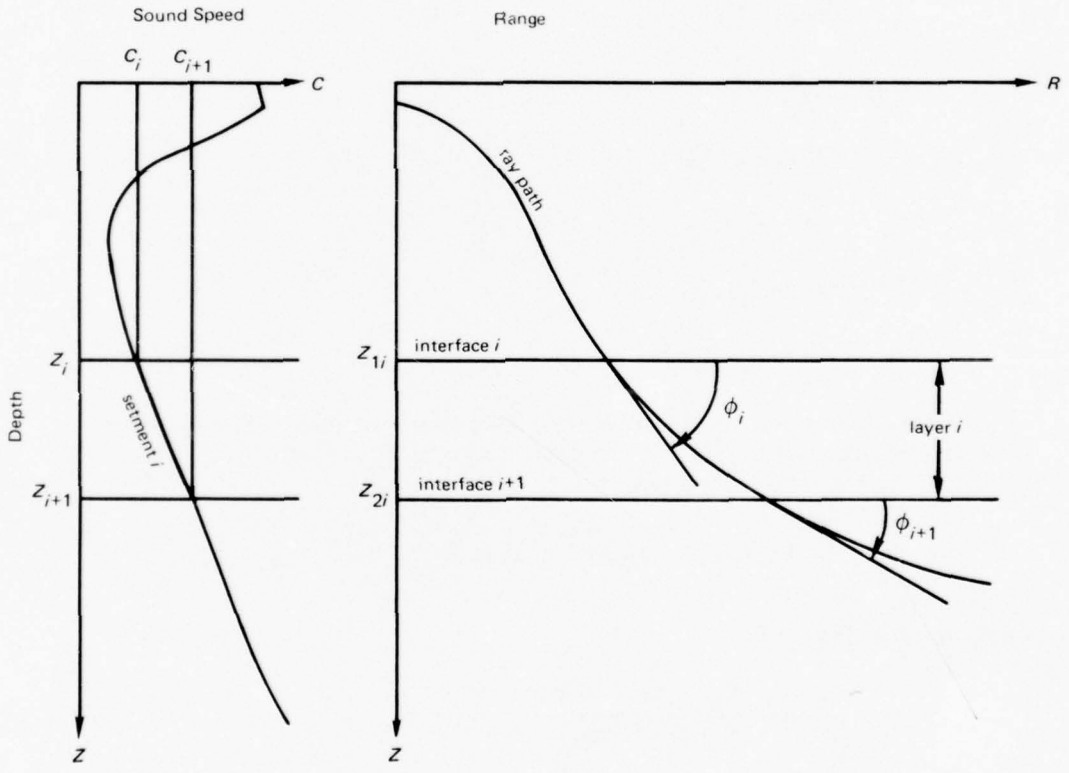


Figure 7. Layer geometry.

Let $C_{ai}$, $K_{ai}$, and $Z_{ai}$ be the segment parameters for the curvilinear sound-speed profile layer $i$ between interfaces $i$ and $i + 1$. Let the upper and lower depths for layer $i$ be $Z_{1i}$ and $Z_{2i}$, respectively. (Notice that $Z_{1i} = Z_i$ and $Z_{2i} + Z_{i+1}$.) Let $C_v$ be the vertex sound speed, the maximum sound speed the ray can achieve, the sound speed at which the ray becomes horizontal. Let $\phi_i$ be the angle which the ray makes with the horizontal (downward is positive). Pedersen and Gordon[14] define nine auxiliary quantities:

$$A_i = \pm C_v \left| \frac{K_{ai}}{C_{ai}^2} \right|^{1/2}$$

$$D_i = C_{ai}/(C_v^2 - C_{ai}^2)$$

$$E_i = (C_v^2 + C_{ai}^2)/C_{ai}^2$$

$$R_{1i} = A_i(Z_{1i} - Z_{ai})$$

$$R_{2i} = A_i(Z_{2i} - Z_{ai})$$

$$B_{1i} = \cot \phi_i(Z_{1i} - Z_{ai})$$

$$B_{2i} = \cot \phi_i(Z_{2i} - Z_{ai})$$

$$T_{1i} = \tan \phi_i(Z_{1i} - Z_{ai})$$

$$T_{2i} = \tan \phi_i(Z_{2i} - Z_{ai})$$

The ray parameters $R_i$, $T_i$, and $B_i$ for a ray passing completely through layer $i$ can now be expressed in terms of the above nine quantities. For a Type I curvilinear segment (see Fig. 6) the range in layer $i$ is

$$R_i = \frac{1}{A_i} \cos^{-1} \left[ D_i \left| R_{1i} R_{2i} \right| + \tan \phi_i \tan \phi_{i+1} \right] \tag{20}$$

and for Types II and III

$$R_i = \frac{1}{A_i} \ln \left[ \frac{\left| R_{1i} \right| + \tan \phi_i}{\left| R_{2i} \right| + \tan \phi_{i+1}} \right] \tag{21}$$

The travel time in layer $i$ is

$$T_i = \frac{1}{2C_v} (E_i R_i - T_{1i} + T_{2i}) \tag{22}$$

The derivative of range with respect to vertex sound speed is

$$C_v \left(\frac{\delta R_i}{\delta C_v}\right)_Z = B_i = D_i(B_{1i} - B_{2i}) - R_i$$

The derivative with constant $Z$ indicates ray tracing is between two constant depths. Using Snell's law

$$\left(\frac{\delta R_i}{\delta \phi_X}\right)_Z = \tan \phi_X \left(\frac{\delta R_i}{\delta C_v}\right)_Z$$

where

$\phi_X$ is the starting angle of the ray at the transmitter

Thus

$$\left(\frac{\delta R_i}{\delta \phi_X}\right)_Z = \frac{\tan \phi_X}{C_v} \{D_i(B_{1i} - B_{2i}) - R_i\} = \frac{\tan \phi_X}{C_v} B_i \tag{23}$$

If a ray forms an apex in layer $i$, $R_{1i}$ is replaced by $|D_i|^{-1/2}$, $\tan \phi_i$ is set to zero, and Eq. 20 and 23 are still applicable. If a ray forms a nadir in the layer, $R_{2i}$ is replaced by $|D_i|^{1/2}$ and $\tan \phi_{1+i}$ is set to zero. Pedersen and Gordon[14] list problems and solutions for cases when a vertex sound speed is at an interface. The LORA program selects vertex sound speeds in such a way that these problems will never occur; however, the ray tracing algorithm is written to handle them according to the specifications of Pedersen and Gordon.

The total range, $R$, time, $T$, and range derivative, $D$, are obtained by summing the appropriate quantities calculated for each layer over the total number of layers traversed from one end of the ray path to the other. Thus, some layers contribute more than once in the summation. Using Eq. 20–23 and converting from feet to kiloyards

$$\left.\begin{aligned} R &= \Sigma R_i/3000 \text{ kyd} \\ T &= \Sigma T_i \text{ sec} \\ D &\equiv \left(\frac{\delta R}{\delta \phi_X}\right)_Z = (\tan \phi_X/3000\, C_v) \Sigma B_i \text{ kyd} \end{aligned}\right\} \tag{24}$$

$R$ and $D$ are used directly in Eq. 17 for the calculation of propagation loss. $T$ is to be used to obtain the reverberation level at the time at which target echo arrives at the receiver.

**Absorption Loss Along the Ray**. The path length in the $i$th layer is approximated by the slant range

$$S_i = [R_i^2 + (Z_{i+1} - Z_i)^2]^{1/2} / 3000 \text{ kyd}$$

where

$R_i$ is the range in feet given by Eq. 20 and 21

$Z_i$ is the upper interface depth in feet

and

$Z_{i+1}$ is the lower interface depth in feet

The total absorption loss is

$$H_A = \sum_i S_i a_i$$

where

$a_i$ is the absorption loss in dB/kyd calculated for the mid-depth at each layer of the sound-speed profile after curve-fitting

and

$\sum_i$ indicates that the summation is over all the layers a given ray path enters (some layers may have more than one contribution)

This value for $H_A$ is used in Table 1 in all propagation modes except the duct modes.

The absorption loss is calculated by using Eq. 8. The pressure is calculated for the mid-depth of each layer, $Z_m$, and the relaxation frequency is calculated for the temperature, $T_m$, at $Z_m$. The temperature is given by

$$\left.\begin{aligned} T_m &= A_1 - (0.000434\, Z_m)^2 / A_1 \\ \text{with} \\ A_1 &= 122.83 - 4.6676 \sqrt{5132 - C_m + 0.0165\, Z_m} \end{aligned}\right\} \qquad (25)$$

where

$Z_m$ is the mid-depth of the layer

and

$C_m$ is the corresponding sound speed

The form of Eq. 25 results from an approximation to Wilson's equation,[16] inverted to obtain temperature by the *regula falsi* method. It is understood that Wilson's equation is properly a least-squares polynomial fit to the regression variables temperature, pressure, and salinity, and that inversion to obtain temperature as a function of sound speed, pressure, and salinity produces a larger standard deviation than if a new regression were performed on the original data. However, absorption loss is not severely influenced by temperature, and the errors introduced by inverting Wilson's equation and by using Eq. 25 are negligible for the total propagation loss along a ray path.

Equation 25 is a trial and error fit as to form, but some of the coefficients have been adjusted to produce a minimum standard deviation in temperature prediction. H. W. Frye's regression analysis program[17] was used to fit polynomials to a large set of temperatures obtained by inverting Wilson's equation for specific sound speeds, pressures (depths), and salinities. Realistic values for ocean parameters produced a standard deviation of less than 0.1°F. McGirr and Hall[18] have shown that an error of even 1°F would not seriously debilitate the prediction for the absorption coefficient.

**Surface Loss.** Loss caused by a ray reflecting from the ocean surface is a model input. The user of the LORA computer program can, as an option, use the value for surface loss per bounce calculated by Eq. 9. The total loss caused by surface reflections is the number of surface bounces a ray path undergoes times the surface loss per bounce. This loss is added to the other components of propagation loss for one of the modes of propagation described in Table 1.

**Bottom Loss.** Loss caused by a ray bouncing off the ocean bottom is a model input. In the computer program it is calculated by linearly interpolating a user-supplied piecewise linear array of bottom loss values versus grazing angle. The bottom loss per bounce is multiplied by the number of bottom bounces to obtain total bottom loss, which is used in the equation for bottom bounce propagation in Table 1.

**Ray Paths.** Vertex sound speed, the maximum sound speed a ray can obtain, is given by Snell's law. At this sound speed, the ray becomes horizontal and thereafter traces a mirror-image path about the vertical. With the ending angle $\phi = 0$, Eq. 19 gives the expression for vertex sound speed:

$$C_v = \frac{C_0}{\cos \phi_0} \tag{26}$$

where

$\phi_0$ and $C_0$ are ray angle and sound speed, respectively, at the same depth

The sound-speed profile, $C(Z)$, is a single-valued function of depth. The inverse of $C(Z)$, depth as a function of sound speed, is multivalued. Thus, given $C_v$, a number of values for the vertex depth, $Z_v$, may be obtained. Given a sound-speed profile and the depth and angle at which a ray starts, one upper and one lower vertex depth can be found by scanning the profile upward and downward from the starting depth and finding the depths (upward–downward) at which the ray achieves the sound speed $C_v$. The ray is confined between these upper and lower vertex depths, and mirror-image paths are produced as the ray travels on. In some cases $C_v$ is greater than any sound speed found in the upward–downward scan of the sound-speed profile; this indicates that the ray will strike the surface or bottom of the ocean. In this model these boundaries provide mirror images of the path with range and give the same replication of path as if the ray had gone through a refractive turning point. Once a ray is traced from its upper vertex depth (or the surface) to its lower vertex depth (or the bottom), one-half of a cycle of the ray is obtained (in range versus depth). The second half of the cycle is obtained by annexing the mirror image to the first half. As many cycles as desired can be appended to extend the horizontal range of the ray. This model uses a maximum of 30 cycles (up to 30 cycles appended to points on the basic ray path in the first cycle) for both active sonar two-way propagation loss and passive one-way propagation loss. The program user can specify the maximum number of refractive cycles or bottom bounce cycles to be used.

This model is concerned with tracing rays between several depths, computing propagation loss for the resultant ranges, and using these losses to determine the signal return from a target or the reverberation from surface, bottom, or volume acoustic scatterers. Thus, rays are traced from transmitter depth to target depth, as well as to the surface and bottom. When a ray is traced from one depth to another, five ray parameters are calculated for later use in the calculation of propagation loss and for interpolation: absorption loss, $H_A$, range, $R$, time, $T$, derivative of range with respect to starting angle, $D$, and boundary loss, $B$. *For convenience in subscripting, A will be used for* $H_A$ *in the following discussion.* The parameters $A$, $R$, $T$, $D$, and $B$ are associative from segment to segment on a ray path, so that several segments can be annexed together by adding the corresponding components. The parameters for a path segment can be thought of as forming a vector space

$$\overline{V} = (A, R, T, D, B)$$

where the linear combination of the components is the only property of interest in this study (scalar product and norm have no physical significance here). $\overline{V}$ will be used as a shorthhand notation for its components, and when $\overline{V}$ is subscripted, the subscript applies to each of the components. An example of $\overline{V}$ for a ray traced from depth $a$ to depth $b$ is

$$\overline{V_{ab}} = (A_{ab}, R_{ab}, T_{ab}, D_{ab}, B_{ab})$$

One of the many possible range components, $R_{ab}$, is depicted in Fig. 8.

Because of the cyclic nature of the ray path, there are an infinite number of vectors $\overline{V_{ab}}$ which can connect two depths. Thus, following the dotted ray path in Fig. 8, one can see that the path will cross depths $a$ and $b$ infinitely. A ray path connecting two depths which does not contain cyclic components or mirror image components about some vertical (range = constant) is defined as a ray path segment.

In computing propagation loss from transmitter to target, it is only necessary to trace three segments: (1) upper vertex depth or surface-to-transmitter depth, (2) transmitter depth to target depth, and (3) target depth to lower vertex or bottom depth.* These segments are depicted in Fig. 9, with one of the vector components, $R$, the horizontal range, also shown. The vectors resulting from calculating the segments are

$$\overline{V_{SX}} = (A_{SX}, R_{SX}, T_{SX}, D_{SX}, B_{SX})$$

$$\overline{V_{XT}} = (A_{XT}, R_{XT}, T_{XT}, D_{XT}, B_{XT})$$

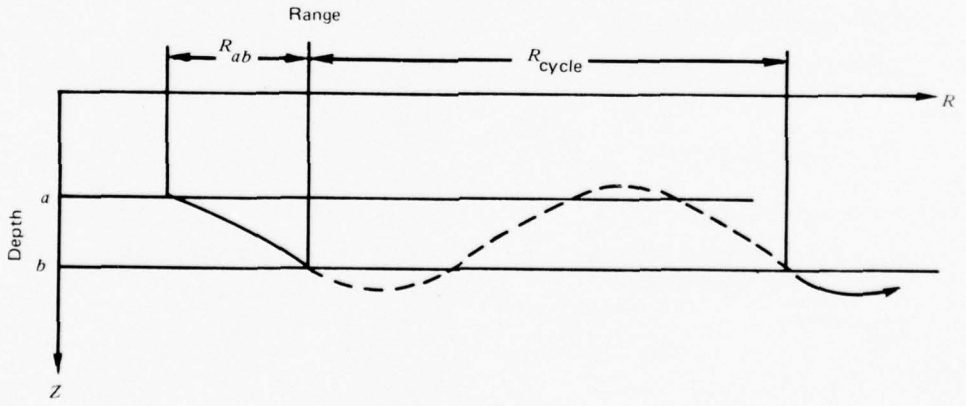


Figure 8. Range component and range cycle.

*These segments apply when transmitter depth is less than the target depth. If the transmitter depth equals the target depth, then segment 2 is null. If the transmitter and target depths are reversed, then "transmitter" and "target" designations in the description of the three segments should be reversed.

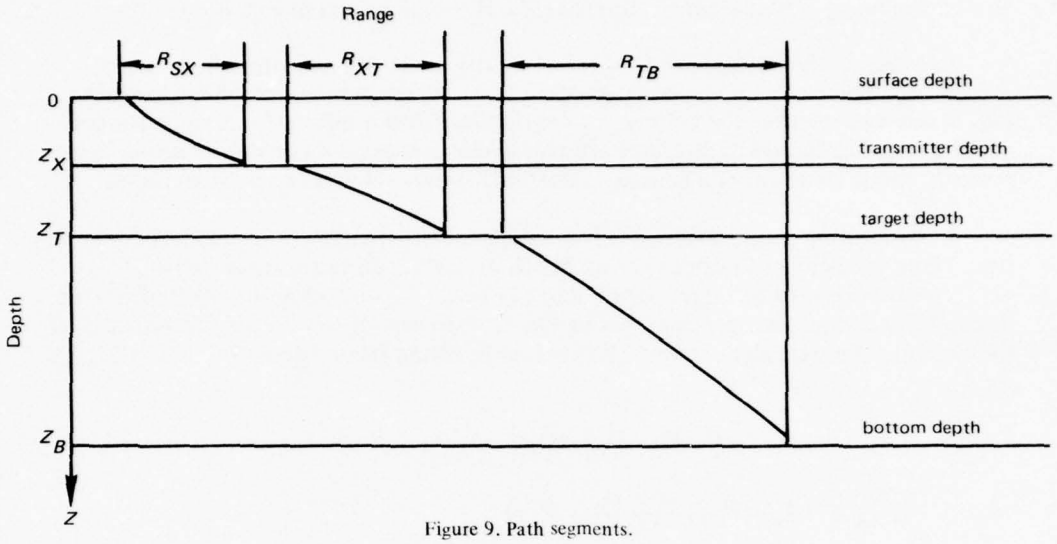


Figure 9. Path segments.

and

$$\overline{V_{TB}} = (A_{TB}, R_{TB}, T_{TB}, D_{TB}, B_{TB})$$

where the subscripts imply the following:

$SX \rightarrow$ surface to transmitter

$XT \rightarrow$ transmitter to target

and

$TB \rightarrow$ target to bottom

The $B$ components are

$B_{SX}$ = 1/2 × surface-loss-per-bounce or zero if the ray does not strike the surface

$B_{XT} = 0$

and

$B_{TB}$ = 1/2 × bottom-loss-per-bounce or zero if the ray does not strike the bottom

Once the path segments are determined for a given starting angle at the transmitter, they can be combined through addition to give four basic path types. These basic path types are illustrated in Fig. 10.

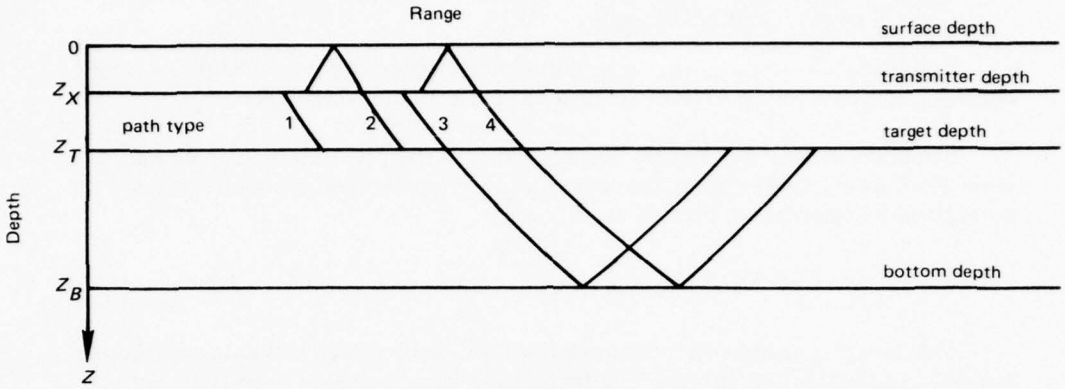


Figure 10. Four basic path types connecting transmitter and target depths.

The vector representation for the basic path types is

$$\left.\begin{aligned} \overline{V_1} &= \overline{V_{XT}} \\ \overline{V_2} &= 2\overline{V_{SX}} + \overline{V_{XT}} \\ \overline{V_3} &= \overline{V_{XT}} + 2\overline{V_{TB}} \\ \overline{V_4} &= 2\overline{V_{SX}} + \overline{V_{XT}} + 2\overline{V_{TB}} \end{aligned}\right\} \tag{27}$$

These four basic path types are the only ways in which a ray with angle $\pm\phi_X$ at the transmitter can travel from the source to the target depth without completing a cycle. The vector describing a cycle is

$$\overline{V_C} = 2(\overline{V_{SX}} + \overline{V_{XT}} + \overline{V_{TB}}) \tag{28}$$

All possible paths and their parameters from the source to the target may now be described by

$$\overline{V_{kn}} = \overline{V_k} + n\overline{V_C}, \quad k = 1,2,3,4; \quad n = 1,2,3,\ldots, \tag{29}$$

where

$\overline{V_{kn}}$ = is the vector whose components are absorption loss, range, time, range derivative, and boundary loss*

Equations 27–29 define every possible path connecting transmitter and target depths, given that the complete ray path has a maximum sound speed $C_v$.

**Selection of Starting Angles.** The ray paths of the previous section all had the same absolute starting angle at the source, $\phi_X$. Given the maximum sound speed $C_v$, $\phi_X$ is given by Snell's law, Eq. 18, as

$$\phi_X = \pm \cos^{-1} (C_X/C_v)$$

This model considers two categories of rays, those which ultimately strike the bottom and those which do not. The former category is called the bottom bounce (*BB*) propagation mode, and the latter, the convergence zone (*CZ*)** propagation mode. For *BB* rays $C_v$ exceeds the bottom sound speed, $C_B$. For *CZ* rays $C_v$ is less than $C_B$. For each propagation mode, *BB* and *CZ*, 40 $C_v$'s are selected, giving a total of 80 unique $\phi_X$'s. By using both positive and negative values for $\phi_X$, 160 ray paths are obtained.

The 40 *BB* $C_v$'s are selected by using the equation

$$C_v^{(j)} = \frac{C_X}{\cos\left\{\phi_m - [1-\exp(j/4)](\phi_m - \phi_B)\right\}}$$

where

$C_v^{(j)}$ is the $j$th vertexing sound speed to be used in ray tracing

$C_X$ is the sound speed at the source depth

$\phi_m$ = 1.553343033, the radian value for 89 degrees

$j$ = 0,1,...,39

and

$$\phi_B = \cos^{-1}(C_X/C_B), \quad C_X < C_B$$

$$= 0, \quad C_X \geq C_B$$

is the angle in radians at the source depth of the ray which just grazes the bottom

*The boundary-loss component is one-half the actual loss, since the segments containing nonzero boundary losses are always doubled in Eq. 27.

**This categorization is somewhat arbitrary in that refracted and surface reflected ray paths are also included.

In addition, each of the following sound speeds is included in the set if it is greater than both $C_X$ and $C_B$:

$$C_S \pm \delta$$

$$C_{RM} \pm \delta$$

where

$C_S$ is the surface sound speed

$C_{RM}$ is any relative maximum in the sound-speed profile

and

$\delta$ is a small constant increment

Selection of the 40 values of $C_v$ for the *CZ* propagation mode is as follows: First, all interface sound speeds are found with values between $C_X$ and $C_B$. Then $\delta$ is subtracted from each and the result stored. If the interface sound speed is a relative maximum, $\delta$ is added and the result is included in the set. The surface sound speed is treated in the same way as a relative maximum. The source and target sound speeds plus $\delta$ are included in the set. Then all these sound speeds are ordered in increasing magnitude. The spacing between successive sound speeds in the ordered set is examined, and more sound speeds, approximately evenly spaced, are added to the set to fill up an array of 40 vertex sound speeds.

The *BB* and *CZ* vertex sound-speed arrays are used as drivers to step through the starting angles at the source. They have been chosen to reduce caustic effects and accurately outline the shadow zones. These sets of vertex sound speeds also produce roughly evenly spaced range values between successive rays for average sound-speed profiles with the following qualifications: in range regions with highly fluctuating propagation losses, the rays tend to be spaced very close together (say, 0.1 kyd), and in range regions with slowly varying propagation losses, the rays are spaced farther apart (say, 2 kyd). The angular coverage is ±89 degrees; thus, the ocean is effectively filled with sound.

**Ray Path Interpolation.** Ray-tracing methods involve specifying a ray's starting depth and starting angle (or its equivalent, vertex sound speed) and following the ray through the medium to see where it goes. Range and range derivative are obtained, from which propagation loss can be calculated. Range and range derivative are outputs of the ray-tracing algorithm. But for exceptional cases, a specific range for a given depth cannot be produced except by iterative techniques or interpolation. The technique for producing propagation loss for specific ranges becomes a part of the model.

For interpolating propagation loss between adjacent rays of the same class, this model uses an interpolation technique whose basic assumption is that

$$H = 20 \log (R/R_0) + H_0 \tag{30}$$

where

$H$ is propagation loss at range $R$

and

$H_0$ is a reference propagation loss at a reference range $R_0$

Two adjacent rays at a given depth produce the propagation losses $H_a$ and $H_b$ at the ranges $R_a$ and $R_b$. Equation 30 can then be solved for $R_0$ and $H_0$ to produce the following equation for $H$:

$$\left.\begin{aligned} H &= 20 \log \left[(1-F)\, 10^{H_a/20} + F\, 10^{H_b/20}\right] \\ \text{where} \\ F &= \frac{R - R_a}{R_a - R_b} \end{aligned}\right\} \tag{31}$$

The computer program interpolates in 1-kyd increments. Thus, interpolation is made for propagation loss for all integer range values between $R_a$ and $R_b$. Corresponding times are obtained by linear interpolation. These times are used later for interpolating reverberation arrays.

Interpolation between successive rays means that the two rays have successive vertexing sound speeds in one of the arrays; these arrays are arranged either in increasing magnitude (for convergence-zone loss) or decreasing magnitude (for bottom-bounce loss). Also, the ray paths must be of the same class: both ray paths must have the same value of $k$ and $n$ for the $V_{kn}$ defined in Eq. 29. In Fig. 11 rays $a$ and $b$ would be interpolated, but ray $c$ would not be interpolated with either ray $a$ or ray $b$, even though ray $c$ has the same vertex depth as ray $a$ and the next successive vertex depth compared to ray $b$. The key to the interpolation lies in the path type $k$ and cycle number $n$ subscripts. See Fig. 10 and Eq. 29 to obtain relationships in Fig. 11.

There is one very important exception to the interpolation rule of only interpolating between successive rays of the same class: the LORA program does not calculate rays which vertex exactly at the source or target depths; the rays vertexing near these depths have vertexing sound speeds slightly larger than the sound speeds at the source and target depths. If the source or target depth falls in a region of the sound-speed profile where the sound speed changes very slowly with depth, a ray vertexing

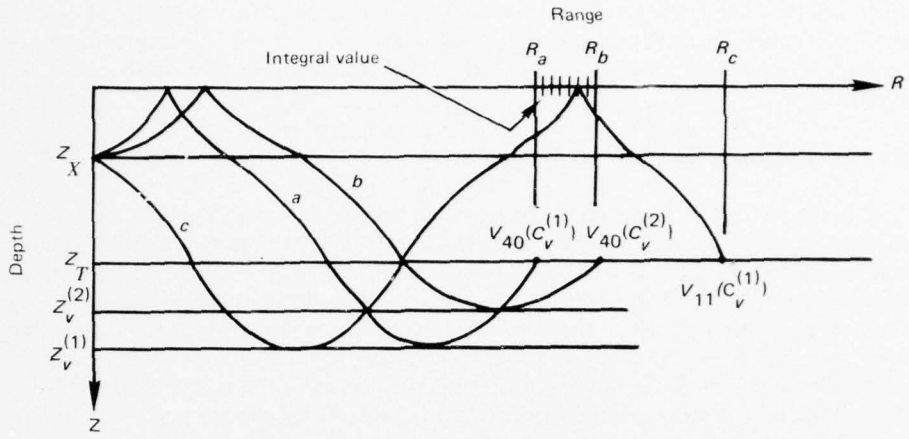


Figure 11. Example of ray interpolation.

near the source or target depth may travel for several kiloyards before it recrosses that depth. The distance between crossings, as depicted by the "hole" in Fig. 12, is omitted from interpolation if the rule that "only rays of the same class may be interpolated" is followed. This is an unacceptable limitation in the interpolation scheme, since changing the precision of the calculations can change the size of the "hole." For a ray that vertexes very near the source and target depths, interpolation is accomplished between the ray path of the first crossing and the same path at the second crossing, even though the ray paths constitute two different classes. This interpolation scheme is reasonable, since $A$, $R$, $T$, $D$, and $B$ are continuous in the affected region.

Another special case arises when source and target are at the same depth. The first ray, even though it has a very small starting angle, often produces a range value of more than 1 kyd when it crosses the target depth. This case is dealt with easily by setting $R_a$ to 0.001 kyd and $H_A$ to 0 dB, the reference values, and using Eq. 31 for interpolation. A linear interpolator for propagation loss versus range would be inaccurate, but Eq. 31 produces accurate spherical spreading values.

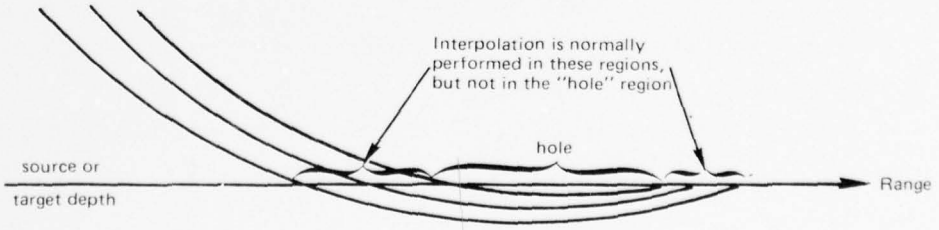


Figure 12. The "hole" in the interpolation scheme.

Equation 31 is valid for interpolation for short ranges, but what about long ranges? Interpolation between successive rays spaced a few kiloyards apart at ranges exceeding 10 kyd is so close to linear interpolation that there is no noticeable difference.

**Beam Pattern Correction to Propagation Loss**

A beam pattern is the relative response in decibels of a transmit or receive array of hydrophones as a function of some angle. Since ray paths in this model are all contained in the vertical plane, the response need only be known as a function of vertical angle in the vertical plane through own-ship and target positions. The angle of maximum response defines the main axis of a beam pattern. The angle that this axis subtends with the horizontal is called the depression–elevation (D/E) angle. The maximum response is 0 dB, with all other responses measured relative to it. The abscissal angular values used in defining the response function are positive when measured downward (clockwise) with respect to the main axis. Since the maximum of the response function is 0 dB, responses at all other angles must be less than 0 dB.

Beam patterns as inputs to the computer program are represented as piecewise linear functions of angle, and the response values are in decibels *down* from the main axis response. Thus, all response values are entered as positive numbers, and the program makes the change of sign at the time of interpolation. Intermediate responses as a function of angle are obtained by linear interpolation. The remainder of the discussion here will treat responses as negative, according to the usual definition.

The computer program uses the theoretical response of a long line as a default function for beam pattern. Both the transmit and receive beam patterns can be represented by this function, and each can have its own respective beamwidth. The response function for a continuous line of length $L$ is[19]

$$B(\phi) = 20 \log \left[ \frac{\sin \left( \frac{\pi L}{\lambda} \sin |\phi - \phi_0| \right)}{\frac{\pi L}{\lambda} \sin |\phi - \phi_0|} \right] \tag{32}$$

where

$\lambda$ is the wavelength of the acoustic energy

$\phi$ is the look-angle for calculating response

$\phi_0$ is the depression angle of the main axis and is obtained by mechanically rotating the line array, not electronically steering it

Equation 32 can be represented in terms of the absolute value of the main-lobe half-power beamwidth $2\alpha$ as

$$B(\alpha) = 20 \log \frac{1}{\sqrt{2}} = 20 \log \left[ \frac{\sin \left( \frac{\pi L}{\lambda} \sin \alpha \right)}{\frac{\pi L}{\lambda} \sin \alpha} \right]$$

The above equation is in the form

$$\frac{1}{\sqrt{2}} = \frac{\sin x}{x} \tag{33}$$

where

$$x = \frac{\pi L}{\lambda} \sin \alpha \tag{34}$$

Solving Eq. 33 for $x$ numerically gives $x = 1.39155738$. If this value for $x$ is used in Eq. 34, the beam pattern response function of Eq. 32 can be written as

$$B(\phi) = 20 \log \left[ \frac{\sin \left( \frac{1.39}{\sin \alpha} \sin |\phi - \phi_0| \right)}{\frac{1.39}{\sin \alpha} \sin |\phi - \phi_0|} \right]$$

where

$2\alpha$ is the beamwidth at 3.0103 dB shown on each side of the main lobe

The active sonar equation, Eq. 5, includes the term $H_2$, which is two-way propagation loss from the source to the target and back to the receiver plus signal degradation caused by the transmit and receive beam patterns. It is convenient at the time of interpolating for propagation loss to use $F$ (given by Eq. 31) to interpolate linearly for the angle at the source–receiver. The beam pattern response is obtained by interpolating the input transmit and receive beam patterns (or by calculating the $\sin(x)/x$ response function) using the angle at the source. These beam pattern values are added to two-way propagation loss and the result is called $H_2$. The total transmit and receive beam pattern degradation is $H_0$, which is used in Table 1.

Except for surface-duct propagation loss outputs, the LORA program never displays true two-way propagation loss values; all displayed values contain beam pattern corrections. If the user desires to see uncorrected propagation loss outputs, he should input an omnidirectional beam pattern, that is, zero response for all angles.

## MASKING BACKGROUND

The total masking background level, $M$, may be decomposed into two basic components, total noise level, $L_N$, and total reverberation level, $L_R$. Both noise level and reverberation level are expressed in decibels (re 1 $\mu$bar) and, when added incoherently, yield masking level:

$$M = 10 \log (10^{L_N/10} + 10^{L_R/10})$$

The quantities $L_N$ and $L_R$ are composed of primary sources of noise and reverberation.

### Noise

The total noise level is assumed to include both self-noise and ambient noise. Self-noise, $L$, is primarily composed of electrical receiver noise, other electrical interference, and acoustic noise generated by own-ship motion and machinery. Ambient noise is produced by rain and wind agitating the ocean surface, distant shipping, and biological activity. Data for these separate noise components are difficult to obtain; measurements of the equivalent isotropic noise spectrum level, $N_S$, are more readily available.[20,21,22]

Assuming the noise to be isotropic and noise spectrum level to be constant over the receive band, the equivalent total plane-wave noise level in the active band is

$$L_N = N_S - DI + 10 \log (B_{WR}) \text{ (dB)} \tag{35}$$

where

$N_S$ is the noise spectrum level (dB re 1 $\mu$bar in a 1-Hz bandwidth) for the active receiving frequency at the receive array (with self-noise added incoherently)

$DI$ is the directivity index of the receive array

and

$B_{WR}$ is the receive bandwidth (Hz)

The user may enter his own value for directivity index. Otherwise, he has the option of using an approximate expression obtained using horizontal and vertical half-power beamwidths, $\Delta\theta$ and $\Delta\phi$:

$$b(\theta,\phi) = 1, \text{ if } -\frac{1}{2}\Delta\theta \leq \theta \leq \frac{1}{2}\Delta\theta, \text{ and } -\frac{1}{2}\Delta\phi \leq \phi \leq \frac{1}{2}\Delta\phi$$

$$= 0, \text{ otherwise}$$

with

$$DI = 10 \log \left[ \frac{4\pi}{\int_0^{2\pi} \int_{-\frac{\pi}{2}}^{\frac{\pi}{2}} b(\theta,\phi) \sin \phi \, d\phi \, d\theta} \right]$$

$$= 10 \log \left[ \frac{2\pi}{\Delta\theta \sin \left(\frac{\Delta\phi}{2}\right)} \right] \tag{36}$$

where

$DI$ is directivity index, given in Urick*

$b(\theta,\phi)$ is the beam pattern (intensity ratio)

$\theta$ is the azimuthal angle

$\phi$ is the vertical angle

$\Delta\theta$ is the horizontal half-power beamwidth in radians

and

$\Delta\phi$ is the vertical half-power beamwidth in radians

Notice that for omnidirectional transmission in the vertical plane, that is, $\Delta\phi = \pi$, Eq. 36 gives

$$DI = 10 \log \left(\frac{2\pi}{\Delta\theta}\right) \text{(vertical omnidirectionality)}$$

which reduces to zero if the horizontal beamwidth is $2\pi$. With horizontal beamwidth and vertical beamwidth in degrees, the directivity index of Eq. 36 is

$$DI = 10 \log \left[ \frac{360}{\Delta\theta \sin (0.0087266463 \, \Delta\phi)} \right]$$

The directivity index is only used to calculate the bandlevel noise, $L_N$, at the output of the beamformer. Often, in system studies, $L_N$ is known and need not be calculated by using Eq. 35, but instead can be entered directly as a program input.

*Ref. 19, p. 48.

## Reverberation

Acoustic energy generated by the active sonar transmitter propagates through the ocean medium, reflects and reradiates from a target, and propagates back to the sonar receiver. This return energy is the signal. Some of the energy put into the water by the active sonar scatters from the ocean boundaries, the surface and the bottom, and from volume scatterers such as marine organisms, bubbles, and suspended particulate matter. The return energy from scatterers other than the target is called reverberation. Reverberation masks the signal, just as does noise, but differs from noise in its spectral characteristics. Noise has many frequency components over a broadband. Reverberation is narrowband, with the same frequency as the transmit frequency except, perhaps, for a small frequency shift (doppler) due to transmitter motion relative to the environment. This model assumes that the transmitter is stationary relative to the environment and that the doppler correction is made to the signal because of target motion along the range track between the source and the target.

There are three components of reverberation level (all levels given in decibels): surface reverberation level, $L_S$, bottom reverberation level, $L_B$, and volume reverberation level, $L_V$. The total reverberation level, $L_R$, is expressed in terms of these components as

$$L_R = 10 \log (10^{L_S/10} + 10^{L_B/10} + 10^{L_V/10}) \tag{37}$$

For each scattering mechanism, the LORA model uses only backscattering; that is, the propagation path to the scattering center is identical to the path from the scattering center back to the receiver.

The bandwidth of energy returned from scatterers may be broadened due to the dispersive effects of the scattering mechanisms. Also, the surface (wave motion) may cause a slight frequency shift, which is of interest in high-resolution sonars. These effects, however, are not considered here.

Both surface and bottom reverberation are strongly dependent upon grazing angle and boundary roughness. Volume reverberation is mainly characterized by the biological organisms composing the scattering layer. The scattering layer extends in depth to about 2500 feet and is subject to large diurnal fluctuations.

Regardless of the scattering mechanism encountered, unwanted energy returned to the source is strongly affected by the acoustic propagation paths. Both surface reverberation and volume reverberation can include direct, surface-duct, bottom-bounce, and convergence-zone paths. Bottom reverberation can include direct and surface-bounce paths.

The scattering strengths attributed to the various layers of scatterers may be represented approximately by a single number, the scattering strength integrated over

the water column, that is, the column scattering strength. Such an approximate representation allows the volume element of scatterers to be replaced by an effective scattering "area." This concept is consistent with most active sonar systems operating in deep waters, since most currently operational sonars employ pulse lengths exceeding 100 $\mu$'s. Pulse lengths of this order correspond to resolution lengths on the order of 2500 feet. Consequently, ensonification of the entire scattering column is usually ensured.

A general expression for reverberation level from one scattering source may be written in the form

$$L_k = L_0 + B_X(\phi_X) + B_R(\phi_X) - 2H_k + S_k(\phi_k) + 10 \log (A_k/A_0) \text{ in dB} \qquad (38)$$

where

$L_0$ is the source level

$B_X$ is the transmit beam pattern response

$B_R$ is the receive beam pattern response

$\phi_X$ is the ray angle at the transmitter (and also at the receiver)

$H_k$ is the one-way propagation loss for a ray propagating between the transmitter and $k$th scattering element

$S_k$ is the backscattering strength of the $k$th scattering element and is 10 log of the ratio of intensity in the direction of backscatter at 1 yard from the center of a scattering element of area $A_0$ to the intensity of a plane wave incident to the element with angle $\phi_k$

$A_k$ is the effective scattering area of the $k$th scattering surface or the cross-sectional areas associated with column volume scattering

and

$A_0$ is a reference area which has the same spatial units as the element producing $S_k$; $A_0$ is 1 yd$^2$ in the LORA model

Watson and McGirr[1] describe a technique for approximating the effective total scattering areas for the surface and bottom backscatterers as well as the equivalent scattering area for the backscattering water column. Table 3 summarizes these approximations. If the units of the scattering areas in Table 3 are adjusted to square yards, then the scattering areas are numerically equal to $A_k/A_0$ of Eq. 38. The parameters in the expressions for scattering area are: $C_S$, $C_B$, and $C_V$, sound speeds at the ocean surface, ocean bottom, and center of the volume scattering column; $\phi_S$, $\phi_B$, and $\phi_V$, angles down from the horizontal for rays incident at the surface, bottom and volume scatterers; $\tau$, pulse length; $R$, horizontal range; $\Delta\theta$, horizontal beamwidth.

Table 3. Approximations for effective scattering areas for surface, bottom, and volume backscatters.

| Reverberation Source | Scattering Strength | Scattering Area |
|---|---|---|
| Surface | $S_S$ | $(1/2C_S\tau)R\Delta\theta/\cos\phi_S$ |
| Bottom | $S_B$ | $(1/2C_B\tau)R\Delta\theta/\cos\phi_B$ |
| Volume | $S_V$ | $(1/2C_V\tau)R\Delta\theta/\cos\phi_V$ |

**Surface Backscattering Strength.** For surface backscattering strength, $S_S$, the LORA model uses the Chapman–Harris expressions for diffuse backscattering,[23] merged with Eckart's high-angle expression for facet reflection from the ocean surface,[24,25] and interpolated values representing Richter's data[26] for low grazing angles. The empirical Chapman–Harris expressions apply for grazing angles from 10–20 degrees to 40–60 degrees, depending on wind speed. The Chapman–Harris expressions for backscattering strength, $S_{CH}$, are

$$\left.\begin{aligned} S_{CH} &= 3.3\,\beta \log(\phi_S/30) - 42.1 \log\beta + 2.6 \\ \beta &= 41.6\,(V_W\, f^{1/3})^{-0.58} \end{aligned}\right\} \tag{39}$$

where

$\phi_S$ is the grazing angle in degrees at the surface

$V_W$ is the wind speed in knots

and

$f$ is the frequency in kHz

Eckart[24] derived theoretical equations for surface backscattering strength for sound impinging on the ocean surface at angles steep enough to preclude self-shadowing at the surface. His general expression requires knowledge of the spatial spectrum of the surface waves: the ocean surface must be described by two components of the surface wave-number vector, depending on the direction and wavelength of the sinusoidal components of the surface waves. With the simplification that the wavelength of the incident sound is much shorter than the ocean surface wavelengths reflecting the sound, the following expressions describe surface backscattering strength:

$$S_E = -10 \log(8\pi\alpha^2) - 2.17\,\alpha^{-2}\cot^2\phi_S \tag{40}$$

where

$$\alpha^2 = 0.003 + 0.00294\,V_W \text{ (mean-square waveslope)} \tag{41}$$

$\phi_S$ is the grazing angle (off the horizontal) at the surface

and

$V_W$ is the wind speed in knots

Chapman and Scott[25] reported data for high angles of incidence and recommended the use of Eckart's theory, which they expressed in the form of Eq. 40. They also recommended the Cox and Munk[27] empirical expression for random-direction mean-square waveslope given by Eq. 41, modified for units. Incidentally, Cox and Munk also give with-the-wind ($\alpha_W^2$) and crosswind ($\alpha_C^2$) mean-square waveslopes of

$$\alpha_W^2 = 0.00316\, W$$

and

$$\alpha_C^2 = 0.003 + 0.00192\, W$$

where

$W$ is wind speed in m/s

The LORA model does not consider wind direction, but may in the future if a satisfactory low-grazing-angle theory supported by data over the full active sonar frequency range becomes available.

Gardner[28] finds significant backscattering at low grazing angles at the ocean surface for 5-kHz sound. His reported data and theoretical derivation, which uses diffuse backscattering from a self-shadowing surface, indicate that the surface backscattering strengths should be 20 to 40 dB higher, for grazing angles less than 10 degrees, than those predicted by the Chapman-Harris expressions, Eq. 39. Almost every investigator in the field who noticed the high backscattering strengths at low grazing angles attributed the effect to near-surface volume scatterers such as biological organisms or resonating air bubbles. Gardner's work shows the theoretical possibility of high backscattering strengths at low grazing angles. Unfortunately he validates his predictions at only one frequency, 5 kHz. His reported backscattering strengths are 12 dB higher than Richter's data[26] at the same frequency. Richter's data spans the frequencies 0.8–12.8 kHz and the grazing angles 2–38 degrees. Richter interpreted his high backscattering strengths at low grazing angles to be caused by near-surface volume scatterers. The trends in his data at the various frequencies would seem to support his view. Since Richter's data spans the frequencies, grazing angles, and wind speeds of interest, and since Richter's data indicates substantially higher values than those predicted by Eq. 39 for low grazing angles, Richter's data will be used for a lower limit on surface backscattering strength for grazing angles of 0–20 degrees. This choice is a compromise in Gardner's direction, for he says the low-angle backscattering strengths are even higher. Since Richter did not summarize his data as some

function of wind speed, frequency, and grazing angle, a reduced data set based on his reported data set will be interpolated. The reduced data set is given in Table 4. In the LORA computer program the data is linearly interpolated, with the appropriate end value used as the default value if any of the parameters of wind speed, frequency, or grazing angle is out of range.

Table 4. Reduced Richter data[26] for surface backscattering strength.

| Geometric Frequency (kHz) | Wind Speed 5 knots | | | Wind Speed 20 knots | | |
|---|---|---|---|---|---|---|
| | Grazing Angle, deg | | | Grazing Angle, deg | | |
| | 6 | 15 | 38 | 6 | 15 | 38 |
| 1.15 | -57 | -57 | -46 | -57 | -48 | -39 |
| 2.3 | -58 | -63 | -45 | -58 | -50 | -39 |
| 4.5 | -52 | -57 | -51 | -52 | -45 | -42 |
| 9.0 | -48 | -55 | -51 | -48 | -46 | -30 |

The model for surface backscattering strength is a combination of the Richter data, the Chapman–Harris expressions, and the Chapman–Scott expressions. Surface backscattering strength is calculated by each method for the grazing angle of interest, and the maximum value is retained. The results for some selected frequencies and wind speeds are shown in Fig. 13.

**Bottom Scattering Strength.** The expression for backscattering from the bottom includes a term for diffuse scattering at small angles, in accordance with Lambert's law. This term was derived by Mackenzie[29] and merged by Watson[30] with a large-angle facet reflection term based on Schmidt's data from the Norwegian Sea.[31] The resulting expression for scattering strength in decibels for 1 $yd^2$ of bottom measured at 1 yard in the direction of backscattering is

$$S_B = 10 \log [\mu_B \sin^2 \phi_B + \exp (-100 \cot^2 \phi_B)] \tag{42}$$

where

$\mu_B \equiv 10^{U_B/10}$, and is the bottom backscattering coefficient

$U_B$ is the bottom backscattering coefficient in dB

and

$\phi_B$ is the grazing angle at the bottom

Figure 14 shows Lambert's law scattering for $U_B = -27$ dB, facet reflection for the Norwegian Sea, and the merging of the two curves resulting in Eq. 42.

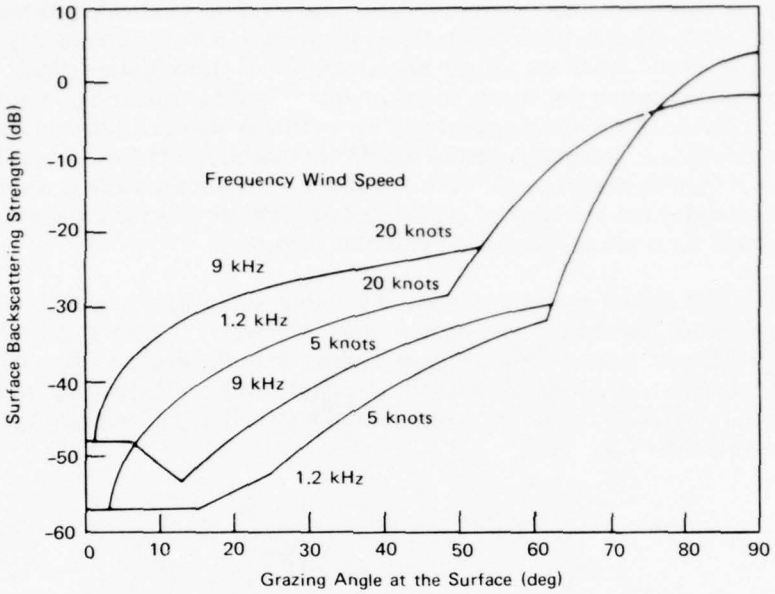


Figure 13. Surface backscattering strength.

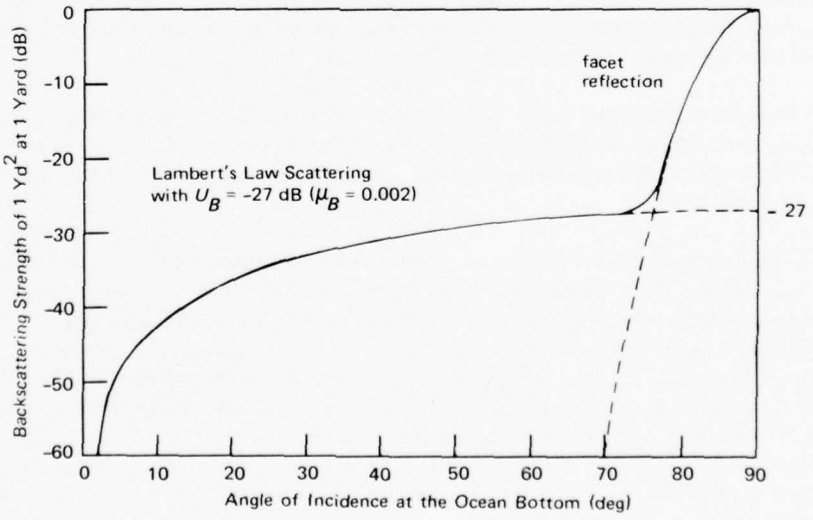


Figure 14. Bottom backscattering strength.

**Volume Backscattering Strength.** The primary mechanism responsible for volume reverberation consists of migrating biological scatterers extending from the surface to depths of about 2500 feet. Often these scatterers occur in identifiable layers which exhibit a diurnal vertical migration. The scattering strengths of these layers depend on geographic location and season as well as time of day. Groups of scatterers have been known to collect and then disperse within a few minutes, giving rise to transient scattering strengths of significant magnitude.[32] Consequently, measurements of volume scattering strength as a function of depth, while providing a means of studying the behavior of migrating scatterers, do not yield values considered stable enough for most performance prediction efforts.

The LORA model uses the concept of backscattering from a water column containing uniformly distributed volume scatterers. The water column is defined as a column with 1 $yd^2$ cross-sectional area extending from the ocean surface to the bottom of the deepest scattering layer. If the backscattering coefficient, $\mu_V$, for 1 $yd^3$ is known as a function of depth, then the column backscattering strength, $S_V$, can be obtained by integrating

$$S_V = 10 \log \left( \int_0^{Z_C} 10^{\mu_V(z)/10} \frac{dz}{3} \right)$$

where

$Z_C$ is the depth of the deepest scattering layer in feet

The user must supply the value for $S_V$ for input to the LORA computer program. He must find data either for column strength or for depth-dependent volume scattering strength and perform his own numerical integration. Comprehensive discussions of column strength can be found in Ref. 33 and 34.

**Reverberation Ray Paths.** Rays are traced from the source depth to bottom, surface, and volume backscatterers. Many different classes of ray paths are defined. Ray paths within the same class can be interpolated; rays in different classes cannot be interpolated.

Figure 15 shows 17 classes of ray paths which may contribute to the reverberation level at the time the echo returns to the receiver from a target in Zone 1 (this is the approximate region where there exists some ray path to the target which has not completed a cycle). All of the paths in Fig. 15 are specular. Also, the direction of backscattering is along the path of the incident ray. Paths 4 and 5 in Fig. 15 appear to be redundant but are not. Path 4, if continued, would strike the bottom, like Path 7. Path 5, if continued, would not strike the bottom, like Path 9. The surface–bottom–surface path which terminates at a bottom backscatterer is not included because it contributes less to reverberation level than Path 3, which itself usually makes a negligible contribution to the reverberation level in a deep ocean.

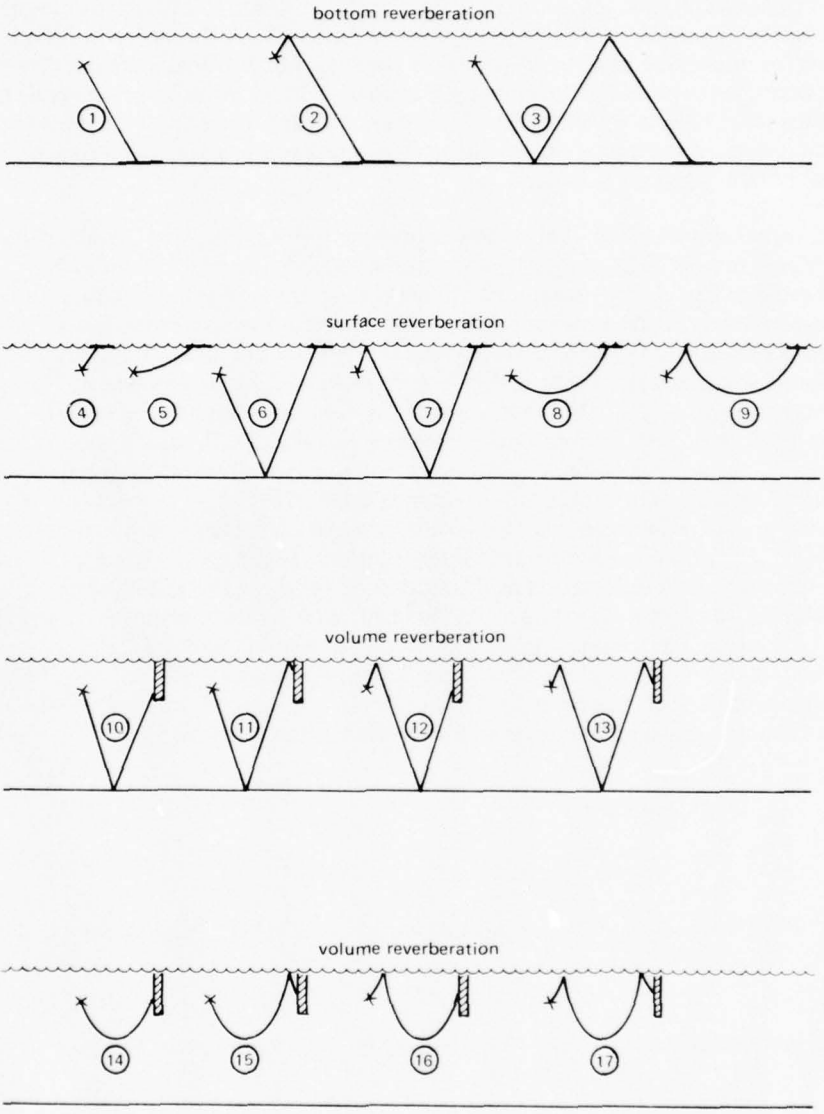


Figure 15. Reverberation paths for first-zone backscatterers.

Long-range reverberation paths are shown in Fig. 16. One to four cycles are added to Paths 8, 9, 14, 15, 16, and 17 of Fig. 15 in order to obtain multizone reverberation (Zones 2 through 5). Only those paths which do not strike the bottom are used for multizone reverberation, since the high bottom loss associated with active sonar frequencies reduces multiple-bottom-bounce reverberation levels to insignificance. Shallow-water studies, however, warrant using contributions to reverberation from multi-bottom-bounce paths. The appropriate paths can be incorporated into the LORA program if needed.

Reverberation level is obtained by summing the contributions from all backscatterers. There are 41 different classes of reverberation paths, 17 shown in Fig. 15 and 24 indicated in Fig. 16. A maximum of 40 rays are traced for each path, and corresponding two-way travel times are calculated. Propagation loss is computed for each ray, and transmit and receive beam pattern corrections are added to the loss. The appropriate backscattering area in Table 3 is calculated, as well as one of the appropriate scattering strengths: bottom, surface, or volume. These values and the source level are used in Eq. 38 to obtain reverberation in dB re 1 $\mu$B, which theoretically is measured at the output of the beamformer. These reverberation levels and their corresponding times are stored in two-dimensional arrays of 41 ray classes, with 40 rays in each class. Minimum and maximum times of each group of 40 rays are stored for later examination to determine if interpolation is appropriate for a given two-way travel time from source to target as a function of range. If the minimum and maximum times bracket the target echo time, the array of reverberation values is interpolated. If a reverberation array is multivalued in time, the array is interpolated for each instance in which reverberation time crosses the target echo time. All reverberation components contributing power to the receiver at the time of the target echo return are added incoherently (the phases of the levels are random), so that

$$L_k = 10 \log \left( \sum_i 10^{L_{ki}/10} \right) \tag{43}$$

where

$L_k$ is the bottom, surface, or volume reverberation level, depending on the value of $k$ ($k$=1,2,3)

and

$L_{ki}$ are reverberation levels which belong to the various paths shown in Fig. 15 and 16, grouped according to bottom, surface, or volume backscattering mechanism

The $L_k$ are summed by Eq. 37 to give total reverberation.

**Surface and Subsurface Duct Reverberation.** Because predicted propagation losses are suspect when ray tracing is used for relatively shallow ducts, the duct reverberation calculations use propagation losses predicted by the empirical AMOS equations. If a surface duct is present and the source depth is both less than 1000 feet and less than $32\sqrt{Z_l}$ feet, where $Z_l$ is the layer depth in feet, then the AMOS

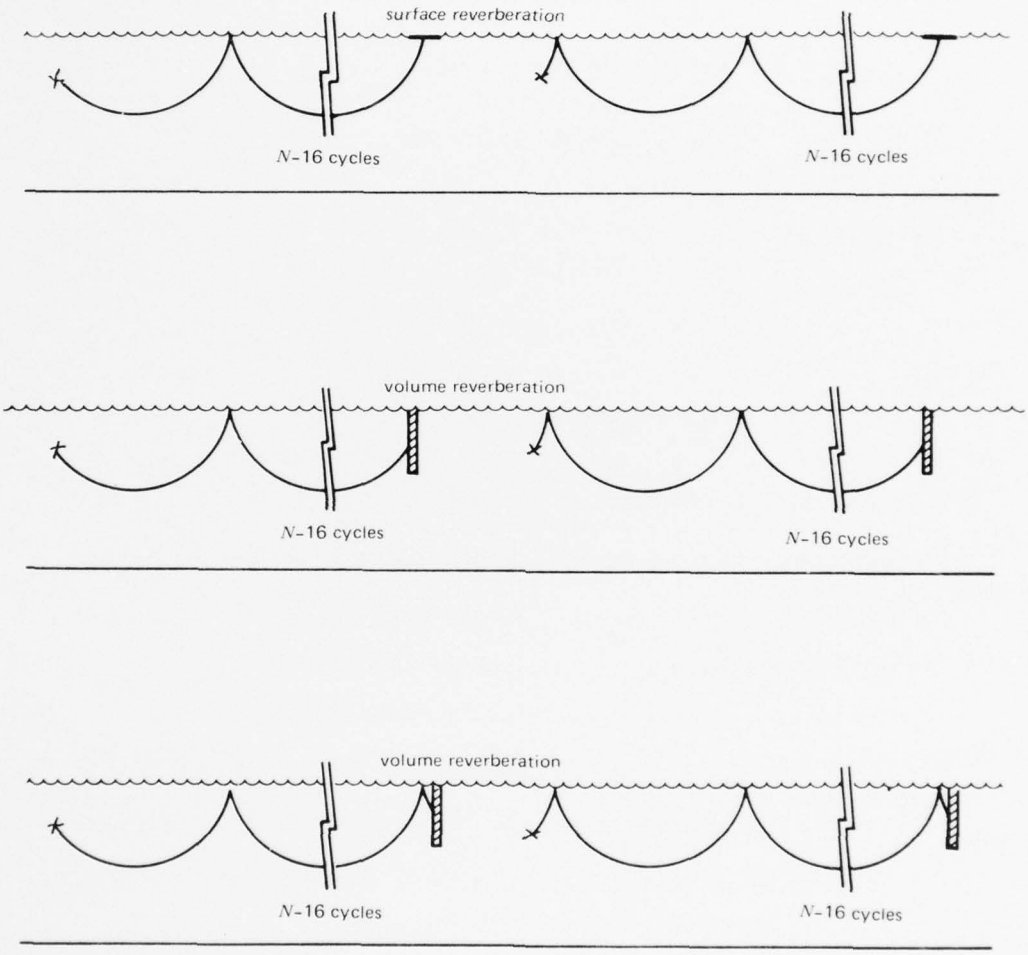


Figure 16. Reverberation paths for *n*th-zone backscatterers.

equations are used. Propagation loss from source to surface is equivalent to propagation loss from source to a target depth of zero. Propagation loss from source to volume backscatterers is obtained by setting target depth to one-half the layer depth.

The reverberation equation, Eq. 38, is applicable for reverberation calculations based on the AMOS equations, with certain assumptions for angles of incidence. The transmit and receive beam pattern responses needed in Eq. 38 are computed by using

$$\phi_X = \frac{1}{2}\,\phi_L, \quad \text{source in the surface duct}$$

$$= \phi_L, \quad \text{source below the surface duct}$$

where

$$\phi_L = \cos^{-1}\frac{C_X}{C_L}$$

and where

$C_X$ is the sound speed at the source

and

$C_L$ is the sound speed maximum in the layer

The surface backscattering strength is computed for the angle at the surface given by

$$\phi_S = \cos^{-1}\left(\frac{C_S}{C_L}\cos\phi_X\right)$$

where

$C_S$ is the surface sound speed

and

$C_X$ and $\phi_X$ are defined above

The surface backscattering area needed in Eq. 38 is easily calculated from Table 3, since all the parameters are known.

The volume scattering strength for a uniform scattering column is functionally related to the depth of the scattering column, $Z_C$, by

$$S_V = U_V + 10\log Z_C$$

where

$U_V$ is a constant containing scattering strength per unit volume and a constant for conversion of units

The assumption that the backscatterers are uniform with depth gives the scattering strength in the duct, with layer depth, $Z_L$:

$$S_{DV} = U_V + 10 \log Z_L , \qquad Z_L < Z_C$$

$$= U_V + 10 \log Z_C , \qquad Z_L \geqslant Z_C$$

Thus, the volume scattering strength of the duct is related to the scattering strength of the column, $S_V$, by

$$S_{DV} = S_V + 10 \log (Z_L/Z_C), \quad Z_L < Z_C$$

$$= S_V , \qquad Z_L \geqslant Z_C$$

$S_V$ is input parameter, and $S_{DV}$ is automatically calculated in the program. The scattering area associated with the backscattering column in the duct is easily computed from Table 3.

Subsurface ducts provide only volume reverberation and only if the source is located within the boundaries of the duct. The columnar volume backscattering strength for the subsurface duct is

$$S_{SDV} = S_V + 10 \log (Z_W/Z_C)$$

where

$Z_W$ is the width of the duct or the portion that overlaps the scattering column whose maximum depth is $Z_C$

**Multiple-Ping Reverberation**. Reverberation level is a function of time and is the incoherent sum of squared pressure levels produced by all of the backscattering mechanisms described above. If a sonar system broadcasts more than one ping, later pings will have their target echo signals masked by the additional incoherent reverberation levels of earlier pings. The LORA program allows the user to specify total number of pings, $N_P$, and the time between pings, $T_P$. To the reverberation level at time $T$, the two-way time from source to target, are added (incoherently, according to the form of Eq. 43) the reverberation levels at times $T + T_P$, $T + 2T_P$, . . . , $T + (N_P-1)T_P$. These reverberation levels are obtained by interpolating all members of the stored reverberation table which have starting and ending times bracketing the extended time of an earlier ping. The user can specify one to nine pings, with single-ping reverberation as the default option.

**Doppler Gain.** In many active sonar tactical situations, target doppler can be the determining factor in target detectability. Doppler gain is the increase of signal-to-reverberation ratio caused by the shifting of the target echo frequency band away from the reverberation frequency band. Doppler gain occurs when the target has a velocity component relative to the ocean along the range track between the target and the transmitter–receiver. A doppler shift in frequency, $\Delta f$, occurs between the target echo and reverberation center frequencies. If the receiver is tuned to the target return frequency, $f + \Delta f$, then the reverberation level is reduced in the doppler receive band as compared to the reverberation level in the receive band if no shift had occurred. It is difficult to obtain an accurate estimate of doppler reduction of reverberation, since pulse shape (in the frequency domain), target and reverberation echo distributions, and sonar operator skill in finding the proper receive frequency and bandwidth are not model inputs. However, some assumptions are possible which can give a rough but tidy model for estimating doppler gain.

The first assumption is that if the source emits a tone pulse at frequency $f$, then the return intensities from backscatterers or target are gaussian distributed. The second assumption is that all distributions have the same standard deviation equal to one-half the receive frequency bandwidth, $B_{WR}$. Thus, it is assumed that the sonar operator can match the bandwidth of the target echo. The third assumption is that the sonar operator can set the receive frequency precisely at $f + \Delta f$, the doppler-shifted target-echo frequency. The fourth assumption is that all significant energy to be used for target detection falls in the new band, $f + \Delta f \pm 1/2\, B_{WR}$.

Figure 17 shows the assumed standardized normal distributions for the target-echo intensity and reverberation intensity. Since all energy for detection is in the bandwidth $B_{WR}$, only the shaded area under the reverberation distribution curve within that band will mask the signal. It must be noted that since each of the distributions is normalized, the actual intensity distributions are obtained by a multiplicative constant or an additive level in decibels. The difference in area of the two curves in Fig. 17 is used to determine a bias in decibels which is subtracted from the reverberation level, either from the separate reverberation components of Eq. 37 or from the total reverberation level.

The standardized normal distribution is

$$\Phi(x) = \frac{1}{\sqrt{2\pi}} \int_{-\infty}^{x} \exp\left(\frac{-y^2}{2}\right) dy \tag{44}$$

where

$x$ is in units of one standard deviation

The area under the target return curve within the receive band, $B_{WR}$, is

$$A_T = \Phi(1) - \Phi(-1) = 0.68$$

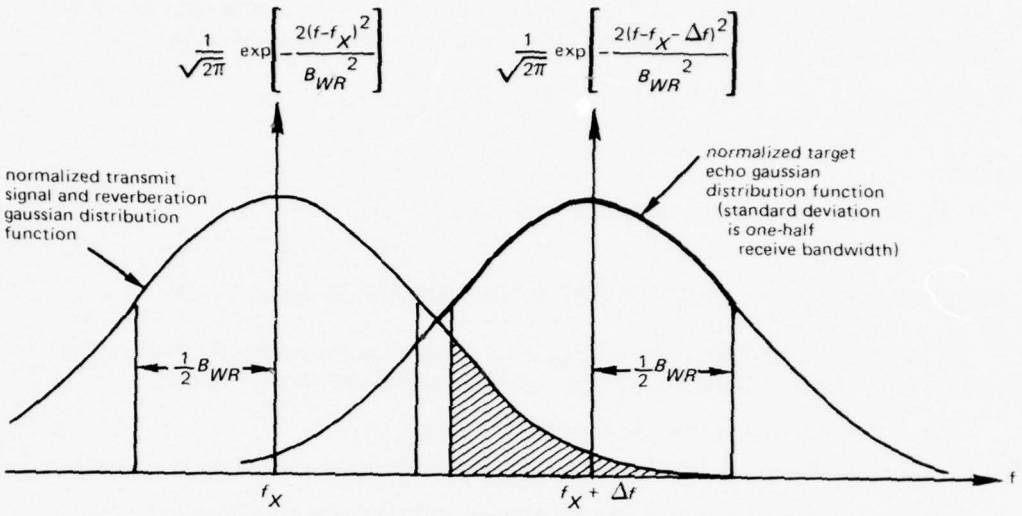


Figure 17. Fraction of the doppler-shifted reverberation in the receive band (ratio of shaded area to area under heavy line).

The area under the normalized reverberation intensity distribution within the band $B_{WR}$ centered on $f + \Delta f$ is

$$A_R = \Phi[(\Delta f + 0.5\, B_{WR})/0.5\, B_{WR}] - \Phi[(\Delta f - 0.5\, B_{WR})/0.5\, B_{WR}]$$

$$= \Phi(2\Delta f/B_{WR} + 1) - \Phi(2\Delta f/B_{WR} - 1)$$

The doppler gain is $G_D = 10 \log (A_T/A_R)$ or

$$G_D = 10 \log \left( \frac{0.68}{\Phi(2\Delta f/B_{WR} + 1) - \Phi(2\Delta f/B_{WR} - 1)} \right)$$

where

$\Delta f = 0.7 V_C f$ Hz[12]

$V_C$ is target velocity component (along the range track between the source and the target and relative to the ocean as the frame of reference)

and

$f$ is the transmitter frequency in kHz

The total reverberation level, $L_R$, from stationary boundary and volume backscatterers is corrected for the doppler shift away from the receive band by

$$L'_R = L_R - G_D$$

where

$L'_R$ is the corrected reverberation level

## SIGNAL PROCESSING MODELS FOR PROBABILITY OF DETECTION

The LORA model contains five optional models for predicting the probability of detection of a signal masked by white gaussian noise and reverberation:

1. Linear correlator and a known receive signal.
2. Linear correlator and a constant-amplitude, phase-distorted receive signal.
3. Quadrature correlator and a constant-amplitude, phase-distorted receive signal.
4. Quadrature correlator and a random-amplitude, random-phase-distorted receive signal (Rayleigh channel).
5. Threshold detector for total energy in the receive band and a random-phase, gaussian-amplitude receive signal.

The first four signal processing models are presented by Schumacher and Teeter.[35] L. K. Arndt of NUC made modifications to those models to replace the time-bandwidth products with a functional dependence on recognition differential. The fifth signal processing model is presented by Watson and McGirr.[1] All five models will be presented after the following sections, which describe the probability of false alarm and the modification to recognition differential to account for reverberation-limited masking noise and signal-clipping losses.

### Probability of False Alarm

The probability of false alarm, $P_{fa}$, is the probability that some threshold is exceeded in some resolution cell of a sonar plan position indicator (or some equivalent display) so that an operator is convinced that a target is present when it is not. Since $P_{fa}$ applies only to one resolution cell, the total probability of false alarm for the indicator is given by

$$P_{FA} = 1 - (1-P_{fa})^N \tag{45}$$

where

$N$ is the total number of resolution cells in the display

If the display is divided into 1-degree sectors and 20 range bins, a 360-degree indicator would have 7200 resolution cells. Thus, in practice $P_{fa}$ assumes a small magnitude, with typical values ranging between $10^{-2}$ and $10^{-12}$. Usually $P_{fa}$ falls in between $10^{-4}$ and $10^{-6}$ (L. K. Arndt, discussion). The model input is $P_{fa}$ and not $P_{FA}$. In the sonar setting, the operator can change his $P_{fa}$ by increasing or decreasing the gain on the indicator. Certain subjective influences on the operator, such as a requirement that no false alarms be reported, can produce wide variance in estimates of $P_{fa}$. However, the probability-of-detection models are relatively insensitive to $P_{fa}$. In all the detection models presented here, the probability of detection is much more sensitive to the recognition differential.

### Recognition Differential

**The Case of Reverberation-Limited Masking Background.** The recognition differential is the ratio in decibels of the signal level to the masking level required for a 0.5 probability of detection. The recognition differential is a psychoacoustic function of the sonar operator's mental outlook and the characteristics of the masking noise. At the same false alarm rate, operators will tend to detect a signal less often in a reverberation-limited background than in an ambient-noise-limited background. The performance of the linear correlator has been investigated for the presence of a known signal in gaussian white noise and in reverberation-limited noise.[36,37] The results indicate that reverberation-limited noise increases the recognition differential 2 dB over an ambient-noise-limited background for both *CW* and *FM* transmit signals. Arndt has produced an expression to give a smooth transition for the correction term $\Delta_r$ to be added to the recognition differential (see Fig. 18):

$$\Delta_r = 2 - 2\,\mathrm{erfc}\left(\frac{R_{NR}}{3}\right) \tag{46}$$

where

$$\mathrm{erfc}(x) = \frac{1}{\sqrt{2\pi}} \int_x^{\infty} \exp\left(\frac{-y^2}{2}\right) dy \tag{47}$$

and

$R_{NR}$ is the ratio of reverberation to ambient noise in dB

The input recognition differential supplied by the user of the computer program is the recognition differential for the ambient-noise-limited performance model.

**Clipping Correction for Recognition Differential.** For multielement receiving arrays, signal digitization can produce effective loss, since the discrete time sampling and nonlinear quantization of the signal level produce a nonoptimum signal at the replica correlator as compared to a signal received by an analog linear receiver. For the assumption of a very low signal-to-noise ratio, Horton[37] and Schultheiss[38] have

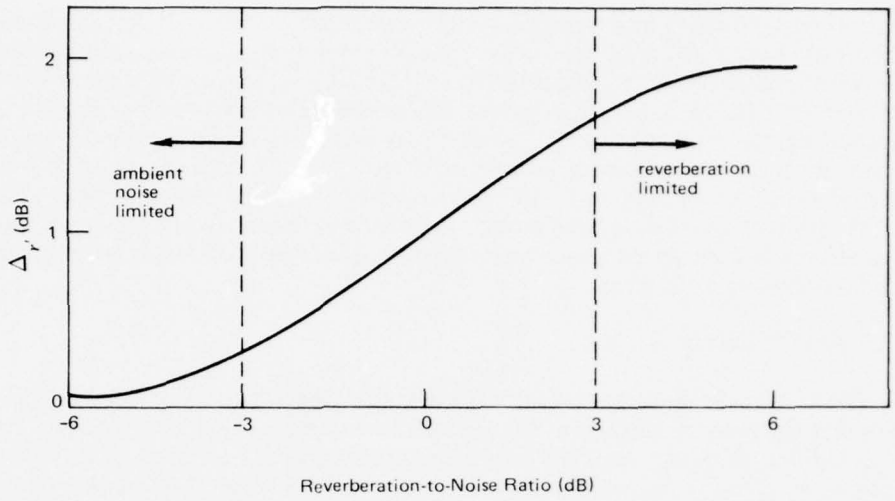


Figure 18. Correction curve for recognition differential, showing the transition from a noise-limited to a reverberation-limited situation (L. K. Arndt, discussion).

determined upper bounds on clipping loss for a replica correlator. Horton specifies clipping loss as a 2-dB response deterioration or as a 1-dB signal-to-noise loss. Experimental results by Teeter[36] for pulsed *CW* and linear *FM* signals indicate the following clipping losses to be subtracted from the signal level:

Clipping Loss, Ambient-Noise-Limited: 2 dB

Clipping Loss, Reverberation-Limited: 1 dB

Instead of the correction being applied to the signal level, it is here applied to the recognition differential. Arndt's smooth transition curve (see Fig. 19) can be used to obtain the correction term, which is

$$\Delta_c = 1 + \operatorname{erfc}\left(\frac{R_{NR}}{3}\right) \quad \text{for clipping} \tag{48}$$

$$= 0 \qquad \text{for no clipping}$$

where

$R_{NR}$ is the ratio of reverberation to noise in dB

and

erfc($x$) is defined by Eq. 47

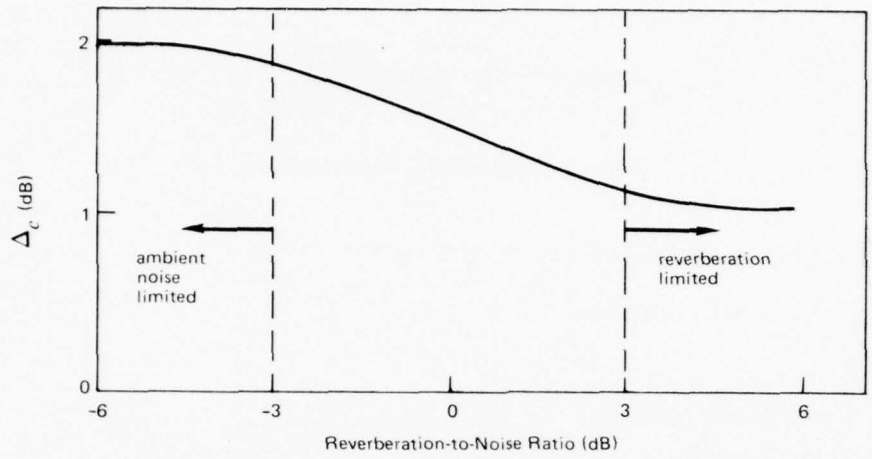


Figure 19. Clipping loss in the presence of reverberation.

**The Corrected Recognition Differential.** The corrected recognition differential, $R_{DC}$, is obtained by combining Eq. 46 and 48:

$$R_{DC} = R_D + \Delta_R + \Delta_C$$

$$R_{DC} = R_D + 2 - 2\,\mathrm{erfc}\left(\frac{R_{NR}}{3}\right), \quad \text{no clipping} \tag{49}$$

$$= R_D + 3 - \mathrm{erfc}\left(\frac{R_{NR}}{3}\right), \quad \text{clipping}$$

## Probability of Detection

The following discussion will deal with several models for probability of detection for various assumptions of signal degradation.

**Model 1 – Performance of the Linear Correlator With a Known Signal in White Gaussian Noise.**[35] The linear correlator (Fig. 20) is (by the maximum-likelihood and minimum-mean-squared-error criteria) the optimum receiver structure for the detection of a completely known signal in the presence of additive white Gaussian noise, $n(t)$.[39] The received signal, $s_R(t)$, is at worst an attenuated, phase-shifted version of the transmitted signal, $s_X(t)$:

$$s_R(t) = kA(t)\sin[\omega t + \phi(t) + \theta], \; 0 \leq t \leq T$$

$$= 0, \text{ otherwise}$$

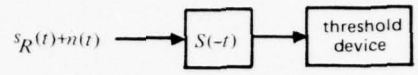


Figure 20. Linear correlator matched filter.

$$s_X(t) = A(t)\sin[\omega t + \phi(t)],\ 0 \leqslant t \leqslant T$$

$$= 0,\ \text{otherwise}$$

where

$k$ is an arbitrary constant

$A(t)$ is the amplitude

$\omega$ is the transmit frequency $\div 2\pi$

$\phi(t)$ is the phase

$\theta$ is an arbitrary constant

and

$T$ is the signal duration

The receiver is matched to $s_X(t)$. This is equivalent to the unlikely situation (especially for echo ranging) where the propagation channel does not distort the signal in amplitude or phase.

The performance of the linear correlator under optimum conditions is[39]

$$P_D = \text{erfc}\,(x-d) \tag{50}$$

where

$P_D$ is the probability of detection

$x$ is the threshold corresponding to a given false alarm rate, $P_{fa}$

and

$d$ is the output signal-to-noise ratio given by

$$d = \frac{2\mathcal{E}}{n_0} = \frac{2ET}{n_0} = \left[2\,TB_{WR}\,(10^{L_{SN}/10})\right]^{1/2}$$

where

$$\mathcal{E} = \int_0^T s_R^2(t)\,dt = ET$$

$E$ is the mean-squared received signal power

$T$ is the signal length

$n_0$ is the mean-squared input noise power in a 1-Hz bandwidth

$L_{SN}$ is the input signal-to-noise ratio in dB

and

$B_{WR}$ is the receiver bandwidth in Hz

A new term, the processing gain, $g_P$, is defined here as

$$g_P \equiv 2\,T\,B_{WR} \tag{51}$$

Then Eq. 50 becomes

$$P_D = \text{erfc}\,[x - (g_P\ 10^{L_{SN}/10})^{1/2}] \tag{52}$$

The probability of false alarm, $P_{fa}$, is the probability that the threshold $x$ is exceeded when there is no signal energy, so

$$P_D = P_{fa} = \text{erfc}\,(x) \tag{53}$$

Thus, given $P_{fa}$, the threshold can be determined by inverting Eq. 53. In the computer program, inversion is done by interpolating tabulated values.

The recognition differential is defined as the value of signal-to-noise ratio where $P_D = 0.5$ for a given $P_{fa}$. Thus, using Eq. 52

$$0.5 = \text{erfc}\,(x - g_P\ 10^{R_D/10})$$

Since

$$\text{erfc}\,(0) = 0.5$$

then

$$x - (g_P\ 10^{R_D/10})^{1/2} = 0$$

with the result

$$g_P = \frac{x^2}{10^{R_D/10}} \tag{54}$$

Using Eq. 52 and 54

$$P_D = \text{erfc}\,[x(1 - 10^{(L_{SR} - R_D)/20})]$$

where

$x$ is obtained by inverting Eq. 53.

This signal processing model is included because it provides an upper bound on signal processor performance. The reverberation-limited case is realized by substituting $R_{DC}$ for $R_D$.

**Model 2 – Performance of the Linear Correlator With a Constant-Amplitude, Phase-Distorted Signal in White Gaussian Noise.** The assumption is made here that the medium causes phase distortion of the signal, but not amplitude distortion. For the transmit signal

$$s_X(t) = A(t)\sin\{\omega t + \phi(t)\}, \qquad 0 \leqslant t \leqslant T \tag{55}$$

$$= 0, \text{ otherwise}$$

A reasonably severe model of the phase-distorted receive signal is

$$s_R(t) = k \sum_{i=1}^{N} A(t)\sin[\omega t + \phi(t) + \theta_i]\;[u(t-t_i) - u(t-t_{i+1})] \tag{56}$$

where

$$u(t) = 0, \quad t < 0$$

$$= 1, \quad t \geqslant 0$$

$$0 = t_1 < t_2 < \ldots < t_n < t_{n+1} = T$$

and

$\theta_i (i=1,2,\ldots,n)$ are independent samples from a uniform distribution over $[0, 2\pi]$

Schumacher and Teeter[35] have shown that this model is very nearly equivalent to Model 1, with the signal-to-noise ratio degraded by 2 dB. The probability of detection is

$$P_D = \text{erfc}\,[x(1 - 10^{L_{SN}\text{-}R_{DC}\text{-}2})]$$

where

$x$ is the threshold obtained by inverting Eq. 53

$L_{SN}$ is the signal-to-noise ratio in dB

and

$R_{DC}$ is the corrected recognition differential of Eq. 49

**Model 3 – Performance of the Quadrature Correlator With a Constant-Amplitude, Phase-Distorted Signal in White Gaussian Noise.** The quadrature correlator matched filter is the optimum receiver (by the maximum-likelihood criterion) for the detection of a constant-amplitude, uniformly distributed random-phase signal, $s_R(t)$, in gaussian white noise, $n(t)$. The transmit signal is described by Eq. 55, and the receive signal is described by Eq. 56. The quadrature correlator is schematically represented in Fig. 21.

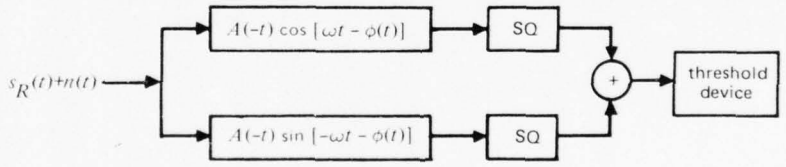


Figure 21. Quadrature correlator matched filter.

The performance of the quadrature correlator under these conditions is[39]

$$P_D = Q(d,x) = \int_x^\infty z \exp\frac{-(z^2 + d^2)}{2} I_0(zd)\,dz \qquad (57)$$

where

$Q$ is known as Marcum's Q Function[40]

$I_0$ is a modified Bessel function of the first kind[40]

$x = \sqrt{-2 \ln P_{fa}}$ is the threshold

and

$$d = \sqrt{2TB_{WR}[10^{L_{SN}/10}]}$$

where

$T$ is the receive signal pulse length

$B_{WR}$ is the receive signal bandwidth

and

$L_{SN}$ is the signal-to-noise ratio in dB

Again, L. K. Arndt has introduced the recognition differential to remove the time-bandwidth product, $TB_{WR}$. Using Eq. 51 and 57

$$P_D = Q[(g_P\ 10^{L_{SN}/10})^{1/2}\ ,\ \sqrt{-2\ln P_{fa}}\ ]$$

By the definition of recognition differential

$$0.5 = Q[(g_P 10^{R_D/10})^{1/2}\ ,\ \sqrt{-2\ln P_{fa}}\ ] \tag{58}$$

Since $R_D$ and $P_{fa}$ are model inputs, $g_P$ can be found by interpolation. The probability of detection is

$$P_D = Q[(g_P 10^{(L_{SN}-R_{DC})/10})\ ,\ \sqrt{-2\ln P_{fa}}\ ]$$

where

$Q$ is defined by Eq. 57

$g_P$ is numerically evaluated using Eq. 58

$L_{SN}$ is the signal-to-noise ratio in dB

$R_{DC}$ is the corrected recognition differential of Eq. 49

and

$P_{fa}$ is the single-resolution-square probability of false alarm

**Model 4 – Performance of the Quadrature Correlator for a Random-Amplitude and Random-Phase-Distorted (Rayleigh Channel) Signal in White Gaussian Noise.** This is the most reasonable of all the models presented for representation of the receive signal in echo ranging. The two-way propagation and target reflection distort

the signal in amplitude and phase. The transmit signal is given by Eq. 55 and the receive signal by

$$s_R(t) = k \sum_{i+1}^{N} a_i A(t) \sin[\omega t + \phi(t) + \theta_i] \; [u(t-t_1) - u(t-t_{i-1})]$$

where

$a_i (i = 1,2,...,N)$ are independent samples from a Rayleigh distribution

and

$\theta_i$, $u(t-t_i)$, and $t_i$ are defined in Eq. 56

The performance of this model is characterized by the probability of detection[39]

$$P_D = P_{fa}^{\left(\frac{1}{1+d^2}\right)} \tag{59}$$

where

$$d^2 = 2\, TB_{WR}\; 10^{L_{SN}/10}$$

Again if Eq. 51 and the definition for $R_D$ are used, $TB_{WR}$ can be eliminated for $R_D$:

$$0.5 = P_{fa}^{\left(\frac{1}{1+g_P\, 10^{R_{DC}/10}}\right)}$$

Thus, the processing gain is

$$g_P = \frac{\log\left(\frac{1}{2P_{fa}}\right)}{\log 2} 10^{-R_{DC}/10}$$

and

$$d^2 = \frac{\log\left(\frac{1}{2P_{fa}}\right)}{\log 2} 10^{(L_{SN}-R_{DC})/10}$$

for use in Eq. 59.

**Model 5 – Random-Phase, Gaussian-Amplitude Signal in White Gaussian Noise.** From the Central Limit Theorem, the distribution of the signal level, $L_{SN}$, tends to be gaussian when it is the sum of independent variables having the same distribution as the others. The signal level in the presence of noise is

$$L_{SN} = S_L - 2H + B_X(\phi_X) + B_R(\phi_R) - M$$

which is assumed to be gaussian, since the source level, $S_L$; one-way propagation loss, $H$; transmit, $B_X$, and receive, $B_R$, response patterns; and masking noise, $M$, are random. The signal excess is

$$S_{EX} = L_{SN} - R_{DC}$$

where

$R_{DC}$ is the recognition differential corrected for the presence of reverberation and for signal clipping, as in Eq. 49

The probability of detection is

$$P_D = \Phi\left(\frac{S_{EX}}{\sigma}\right)$$

*where*

$\sigma$ is the standard deviation of the signal excess in decibels

and

$\Phi$ is the standardized normal distribution function given by Eq. 44

Note that the probability of false alarm plays no part in this model for probability of detection.

## NOTABLE PROGRAM CAPABILITIES

The nominal first-convergence-zone prediction capabilities of NUC models ancestral to LORA have been extended to allow performance predictions for a maximum of five convergence zones and bottom bounces.

Previous NUC active-sonar models apply only to sonars mounted on surface ships. The LORA model allows any source and target depths.

Propagation-loss predictions are useful byproducts of the performance predictions. Active and passive propagation losses may be calculated for a maximum of 30 convergence zones or bottom bounces.

The sound-speed profile is automatically curve-fitted by computer routines designed by C. Bartberger, who used the mathematical techniques of Pedersen and Gordon. Curve-fitting the sound-speed profile reduces false caustics introduced into the propagation loss when the sound-speed profile has discontinuous derivatives.

Multi-ping reverberation is available; that is, reverberation caused by pings preceding the current ping is included in the total reverberation level. Single-ping reverberation is the standard output; multi-ping reverberation for a maximum of nine pings is optional.

If the user wishes, reverberation effects can be reduced because of the doppler motion of the target. The user can enter doppler gain or use the internal calculations to include the doppler effect.

Five optional probability-of-detection models are available, depending on the user's choice of detector characteristics and his assumptions of signal degradation.

The computer program can run nearly without failure. It has been run for thousands of cases. An example of its capability is its processing of 240 sequential data sets in the same program execution; that is, the program read new data 240 times, produced performance predictions, and terminated normally. The total cost for that set of runs was $60 (UNIVAC 1110 computer charges), of which $30 was for paper. The LORA model and supporting computer program can thus give the sonar system designer the ability to compare the performance of active-sonar systems inexpensively.

The LORA program requires 38,000 words of 36-bit core storage.

## RECOMMENDATIONS

Volume reverberation may be estimated more closely by using a scattering strength which varies with depth. The added raytracing would increase program running costs substantially. In addition an algorithm would have to be developed which smooths reverberation peaks due to raytracing caustics. Such an algorithm would depend on propagation mode (that is, direct path, convergence zone, etc.), scattering geometry, beam pattern, and the intuition of the designer of the algorithm.

Nonspecular scattering could also be added to the reverberation model. This is another costly calculation, and the user of the program should be allowed to switch to a cheaper reverberation model if he desires.

The subsurface duct model could be improved. The current model uses cylindrical spreading of sound in the duct. At low wavelength-to-duct-width ratios cylindrical spreading does not apply since some acoustic energy leaks out of the duct. Normal-mode theory can give accurate predictions for propagation loss, but normal-mode models are typically expensive to run. To keep computer costs down a subsurface duct model should be derived which approximates normal-mode theory results. The new model should incorporate such parameters as duct width, source and receiver positions, frequency of the propagating sound, and some indicator for duct strength.

The recognition differential model used here is not representative of some active sonars. A helpful addition to the program would be the ability to enter recognition differential versus signal-to-noise ratio in order to make the program more sensitive to certain active sonars.

## REFERENCES


1. W. H. Watson and R. W. McGirr. "An Active Sonar Performance Prediction Model," NURDC TP 286 (1972).

2. COSMOS, prepared by Ad Hoc Committee on Sonar Model Standards, Naval Ship Systems Command. "Navy Interim Surface Ship Sonar Prediction Model (NISSM) Documentation," (1971).

3. H. W. Marsh, Jr., and M. Schulkin. "Report on the Status of Project AMOS (Acoustic, Meteorological, and Oceanographic Survey) (1 Jan. 1953-31 Dec 1954)," USL Report No. 255A (1967).

4. H. R. Hall and W. H. Watson. Available to qualified requesters.

5. W. H. Thorp. "Analytical Description of the Low-Frequency Attenuation Coefficient," J. Acoust. Soc. Am. 42:270 (1967).

6. M. Schulkin and H. W. Marsh, Jr. "Sound Absorption in Sea Water," J. Acoust. Soc. Am. 34:864–865 (1962).

7. ——. "The Effect of Ocean Scattering on the Propagation of Underwater Sound," J. Underwater Acoust. 10:293-300 (1960).

8. T. Arase. "Some Characteristics of Long Range Explosive Sound Propagation," J. Acoust. Soc. Amer. 31:588-594 (1959).

9. C. S. Clay. "Sound Transmission in a Half-Channel and Surface Duct," Meterology International Incorporated, Project M-153, Technical Note Two 2:1-17 (1968).

10. M. A. Pedersen and D. F. Gordon. Available to qualified requesters.

11. ——. "Normal Mode Theory Applied to Short-Range Propagation in an Underwater Acoustic Surface Duct," J. Acoust. Soc. Amer. 37:105-118 (1965).

12. Department of the Navy. *Physics of Sound in the Sea.* Originally issued as "Summary Technical Report of Division 6," NDRC Volume 8, Washington, D.C. (1946, reprinted in 1969).

13. M. A. Pedersen. "Acoustic Anomalies Introduced by Constant Velocity Gradients," J. Acoust. Soc. Amer. 33:465-474 (1961).

14. M. A. Pedersen and D. F. Gordon. "Comparison of Curvilinear and Linear Profile Approximation in the Calculation of Underwater Sound Intensities by Ray Theory," J. Acoust. Soc. Amer. 41:419-438 (1966).

15. C. L. Bartberger, et al. "The NADC Ray-Tracing Program," NADC-SD-6833 (1968).

16. W. D. Wilson. "Equation for the Speed of Sound in Sea Water," J. Acoust. Soc. Amer. 32:1357 (1960).

17. H. W. Frye. "A Computer Technique for Model Building in the Physical Sciences," NUC TN 54 (1970).

18. R. W. McGirr and J. C. Hall. "FLIRT a Fast Linear Intermediate Range Transmission Loss Model," NUC TN 1282 (1974).

19. R. J. Urick. *Principles of Underwater Sound for Engineers*, McGraw-Hill, New York (1958).

20. V. Knudsen and R. C. Alford. "Survey of Underwater Sound: Report No. 3; Ambient Noise," National Defense Research Committee, Division 6 Report 6.1 – NDRC-1848 (1944).

21. G. W. Wenz. "Acoustic Ambient Noise in the Ocean: Spectra and Sources," J. Acoust. Soc. Amer. 34:1936–1956 (1962).

22. H. R. Hall. Available to qualified requesters.

23. R. P. Chapman and J. R. Harris. "Surface Backscattering Strengths Measured with Explosive Sound Sources," J. Acoust. Soc. Amer. 34:1594–1597 (1962).

24. C. Eckart. "The Scattering of Sound From the Sea Surface," J. Acoust. Soc. Amer. 25:566–570 (1953).

25. R. P. Chapman and H. D. Scott. "Surface Backscattering Strengths Measured Over an Extended Range of Frequencies and Grazing Angles," J. Acoust. Soc. Amer. 36:1735–1737 (ltr) (1964).

26. R. M. Richter. "Measurements of Backscattering From the Sea Surface," J. Acoust. Soc. Amer. 36:864–869 (1964).

27. C. Cox and W. Munk. "Measurement of the Roughness of the Sea Surface From Photographs of the Sun's Glitter," J. Opt. Soc. Amer. 44:838–850 (1954).

28. R. R. Gardner. "Acoustic Backscattering From a Rough Surface at Extremely Low Grazing Angles," J. Acoust. Soc. Am. 53:848–857 (1973).

29. K. V. MacKenzie. "Bottom Reverberation for 530- and 1030-cps Sound in Deep Water," J. Acoust. Soc. Amer. 33:1498–1504 (1961).

30. W. H. Watson. Available to qualified requesters.

31. P. B. Schmidt. "Bottom Reverberation Measurements in the Norwegian Sea and North Atlantic Coast," Informal Report 69-38, Naval Oceanographic Office (1969).

32. P. A. Barakos. "Underwater Reverberation as a Factor in ASW Acoustics," USL Report No. 620 (1964).

33. R. P. Chapman and J. R. Marshall. "Reverberation From Deep Scattering Layers in the Western North Atlantic," J. Acoust. Soc. Amer. 40:405–411 (1966).

34. R. J. Vent. "Acoustic Volume-Scattering Measurements at 3.5, 5.0, and 12.0 kHz in the Eastern Pacific Ocean: Diurnal and Seasonal Variations," J. Acoust. Soc. Amer. 52:373–382 (1972).

35. G. P. Schumacher and J. L. Teeter. "Submarine Echo-Ranging Active Sonar Performance Prediction Model," NUC TN 1308 (1974).

36. J. L. Teeter. Available to qualified requesters.

37. C. W. Horton, Sr. *Signal Processing of Underwater Acoustic Waves,* U.S. Government Printing Office, Washington, D.C. (1969).

38. P. M. Schultheiss. "The Effect of Clipping on the Performance of Replica Correlators," G.D./E.B. Progress Report No. 31 (1967).

39. H. L. Van Trees. *Detection, Estimation, and Modulation Theory, Part 1*, New York: John Wiley and Sons (1968).

40. C. W. Helstrom. *Statistical Theory of Signal Detection*, London: Pergamon Press (1968).

## Appendix A

## LOGICAL STRUCTURE OF THE LORA COMPUTER PROGRAM

The LORA computer program contains three major computational sections: environmental, reverberation, and detection. Figure A-1 shows the computational structure of the LORA program. All inputs are entered through SUBROUTINE READIN. The input parameters are flagged to indicate if they belong to environmental, reverberation, or detection categories. The flag "LOOP" in Fig. A-1 is set in READIN, depending upon which inputs are entered. Table B-1 in Appendix B gives the grouping of the input parameters, environmental, reverberation, or detection. If the user enters only reverberation and detection parameters, the whole environmental section will be skipped automatically, without user specification, eliminating redundant calculations.

OUTP and OUTR in Fig. A-1 are input parameters set by the user if he desires special outputs for propagation loss and reverberation, respectively. The outputs for the detection calculations include summaries of propagation loss and reverberation which are sufficient for active sonar performance prediction work. However, the user may want the optional passive coherent and incoherent propagation loss outputs or the separated components of reverberation – surface, bottom, and volume – as well as the relative contribution to reverberation from previous pings. Use of OUTR and OUTP also allows the user to skip the detection or reverberation calculations if he is interested only in reverberation or propagation loss outputs. If the user does not set OUTP or OUTR, the program sets them to zero, and the detection outputs are the standard outputs.

With successive runs, it may be that environmental parameters are changed which do not influence the sound-speed profile, so that it is unnecessary to curve-fit the profile for every run. The dotted line in Fig. A-1 indicates that the sound-speed profile calculations are considered to be part of the environmental calculations.

The environmental calculations in Fig. A-1 include –

- Searching the sound-speed profile for surface and subsurface ducts and applying the AMOS equations if applicable.
- Curve-fitting the sound-speed profile with continuous-gradient curve segments after the profile has been corrected for earth curvature.

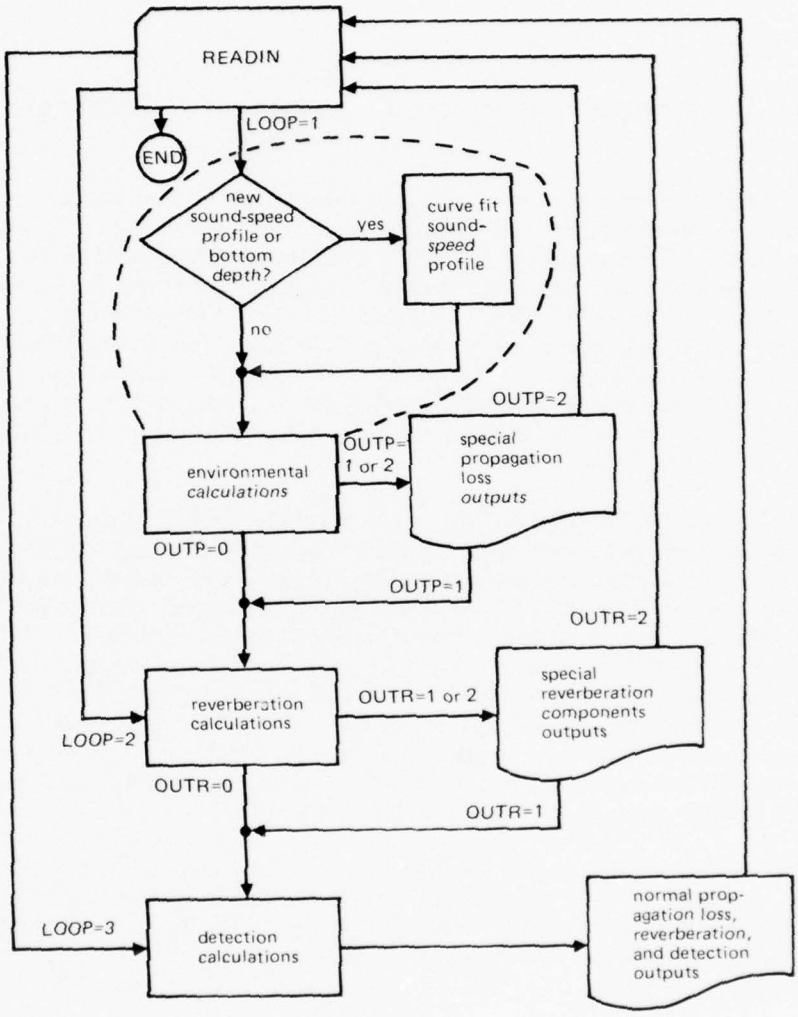


Figure A-1. Logic paths for LORA input-output and calculations.

- Ray tracing to obtain path segments between source and target, source and surface, source and bottom, and source and volume scattering depths.
- Assembling the path segments to obtain a multitude of different paths for the purpose of computing propagation loss and reverberation components.
- Interpolating the ray paths to obtain two-way times and propagation losses corresponding to integer kiloyard steps in horizontal range between source and target.
- Obtaining one-way passive coherent and incoherent propagation losses (optional).

The reverberation section performs the following computations:

- Interpolating arrays of reverberation components (stored during ray path computations) corresponding to the two-way times to the target for integer kiloyard horizontal ranges.
- Grouping (by incoherent summation) the effects of surface, bottom, and volume reverberation.
- Calculating total single-ping reverberation for two-way travel times to the target.
- Calculating total reverberation from time-delayed previous pings.
- Calculating total reverberation from all pings for the current-ping two-way times to the target.

The detection section calculates and prints the following tabular outputs (see the pages in Appendix D labeled "Active Performance Prediction"):

- A heading and a brief statement of the propagation mode.
- A listing of the values of the single-value inputs, with a trailing letter to indicate status.*
- A listing of the values of certain important internally calculated parameters.

---

*The status symbols indicate the following (see p. 95 ff):

U – user has specified this input value on this run.
Blank – set by user on a previous run; unchanged on this run.
T – typical value set in absence of user specification.
C – calculated internally by the program at the user's request.
W – wrong value specified by user. (Out of range of allowable values. The printed value is either a typical or an internally calculated value.)
N – not an input; internally calculated parameter.

and under the following headings:

- RANGE, all integer kiloyard ranges to the target for which the current propagation mode is applicable.
- TIME, corresponding two-way travel times for the rays which give minimum loss to the target.
- LOSS, minimum two-way propagation loss to the target, including beam pattern corrections.
- ANGLE, starting angles for the rays at the source depth which give minimum loss to the target.*
- SIGNAL, signal level of the return signal in the receive band (as measured at the output of the beamformer).
- REVERB, reverberation level before doppler correction (doppler gain "GDOP" is listed with the single-value inputs).
- REV LIM, a "YES" or "NO" to indicate if the masking noise is reverberation limited (that is, doppler-corrected reverberation level exceeds ambient noise level in the receive band by 3 dB).
- S/MN, signal-to-masking-noise ratio in the receive band.
- EXCESS, signal excess.
- PROB DETECT, probability of detection.

*This is useful information for aiming the beam pattern on successive runs. No values for ANGLE are given in the surface-duct or subsurface-duct modes of propagation.

## Appendix B

## INPUTS TO THE LORA COMPUTER PROGRAM

Table B-1 contains a list of the inputs to the LORA computer program. Each input is designated by a name that corresponds to a parameter used in other computer programs at NUC. These names are listed in the column "NUC Names." Modifications to the NUC names were required by users at the Naval Intelligence Support Center (NISC), because their computer word contains four characters rather than six as at NUC. Thus, new and sometimes more mnemonic and acronymistic names were developed. These occur in Table B-1 in the column under "NISC Names." Input parameters identified by either set of parameter names are acceptable to the program without user specification. Output labels, however, are identified by using either of the data literals, "NUC" or "NISC" (see Table B-2) to denote the appropriate set of parameter names. The column under "Description" in Table B-1 contains brief definitions of the input parameters. "Range" is the range of values a given parameter is allowed. Any input value outside this range is either set to a "Typical Value" or calculated in the program.

Table B-2 is the list of data literals used to exert specific control over the program. The user must type these one to a card (line, record).

Not all of the input parameters need to be entered by the user. In fact only one input parameter is required to be entered by the user, the sound-speed profile, "SSP." Typical or calculated values will be produced for every other input parameter that is not entered. Of course the outputs may have little significance to the user who does not exercise his prerogative to enter his own data.

Table B-1. LORA inputs.

ENVIRONMENTAL PARAMETERS

| NUC Name | NISC Name | Description | Units | Range | Typical Value |
|---|---|---|---|---|---|
| OUTP | OUTP | Flag for special output of propagation losses (=0, no special output; =1, print and continue to reverberation calculations; =2, print and go back to read new data) | – | 0 to 2 | 0 |
| ZX | SD | Source depth | ft | 1 to 40,000 | 20 |
| ZTG | TD | Target depth | ft | 1 to 40,000 | 50 |
| FREQ | FREQ | Frequency of transmitter | kHz | 0.099 to 25 | 3.5 |
| LWA | WAVE | Wave height | ft | 0 to 20 | 4 |
| VWI | WIND | Wind speed | knots | 0.1 to 35 | 15 |
| SALT | SALT | Salinity | $^{o}/_{oo}$ | 33 to 37 | 35 |
| HS | SLPB | Signal loss per bounce at the surface | dB | –2 to 10 | 3, calculated if negative |
| ZBM | BD | Bottom depth (if different than the largest depth in the sound-speed profile) | ft | 1 to 40,000 | largest depth in SSP |
| REFLS | NBBB | Maximum number of bottom bounces | – | 1 to 30 | 1 |
| ZONES | ZONE | Maximum number of convergence zones | – | 1 to 30 | 1 |
| PHDX | XDE | Transmit depression–elevation angle of the main axis of the beam pattern | deg | –85 to 85 | 5 |
| PHDR | RDE | Receive depression–elevation angle of the main axis of the beam pattern | deg | –85 to 85 | 5 |
| DELPX | XVBM | Effective vertical beamwidth – transmit | deg | 0.1 to 180 | 10 |
| DELPR | RVBM | Effective vertical beamwidth – receive | deg | 0.1 to 180 | 10, set to 180 if BEAMR is omnidirectional |
| MUB | BSS | Bottom backscattering strength | $dB/yd^2$ | -40 to -5 | -27 |
| MUV | VSS | Volume backscattering strength of the water column | $dB/yd^2$ | –80 to –30 | –49 |
| ZC | SLD | Scattering layer depth (water column depth) | ft | 0 to 10,000 | 2000 |
| LAT | LAT | Latitude | deg | –90 to 90 | 0 |
| DUMP | DUMP | Flag for diagnostic printout (=0, no diagnostic printout; =–1, print ray tracing outputs; =1, print) | | | |
| SSP | SSP | Sound-speed profile – array of alternating depth and sound-speed values or depth and temperature values | ft, ft/sec | 4750 to 5160** | no typical value |
| | | | m, m/sec | 1440 to 1590** | SSP must be input for program to run |
| | | | ft, °F | 30 to 85** | |
| | | | m, °C | 0 to 30** | |
| AHB | BRLP | Bottom reflection loss profile – array of alternating grazing-angle and bottom-reflection-loss values | deg, dB | not checked | zero loss at any grazing angle |

*The input parameter is automatically set to this value in absence of user specification. (Contd)

**This range of values applies only at the ocean surface, that is, the second value in the input array after elements have been ordered with respect to increasing depth.

Table B-1. (Contd)

| NUC Name | NISC Name | Description | Units | Range | Typical Value |
|---|---|---|---|---|---|
| BEAMX | XVRP | Transmit vertical response pattern (i.e., beam-pattern) – array of alternating angle and response values, where response is given as positive dB down from the maximum response, defined as 0 dB at an angle of 0 degrees | deg, dB | not checked | omnidirectional (i.e., 0 dB for all angles); if the array contains one element only, the sin (x)/x response pattern for a continuous line is calculated |
| BEAMR | RVRP | Receive vertical response pattern | Same as for BEAMX | | |
| REVERBERATION PARAMETERS | | | | | |
| OUTR | OUTR | Flag for special output of reverberation values (bottom, surface, and volume components, total contribution from each ping, and overall total reverberation for two-way time to target corresponding to integer ranges in kyd (=0, no special printout; =1, prints and continues to detection section; =2, prints and goes back to read new data) | – | 0 to 2 | 0 |
| MODE | MODE | Flag to indicate sonar operation mode (=1, near-surface or direct path; =2, bottom bounce; =3, convergence zone, surface bounce, or reliable acoustic path) | – | 1 to 3 | 1 |
| SL | SL | Source level | dBre 1$\mu$b | 40 to 160 | 148 |
| DELTH | HBM | Effective horizontal beamwidth | deg | 0 to 360 | 10 |
| MPR | MPR | Number of pings for multi-ping reverberation | – | 1 to 9 | 1 |
| TBP | TBP | Time between pings | sec | 1 to 90 | 20 |
| PULSE | PULS | Pulse length to help determine reverberation backscattering areas | sec | $10^{-4}$ to 5 | 0.1 |
| DETECTION PARAMETERS | | | | | |
| DI | DI | Directivity index (used only to determine the amount of discrimination against isotropic noise due to the directivity of the beam pattern. If NOUT is known, DI need not be input) | dB | 0 to 70 | 0 |
| BWS | BWS | Bandwidth of the return signal | Hz | 1 to 1000 | 100 |
| BWR | BWR | Receiver bandwidth | Hz | 1 to 1000 | BWS |
| NIN | NIN | Omnidirectional noise spectrum level at the receiving-array input | dBre 1$\mu$b | -80 to 0 | -45 |
| NOUT | NOUT | Noise band level at the receiving array output or signal processor input | dBre 1$\mu$b | -105 to 29 | -61.2 |
| TVC | TVC | Target closing velocity (target speed with respect to the ocean along the range track between source and target) – used in estimating doppler gain of signal over reverberation. | knots | -60 to 60 | 0 |

(Contd)

Table B-1. (Contd)

| NUC Name | NISC Name | Description | Units | Range | Typical Value |
|---|---|---|---|---|---|
| GDOP | GDOP | Doppler gain (signal enhancement over reverberation due to shift of reverberation band away from return signal band if target is moving relative to environment) | dB | -2 to 300 | calculated using TVC, negative value results in calculation |
| TGS | TGS | Target strength | dB | 0 to 40 | 15 |
| RDN | RDN | Recognition differential for ambient-noise-limited detection (corrected by program for reverberation-limited detection | dB | -20 to 20 | -2 |
| CLIP | CLIP | Flag to indicate 2-dB clipping of signal at processor (=0, no clipping; =1, clipping) | – | 0 to 1 | 0 |
| SIGMA | SIG | Standard deviation of signal differential to be used with signal processing model given by SP=5 | dB | 0.5 to 16 | 6 |
| PFA | PFA | Probability of false alarm for one resolucell on some display | – | $10^{-12}$ to 0.1 | 0.001 |
| SP | SP | Flag to denote signal processing model<br>=1, linear correlator, known signal;<br>=2, linear correlator, constant signal;<br>=3, quadrature correlator, constant-amplitude signal;<br>=4, quadrature correlator, random-amplitude-and-phase signal<br>=5, energy detector for gaussian signal | – | 1 to 5 | 5 |

Table B-2. Data literals.

| Data Literal | Resulting Control |
|---|---|
| RUN | Calculations are performed for the current values of the input parameters and control is returned to SUBROUTINE READIN for more inputs. |
| XQT | Same as RUN. |
| XEQ | Same as RUN. |
| PAUSE | Same as RUN. |
| END | Program execution is immediately terminated and control is returned to the executive. |
| STOP | Same as END. |
| END-DATA | Same as END. |
| HEADER | Allows the alphanumeric string on the next card to be used for headings on output pages. |
| NUC | Naval Undersea Center input parameter names are used to label the outputs (assumed if "NISC" is not entered by the user). |
| NISC | Naval Intelligence Support Center input parameter names are used to label the outputs. |
| PASY | One-way passive propagation loss, including receiver response pattern and multipath ray summations, is calculated (OUTP=1 or 2 is needed to display the values). |
| PASN | Defeats PASY if it has been entered. |
| COMY | One-way communications propagation loss, including transmit and receive response patterns and multipath ray summation, is calculated (OUTP=1 or 2 is needed to display the values). |
| COMN | Defeats COMY if it has been entered. |
| COHY | Coherent propagation losses are calculated, as well as the incoherent losses, for either the passive or communications options. Semicoherence is also included but not recommended because of the artificiality of the calculations. |
| COHN | Defeats COHY if it has been entered. |
| TTY | Reduces output for demand terminal usage. |
| NOTT | Defeats TTY (assumed if TTY has not been entered); normal outputs and page headings are printed. |

## Appendix C

## INPUT FORMAT

The LORA program accepts all inputs through SUBROUTINE READIN. READIN contains only two read statements. The input characters are scanned in a manner similar to NAMELIST to determine if a string of characters is an input name or an input parameter value (a number). READIN does not use NAMELIST for the following reasons:

- It is important to keep track of the variables which are changed from run to run in order to reduce redundant calculations.
- Column 1 on the input record can now be used.
- Data literals which have no numerical value can be entered.

The user enters single-value variables by typing the name of the variable, followed by a space or an equal sign "=", and then by the numerical value in F, I, E, or D format. All input values are converted to single-precision floating point numbers. There can be no imbedded blanks in either the name or value, although there may be more than one blank separating the name and value. A name and its value must be on the same line. If more than one name–value set occurs on a line, the sets are to be separated by a comma "," or a slash "/". There is no need to use a comma or a slash as a separator between sets occurring on different lines. The parameters can be input in any order or not input at all, as the user desires.

The user enters arrays in a similar fashion to his entering single-value variables, by first typing the name, then a space or equal sign "=", and then the array values in F, I, E, or D format. Successive array values are separated by one or more spaces. If the array is too long for one line, as many lines as are required can be used by typing the continuation symbol "* ", that is, an asterisk and a space, as the first characters on the successive lines. An array is terminated by a comma or a slash or by starting a new line without the continuation symbol.

Data literals are names which are not followed by values. To enter the name is to set a flag or to follow some instructions before reading the next input. When one data literal is read, the line is automatically terminated. Data literals must be entered one to a line and be the last datum on that line. Any other data on the line following the data literal will be ignored.

Figure C-1 illustrates some of the possible ways data may be entered. Column 1 is indicated by the arrow. The line numbers are merely for reference in this discussion. Line 1 in Fig. C-1 shows several examples of separators and spacings and the use and nonuse of the equal sign. Line 2 contains the data literal "PASY," which will cause a flag to be set so that passive propagation losses will be calculated. Line 3 is another data literal, "HEADER," which causes the next card to be read as heading information. Line 5 shows how an array may be entered. A user at a demand terminal may make a mistake. If so, he can reenter the same parameter as on Line 6. The latest entry of any parameter supersedes any value it may have been assigned by previous entries. The user need not specify the number of values in an array; the program automatically counts them. Lines 8-10 illustrate the entering of values in array "AHB," employing continuation cards. On card 11 "TGS=20" follows a data literal, so it is ignored. Thus, TGS=15. On Line 12 PFA is assigned value in E format and on Line 13 in D format. The data literal on Line 12, "RUN," will cause immediate termination of the READIN subroutine, calculations will be performed with the current data set, and control will be returned to READIN to read the new value for PFA on Line 13. The "RUN" on Line 14 will again cause calculations to be performed, this time only in the detection section, since PFA is a detection parameter. Line 15 ends the program with "END," and control is returned to the executive.

```
Col. 1
     ↓
1.   FREQ=1., ZX=20/ZTG  300.,PHDX=5  ,PHDR .5
2    PASY
3    HEADER
4    THIS IS A HEADING
5    SSP=0 5000  100  5001.8 3000
6    SSP  0 5000  100 5001.8  3000 4950   10000 5050
7        AHB  0  5  5.0  8.5  10.  12
8      *  20  13  40  14
9    * 55  15
10         * 90  15
11       TGS=15, COHY, TGS=20
12   PFA=1.E-5,  RUN
13            PFA=1.D-4
14   RUN
15   END
```

Figure C-1. Example of some options in the input format.

A data set equivalent to that represented in Fig. C-1 is shown in Fig. C-2.

```
Col. 1
↓
HEADER
THIS IS A HEADING
FREQ=1 ZX=20, ZTG=300, TGS=15
PFA=.00001, PHDX=5, PHDR=-5
PASY
COHY
SSP=0 5000 100 5001.8 3000 4950 10000 5050
AHB=0 5 5 8.5 10 12 20 13 40 14 55 15 90 15
RUN
PFA=.0001, RUN
END
```

Figure C-2. Rewritten form of the data in Figure C-1.

## Appendix D

## EXAMPLES OF RUNS FOR THE LORA COMPUTER PROGRAM

This Appendix contains examples of inputs and resulting outputs of the LORA computer program. To keep the report unclassified, no attempt is made to make the system and environmental inputs correspond to data or theoretical values, with the exception that the two sound-speed profiles are from unclassified measured data.* These profiles are depicted in Fig. D-1 and D-2 and tabulated in Tables D-1 and D-2. In the computer runs the typical values for sound speed are used rather than the average values.

The transmit and receive beam patterns are the internally calculated response functions for a continuous-line array, with the half-power beamwidths defining the length of the line for the given frequency. It is important to remember that the propagation loss values include beam response degradations.

*J. G. Colborn and J. D. Pugh. "A Procedure for Selection of Typical Sound-Speed Profiles," NUC TN 1006 (1973).

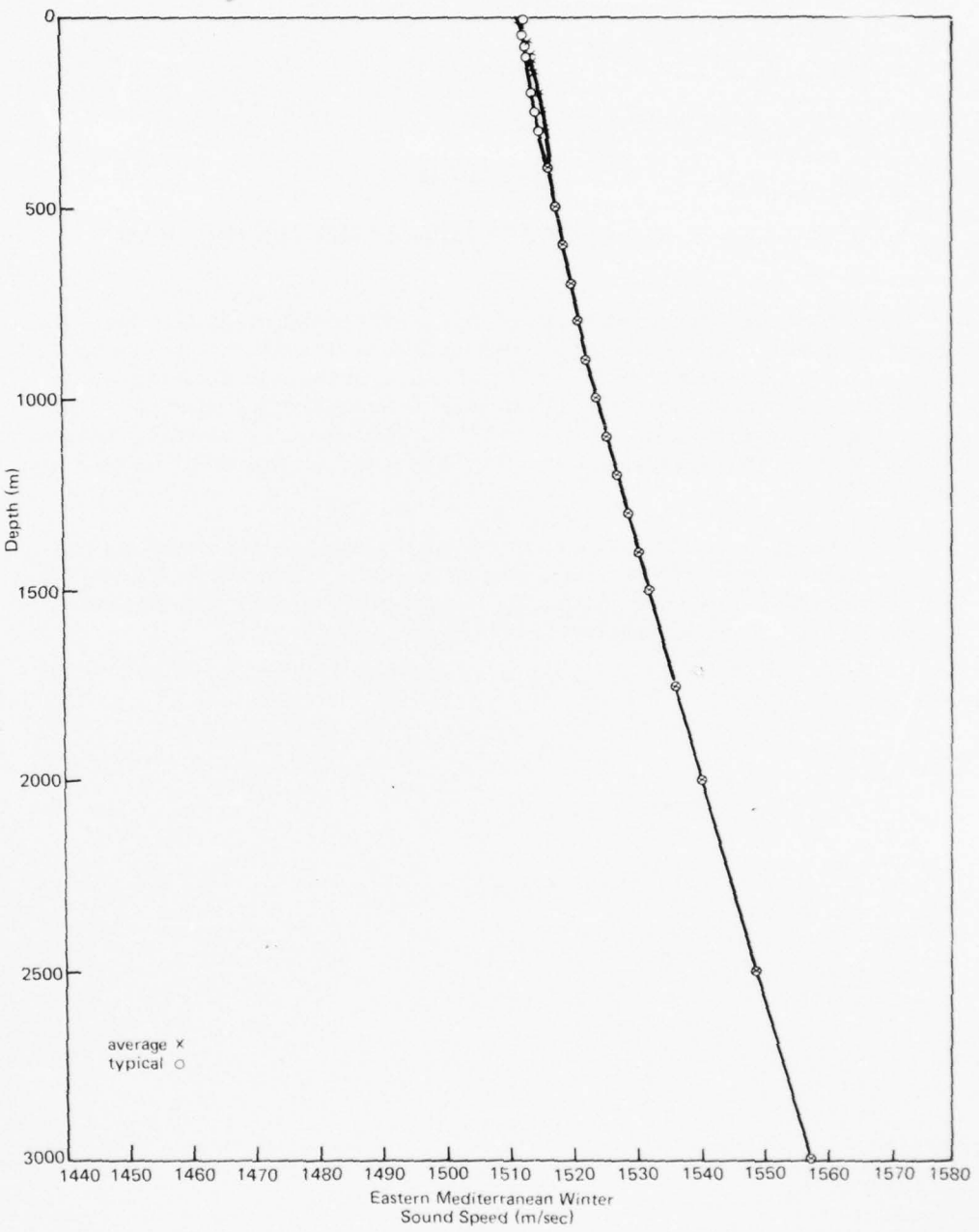


Figure D-1. Sound-speed profile used in computer runs 1 and 2.

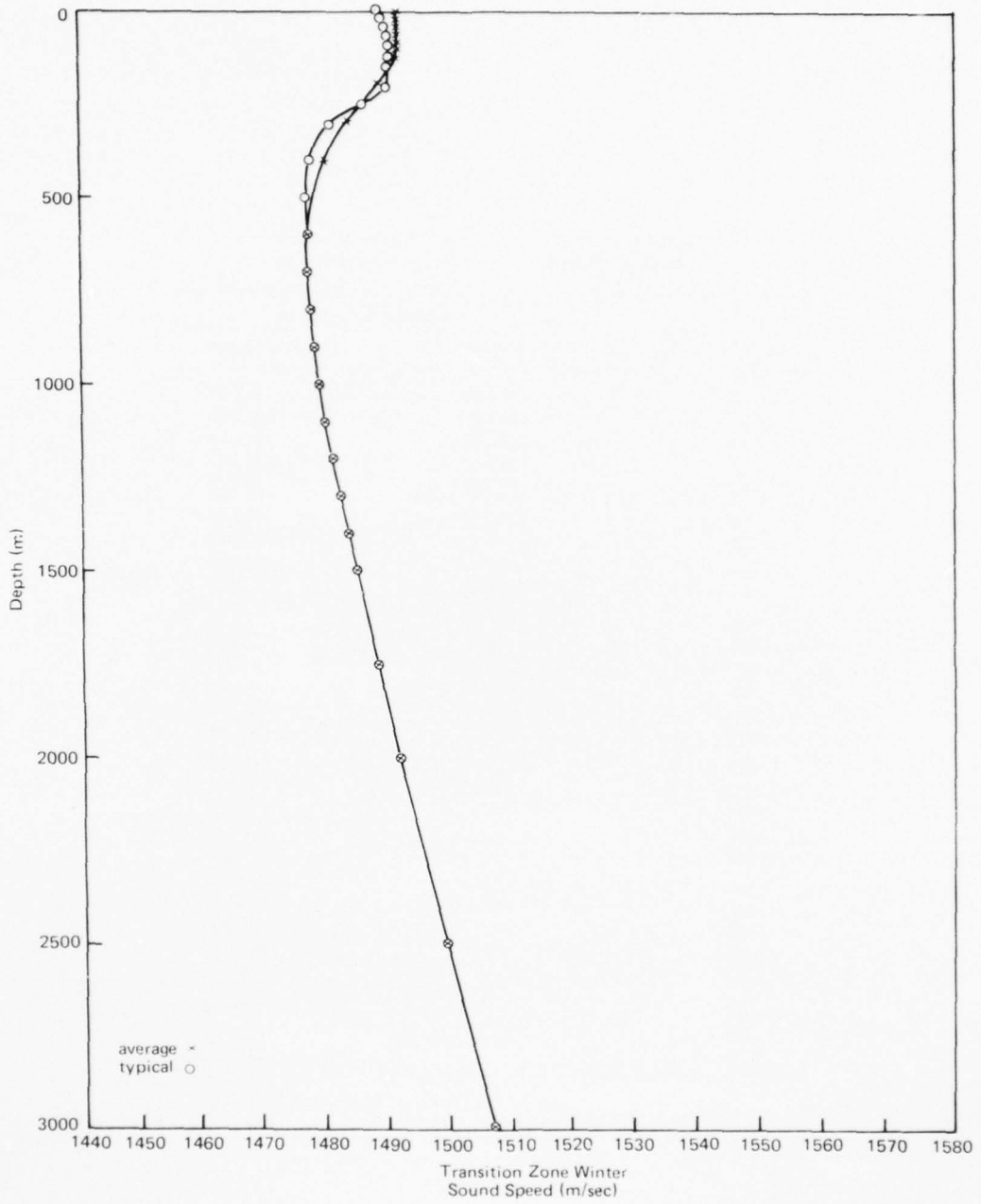


Figure D-2. Sound-speed profile used in computer runs 3, 4, and 5.

Table D-1. Sound speeds at standard depths for typical profile and average profile. Eastern Mediterranean Sea, winter.

| Depth, m | Sound Speed, m/s | |
|---|---|---|
| | Typical | Average |
| 0 | 1511.8 | 1512.46 |
| 10 | 1512.0 | 1512.56 |
| 20 | 1512.2 | 1512.74 |
| 30 | 1512.3 | 1512.85 |
| 50 | 1512.8 | 1513.08 |
| 75 | 1513.5 | 1513.45 |
| 100 | 1514.1 | 1513.86 |
| 125 | 1514.4 | 1514.11 |
| 150 | 1514.5 | 1514.45 |
| 200 | 1514.7 | 1515.44 |
| 250 | 1515.1 | 1515.92 |
| 300 | 1515.8 | 1516.23 |
| 400 | 1516.8 | 1516.95 |
| 500 | 1517.9 | 1517.82 |
| 600 | 1519.0 | 1519.00 |
| 700 | 1520.2 | 1520.25 |
| 800 | 1521.3 | 1521.47 |
| 900 | – | 1522.83 |
| 1000 | – | 1524.41 |
| 1100 | – | 1526.01 |
| 1200 | – | 1527.64 |
| 1300 | – | 1529.26 |
| 1400 | – | 1530.88 |
| 1500 | – | 1532.53 |
| 1750 | – | 1536.64 |
| 2000 | – | 1540.78 |
| 2500 | – | 1549.20 |
| 3000 | – | 1557.87 |

Table D-2. Sound speeds at standard depths for typical profile and average profile. Transition Zone, winter.

| Depth, m | Sound Speed, m/s | |
|---|---|---|
| | Typical | Average |
| 0 | 1488.0 | 1490.36 |
| 10 | 1488.2 | 1490.69 |
| 20 | 1488.6 | 1490.87 |
| 30 | 1488.8 | 1490.98 |
| 50 | 1488.8 | 1491.05 |
| 75 | 1489.0 | 1491.13 |
| 100 | 1489.2 | 1491.21 |
| 125 | 1489.3 | 1490.95 |
| 150 | 1489.6 | 1490.36 |
| 200 | 1489.5 | 1488.31 |
| 250 | 1485.5 | 1485.75 |
| 300 | 1479.9 | 1483.23 |
| 400 | 1477.2 | 1479.46 |
| 500 | 1476.6 | 1477.38 |
| 600 | 1476.6 | 1476.75 |
| 700 | 1476.7 | 1476.81 |
| 800 | 1477.2 | 1477.33 |
| 900 | 1477.8 | 1477.95 |
| 1000 | 1478.6 | 1478.69 |
| 1100 | 1479.4 | 1479.64 |
| 1200 | 1480.5 | 1480.67 |
| 1300 | 1481.7 | 1481.82 |
| 1400 | 1483.0 | 1482.94 |
| 1500 | 1484.4 | 1484.20 |
| 1750 | 1487.9 | 1487.55 |
| 2000 | 1491.3 | 1491.12 |
| 2500 | – | 1498.57 |
| 3000 | – | 1506.52 |
| 4000 | – | 1523.85 |

```
LORA -- LONG RANGE ACTIVE PERFORMANCE PREDICTION PROGRAM

RESPONSIBLE PERSON:   DAVID W. HOFFMAN
                      NAVAL UNDERSEA CENTER
                      CODE 304
                      SAN DIEGO, CA 92132

 TELEPHONE NUMBERS:   (714) 225-2316
                      AUTOVON 933-2316


*********************
* INPUTS,  RUN  1 *
*********************

HEADER
MEDITERRANEAN WINTER SOUND SPEED PROFILE, NUC TN 1006, P. 23
  SSP 0 1511.8 10 1512.0 20 1512.2 30 1512.3 50 1512.8 75 1513.5 100 1514.1
* 125 1514.4 150 1514.5 200 1514.7 250 1515.1 300 1515.8 400 1516.8 500 1517.9
* 600 1519.0 700 1520.2 800 1521.3 900 1522.83 1000 1524.41 1100 1526.01
* 1200 1527.64 1300 1529.26 1400 1530.88 1500 1532.53 1750 1536.64
* 2000 1540.78 2500 1549.20 3000 1557.87
ZBM 6040
BEAMX 0, BEAMR 0
AMB = 0 1   10 2   50 6   70 7   90 7.5
ZX=400, ZTG=1000, FREQ=2, LRA=5, VWI=15, HS=-1, ZONES=2
DELPX=10, DELPR=10, DELTH=10, LAT=35, OUTR=1,
SL=135, MPR=2, TBP=10, TVC=12, BWR=10, OUTP=1, COHY
MODE 1, RUN

**********************
* CALCULATIONS,  RUN  1 *
**********************


 BEAMX IS THE SIN(X)/X RESPONSE FUNCTION FOR A CONTINUOUS LINE ARRAY

 BEAMR IS THE SIN(X)/X RESPONSE FUNCTION FOR A CONTINUOUS LINE ARRAY



 THE LETTERS FOLLOWING THE NUMBERS IN THE HEADING ON THE
 PERFORMANCE PREDICTION PAGE SIGNIFY THE FOLLOWING,

   U      USER HAS SPECIFIED THIS INPUT VALUE ON THIS RUN
BLANK     SET BY USER ON A PREVIOUS RUN
   T      TYPICAL VALUE SET IN ABSENCE OF USER SPECIFICATION
   C      CALCULATED INTERNALLY BY PROGRAM (USER OPTION)
   W      WRONG VALUE SPECIFIED BY USER (OUT OF RANGE OF ALLOW-
            ABLE VALUES.  THE PRINTED VALUE IS A TYPICAL VALUE.)
   N      NOT AN INPUT, CALCULATED INTERNALLY.
```

SOUND SPEED PROFILE AFTER EARTH CURVATURE CORRECTION AND CURVE FITTING

SSP SEGMENT PARAMETERS
(JASA, VOL. 41, NO. 2, PP. 419-438)

| LAYER NUMBER | DEPTH (FT) | SOUND SPEED (FT/SEC) | CA**2 | KA | ZA |
|---|---|---|---|---|---|
| 1 | .000 | 4959.780292 | .2508371+08 | -.1172244-08 | .4098082+04 |
| 2 | 328.141 | 4967.157258 | .2468171+08 | -.5150712-07 | .4125656+03 |
| 3 | 372.683 | 4967.865436 | .2469760+08 | -.5822355-08 | .7257311+03 |
| 4 | 492.136 | 4968.878477 | .2465123+08 | .1181110-08 | -.6572257+03 |
| 5 | 1312.439 | 4976.415117 | .2637136+08 | -.9546943-10 | .2738071+05 |
| 6 | 1591.774 | 4979.649621 | .2752025+08 | -.6010778-10 | .4433693+05 |
| 7 | 1968.612 | 4983.980388 | .2463949+08 | .6438600-09 | -.1572664+04 |
| 8 | 3609.212 | 5007.292068 | .2665761+08 | -.2061638-09 | .2111798+05 |
| 9 | 3820.004 | 5010.857814 | .2674960+08 | -.1959513-09 | .2208231+05 |
| 10 | 4265.457 | 5018.280477 | .9453803+07 | .2437453-11 | -.5019462+06 |
| 11 | 6040.989 | 5047.877286 | .0000000 | .0000000 | .0000000 |

ACTIVE TWO-WAY LOSS, PAGE 1

MEDITERRANEAN WINTER SOUND SPEED PROFILE, NUC TN 1006, P. 23

THE LOSS ENTRIES INCLUDE TWO-WAY PROPAGATION LOSS
AND THE TRANSMIT AND RECEIVE BEAM PATTERN RESPONSES.

| RANGE (KYD) | MINIMUM TWO-WAY LOSS | BOTTOM BOUNCE LOSS | DIRECT PATH, CONVERGENCE ZONE LOSSES |
|---|---|---|---|
| 1 | 131.18 | 212.02 | 131.18 |
| 2 | 132.83 | 211.41 | 132.83 |
| 3 | 139.94 | 203.76 | 139.94 |
| 4 | 145.50 | 215.74 | 145.50 |
| 5 | 149.65 | 201.13 | 149.65 |
| 6 | 153.07 | 203.11 | 153.07 |
| 7 | 156.08 | 215.41 | 156.08 |
| 8 | 158.60 | 202.68 | 158.60 |
| 9 | 160.63 | 196.73 | 160.63 |
| 10 | 162.19 | 197.25 | 162.19 |
| 11 | 163.40 | 201.59 | 163.40 |
| 12 | 164.55 | 210.15 | 164.55 |
| 13 | 165.66 | 215.32 | 165.66 |
| 14 | 166.72 | 222.83 | 166.72 |
| 15 | 167.74 | 216.21 | 167.74 |
| 16 | 169.78 | 209.18 | 169.78 |
| 17 | 171.82 | 205.09 | 171.82 |
| 18 | 173.70 | 202.73 | 173.70 |
| 19 | 175.15 | 201.44 | 175.15 |
| 20 | 176.38 | 200.65 | 176.38 |
| 21 | 177.57 | 200.48 | 177.57 |
| 22 | 178.72 | 200.58 | 178.72 |
| 23 | 177.80 | 200.90 | 177.80 |
| 24 | 177.44 | 201.53 | 177.44 |
| 25 | 177.45 | 202.31 | 177.45 |
| 26 | 177.54 | 203.24 | 177.54 |
| 27 | 177.69 | 204.32 | 177.69 |
| 28 | 168.68 | 205.54 | 168.68 |
| 29 | 178.56 | 206.92 | 178.56 |
| 30 | 184.66 | 208.48 | 184.66 |
| 31 | 187.09 | 210.22 | 187.09 |
| 32 | 186.32 | 212.17 | 186.32 |
| 33 | 185.75 | 214.38 | 185.75 |
| 34 | 185.49 | 216.97 | 185.49 |
| 35 | 191.91 | 220.19 | 191.91 |
| 36 | 192.78 | 224.44 | 192.78 |
| 37 | 193.64 | 227.26 | 193.64 |
| 38 | 194.47 | 229.94 | 194.47 |
| 39 | 195.84 | 233.31 | 195.84 |
| 40 | 197.56 | 237.99 | 197.56 |
| 41 | 199.16 | 267.22 | 199.16 |
| 42 | 200.66 | 273.41 | 200.66 |
| 43 | 202.07 | .00 | 202.07 |
| 44 | 203.17 | .00 | 203.17 |
| 45 | 204.04 | .00 | 204.04 |

ACTIVE TWO-WAY LOSS, PAGE 2

MEDITERRANEAN WINTER SOUND SPEED PROFILE, NUC TN 1006, P. 23

| RANGE (KYD) | MINIMUM TWO-WAY LOSS | BOTTOM BOUNCE LOSS | DIRECT PATH, CONVERGENCE ZONE LOSSES |
|---|---|---|---|
| 46 | 204.89 | .00 | 204.89 |
| 47 | 205.72 | .00 | 205.72 |
| 48 | 206.52 | .00 | 206.52 |
| 49 | 207.30 | .00 | 207.30 |
| 50 | 207.72 | .00 | 207.72 |
| 51 | 208.46 | .00 | 208.46 |
| 52 | 206.55 | .00 | 206.55 |
| 53 | 206.51 | .00 | 206.51 |
| 54 | 206.51 | .00 | 206.51 |
| 55 | 206.57 | .00 | 206.57 |
| 56 | 206.66 | .00 | 206.66 |
| 57 | 206.78 | .00 | 206.78 |
| 58 | 206.92 | .00 | 206.92 |
| 59 | 207.08 | .00 | 207.08 |
| 60 | 207.28 | .00 | 207.28 |
| 61 | 207.51 | .00 | 207.51 |
| 62 | 209.88 | .00 | 209.88 |
| 63 | 214.23 | .00 | 214.23 |
| 64 | 215.96 | .00 | 215.96 |
| 65 | 216.69 | .00 | 216.69 |
| 66 | 216.77 | .00 | 216.77 |
| 67 | 217.75 | .00 | 217.75 |
| 68 | 220.09 | .00 | 220.09 |
| 69 | 220.98 | .00 | 220.98 |
| 70 | 221.90 | .00 | 221.90 |
| 71 | 222.83 | .00 | 222.83 |
| 72 | 223.77 | .00 | 223.77 |
| 73 | 224.71 | .00 | 224.71 |
| 74 | 225.66 | .00 | 225.66 |
| 75 | 226.62 | .00 | 226.62 |
| 76 | 227.59 | .00 | 227.59 |
| 77 | 228.56 | .00 | 228.56 |
| 78 | 229.55 | .00 | 229.55 |
| 79 | 237.57 | .00 | 237.57 |
| 80 | 238.61 | .00 | 238.61 |
| 81 | 239.65 | .00 | 239.65 |
| 82 | 240.70 | .00 | 240.70 |
| 83 | 271.99 | .00 | 271.99 |

AD-A036 539 NAVAL UNDERSEA CENTER SAN DIEGO CALIF F/G 17/1
LORA: A MODEL FOR PREDICTING THE PERFORMANCE OF LONG-RANGE ACTI--ETC(U)
DEC 76 D W HOFFMAN
UNCLASSIFIED NUC-TP-541 NL

2 OF 2
AD
A036539

END

DATE
FILMED
3-77

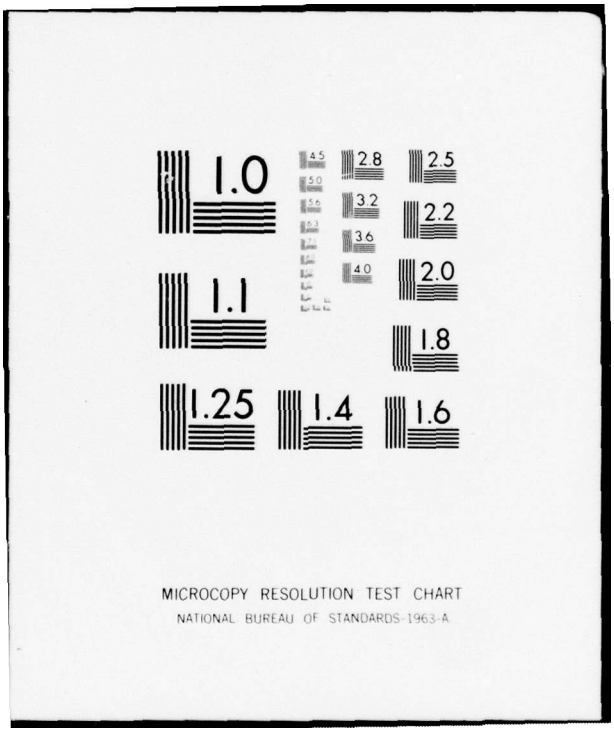
1.0
1.1
1.25
1.4
1.6
1.8
2.0
2.2
2.5
2.8
3.2
3.6
4.0
4.5
5.0
5.6
MICROCOPY RESOLUTION TEST CHART
NATIONAL BUREAU OF STANDARDS-1963-A

PASSIVE ONE-WAY LOSS, PAGE 1

MEDITERRANEAN WINTER SOUND SPEED PROFILE, NUC TN 1006, P. 23

THE LOSS ENTRIES INCLUDE ONE-WAY PROPAGATION LOSS
AND THE RECEIVE BEAM PATTERN RESPONSE. MULTIPATH INTENSITIES
ARE SUMMED, SO THE ONE-WAY PASSIVE LOSSES ARE NOT IN GENERAL
ONE-HALF OF THE TWO-WAY ACTIVE LOSSES.

| RANGE (KYD) | INCOHERENT 1-WAY LOSS | COHERENT 1-WAY LOSS | SEMICOHERENT 1-WAY LOSS |
|---|---|---|---|
| 1 | 65.53 | 64.93 | 64.93 |
| 2 | 66.36 | 65.53 | 65.52 |
| 3 | 69.93 | 70.21 | 70.20 |
| 4 | 72.75 | 72.80 | 72.80 |
| 5 | 74.79 | 74.60 | 74.61 |
| 6 | 76.45 | 76.30 | 76.31 |
| 7 | 77.90 | 78.23 | 78.19 |
| 8 | 79.08 | 79.08 | 79.08 |
| 9 | 80.01 | 80.60 | 80.50 |
| 10 | 80.75 | 82.45 | 82.14 |
| 11 | 81.35 | 81.62 | 81.56 |
| 12 | 81.94 | 82.65 | 82.49 |
| 13 | 82.52 | 85.01 | 84.40 |
| 14 | 83.06 | 82.42 | 82.59 |
| 15 | 83.56 | 82.29 | 82.66 |
| 16 | 84.55 | 85.46 | 85.18 |
| 17 | 85.51 | 86.77 | 86.36 |
| 18 | 86.37 | 88.09 | 87.49 |
| 19 | 87.04 | 89.28 | 88.45 |
| 20 | 87.67 | 93.29 | 91.11 |
| 21 | 88.26 | 88.65 | 88.49 |
| 22 | 88.82 | 89.19 | 89.03 |
| 23 | 88.45 | 95.26 | 92.20 |
| 24 | 88.33 | 87.61 | 87.95 |
| 25 | 88.37 | 89.34 | 88.87 |
| 26 | 88.44 | 88.86 | 88.65 |
| 27 | 88.55 | 88.91 | 88.72 |
| 28 | 81.79 | 88.82 | 84.95 |
| 29 | 85.83 | 89.69 | 87.48 |
| 30 | 88.16 | 88.20 | 88.18 |
| 31 | 88.90 | 97.99 | 92.42 |
| 32 | 88.82 | 85.52 | 87.61 |
| 33 | 89.12 | 92.06 | 90.14 |
| 34 | 89.43 | 86.26 | 88.39 |
| 35 | 91.52 | 93.01 | 91.98 |
| 36 | 92.41 | 89.50 | 91.58 |
| 37 | 93.08 | 90.25 | 92.33 |
| 38 | 95.33 | 93.43 | 94.87 |
| 39 | 96.08 | 96.63 | 96.21 |
| 40 | 97.03 | 102.54 | 98.15 |
| 41 | 97.88 | 99.18 | 98.12 |
| 42 | 99.99 | 97.60 | 99.60 |
| 43 | 100.73 | 101.37 | 100.82 |
| 44 | 101.38 | 101.94 | 101.45 |
| 45 | 101.85 | 102.92 | 101.96 |

PASSIVE ONE-WAY LOSS, PAGE 2

MEDITERRANEAN WINTER SOUND SPEED PROFILE, NUC TN 1006, P. 23

| RANGE (KYD) | INCOHERENT 1-WAY LOSS | COHERENT 1-WAY LOSS | SEMICOHERENT 1-WAY LOSS |
|---|---|---|---|
| 46 | 102.31 | 101.02 | 102.20 |
| 47 | 102.75 | 102.99 | 102.76 |
| 48 | 103.16 | 103.12 | 103.16 |
| 49 | 103.56 | 103.44 | 103.56 |
| 50 | 103.79 | 104.55 | 103.79 |
| 51 | 96.78 | 106.54 | 96.78 |
| 52 | 100.31 | 102.91 | 100.31 |
| 53 | 101.31 | 112.87 | 101.31 |
| 54 | 101.76 | 110.48 | 101.76 |
| 55 | 101.41 | 108.26 | 101.41 |
| 56 | 102.09 | 98.65 | 102.09 |
| 57 | 102.31 | 104.79 | 102.31 |
| 58 | 102.48 | 100.84 | 102.48 |
| 59 | 102.49 | 101.99 | 102.49 |
| 60 | 102.43 | 100.69 | 102.43 |
| 61 | 102.49 | 104.94 | 102.49 |
| 62 | 103.32 | 101.08 | 103.32 |
| 63 | 104.67 | 111.70 | 104.67 |
| 64 | 105.13 | 102.41 | 105.13 |
| 65 | 105.49 | 112.95 | 105.49 |
| 66 | 105.81 | 109.69 | 105.81 |
| 67 | 106.23 | 114.77 | 106.23 |
| 68 | 108.03 | 112.17 | 108.03 |
| 69 | 108.68 | 106.49 | 108.68 |
| 70 | 109.26 | 116.77 | 109.26 |
| 71 | 109.79 | 107.00 | 109.79 |
| 72 | 110.19 | 120.16 | 110.19 |
| 73 | 110.66 | 107.24 | 110.66 |
| 74 | 111.13 | 120.64 | 111.13 |
| 75 | 111.61 | 107.85 | 111.61 |
| 76 | 112.09 | 121.15 | 112.09 |
| 77 | 112.58 | 109.48 | 112.58 |
| 78 | 113.07 | 116.16 | 113.07 |
| 79 | 118.42 | 115.99 | 118.42 |
| 80 | 119.21 | 118.09 | 119.21 |
| 81 | 119.72 | 118.55 | 119.72 |
| 82 | 120.23 | 119.03 | 120.23 |
| 83 | 135.99 | 135.99 | 135.99 |

REVERBERATION LEVELS AT TIMES CORRESPONDING TO 2-WAY
ACOUSTIC TRAVEL TIMES BETWEEN SOURCE AND TARGET.
( 2 PINGS -- TIME BETWEEN PINGS IS 10.00 SECONDS.)
THE SOUND PROPAGATES BETWEEN SOURCE AND TARGET BY

DIRECT PATH

| TARGET RANGE KYD | TWO-WAY TIME SEC | BOTTOM REVERB DB | SURFACE REVERB DB | VOLUME REVERB DB | TOTAL REVERB DB | PING 1 REVERB DB | PING 2 REVERB DB |
|---|---|---|---|---|---|---|---|
| 1.0 | 1.23 | -300.0 | -39.7 | -300.0 | -36.2 | -39.7 | -38.8 |
| 2.0 | 2.43 | -34.0 | -27.0 | -300.0 | -21.5 | -26.2 | -23.4 |
| 3.0 | 3.63 | -41.9 | -27.8 | -300.0 | -22.6 | -27.7 | -24.2 |
| 4.0 | 4.83 | -59.4 | -30.3 | -89.1 | -23.9 | -30.3 | -25.0 |
| 5.0 | 6.04 | -31.1 | -33.9 | -70.0 | -24.3 | -29.3 | -25.9 |
| 6.0 | 7.25 | -36.7 | -37.0 | -73.0 | -25.6 | -33.8 | -26.3 |
| 7.0 | 8.45 | -67.6 | -39.6 | -74.8 | -27.0 | -39.6 | -27.3 |
| 8.0 | 9.66 | -52.3 | -42.1 | -78.9 | -28.7 | -41.7 | -28.9 |
| 9.0 | 10.87 | -41.4 | -44.4 | -64.0 | -29.9 | -39.6 | -30.4 |
| 10.0 | 12.07 | -37.7 | -45.1 | -23.3 | -22.6 | -23.1 | -31.8 |
| 11.0 | 13.28 | -36.7 | -45.9 | -24.2 | -23.4 | -23.9 | -32.6 |
| 12.0 | 14.48 | -37.1 | -46.3 | -25.1 | -24.2 | -24.8 | -33.5 |
| 13.0 | 15.69 | -38.3 | -46.3 | -26.0 | -25.1 | -25.7 | -33.8 |
| 14.0 | 16.90 | -40.1 | -45.8 | -26.8 | -26.0 | -26.6 | -35.0 |
| 15.0 | 18.10 | -42.5 | -45.1 | -27.1 | -26.3 | -26.9 | -35.0 |
| 16.0 | 19.31 | -45.5 | -44.3 | -28.6 | -27.6 | -28.4 | -35.0 |
| 17.0 | 20.51 | -49.2 | -46.1 | -30.3 | -28.6 | -29.8 | -34.9 |
| 18.0 | 21.72 | -54.5 | -42.4 | -31.8 | -29.8 | -31.4 | -34.8 |
| 19.0 | 22.92 | -70.8 | -41.2 | -32.9 | -30.2 | -32.3 | -34.2 |
| 20.0 | 24.13 | -76.3 | -39.8 | -34.3 | -23.6 | -33.3 | -24.1 |
| 21.0 | 25.33 | -89.2 | -38.3 | -35.6 | -30.4 | -33.8 | -33.1 |
| 22.0 | 26.54 | -102.0 | -39.3 | -36.8 | -32.1 | -34.9 | -35.2 |
| 23.0 | 27.74 | -102.1 | -41.8 | -36.1 | -31.6 | -35.0 | -34.3 |
| 24.0 | 28.94 | -94.2 | -43.2 | -35.7 | -32.7 | -35.0 | -36.6 |
| 25.0 | 30.15 | -86.2 | -43.8 | -35.6 | -33.1 | -35.0 | -37.7 |
| 26.0 | 31.35 | -82.2 | -44.4 | -35.3 | -33.1 | -34.8 | -38.0 |
| 27.0 | 32.55 | -78.3 | -42.6 | -35.1 | -33.5 | -34.4 | -40.8 |
| 28.0 | 33.82 | -75.2 | -40.6 | -20.3 | -20.3 | -20.3 | -41.3 |
| 29.0 | 34.95 | -73.8 | -39.4 | -31.5 | -30.6 | -30.9 | -42.8 |
| 30.0 | 36.15 | -72.4 | -38.1 | -38.5 | -34.9 | -35.2 | -45.7 |
| 31.0 | 37.34 | -71.7 | -36.8 | -39.2 | -34.6 | -34.8 | -46.8 |
| 32.0 | 38.64 | -71.2 | -40.1 | -37.7 | -35.6 | -35.7 | -50.9 |
| 33.0 | 39.84 | -70.8 | -43.9 | -38.6 | -37.3 | -37.5 | -52.0 |
| 34.0 | 41.04 | -70.8 | -45.4 | -39.0 | -38.0 | -38.1 | -54.4 |
| 35.0 | 42.27 | -70.8 | -46.1 | -42.0 | -40.4 | -40.6 | -55.9 |
| 36.0 | 43.47 | -71.0 | -47.2 | -42.4 | -41.0 | -41.1 | -56.6 |
| 37.0 | 44.68 | -71.3 | -48.3 | -44.0 | -42.4 | -42.6 | -57.6 |
| 38.0 | 45.89 | -71.7 | -49.4 | -47.8 | -45.3 | -45.5 | -58.7 |
| 39.0 | 47.09 | -72.2 | -50.6 | -48.8 | -46.4 | -46.6 | -59.7 |

ACTIVE PERFORMANCE PREDICTION
MEDITERRANEAN WINTER SOUND SPEED PROFILE, NUC TN 1006, P. 23

DIRECT PATH

| | | | | | | | | | | | |
|---|---|---|---|---|---|---|---|---|---|---|---|
| OUTP | 1.0 | U | ZX | 400.0 | U | ZTG | 1000.0 | U | FREQ | 2.0 | U |
| VWI | 15.0 | U | SALT | 35.0 | T | HS | 5.0 | C | ZBM | 6040. | U |
| ZONES | 2.0 | U | PHDX | 5.0 | T | PHDR | 5.0 | T | DELPX | 10.0 | U |
| MUB | -27.0 | T | MUV | -49.0 | T | ZC | 2000. | T | LAT | 35.0 | U |
| OUTR | 1.0 | U | MODE | 1.0 | U | SL | 135.0 | U | DELTH | 10.0 | U |
| TBP | 10.0 | U | PULSE | .10+00 | T | DI | 25.6 | C | BWS | 10.0 | T |
| NIN | -45.0 | T | NOUT | -60.6 | C | TVC | 12.0 | U | GDOP | 4.4 | C |
| RDN | -2.0 | T | CLIP | .0 | T | SIGMA | 6.0 | T | PFA | .100-02 | T |
| GO | .0000 | N | ALFA | .1265 | N | ZL | .00 | N | ZCJ | 0. | N |
| CX | 4968.13 | N | CT | 4973.07 | N | CL | .00 | N | CS | 4959.97 | N |
| TSUR | 61.6 | N | TAV | 59.9 | N | NOCZ | 2 | N | IRAP | 0 | N |

| LWA | 5.0 | U |
|---|---|---|
| REFLS | 1.0 | T |
| DELPR | 10.0 | U |
| DUMP | .0 | T |
| MPR | 2.0 | U |
| BWR | 10.0 | U |
| TGS | 15.0 | T |
| SP | 5. | T |
| PHIB | 10.20 | N |
| CB | 5047.87 | N |
| IAMOS | 3 | N |

| RANGE (KYD) | TIME (SEC) | LOSS (DB) | ANGLE (DEG) | SIGNAL (DB) | REVERB (DB) | REV LIM | S/MN (DB) | EXCESS (DB) | PROB DETECT |
|---|---|---|---|---|---|---|---|---|---|
| 1.0 | 1.23 | 131.2 | 11.45 | 18.8 | -36.2 | YES | 59.4 | 59.4 | 1.0000 |
| 2.0 | 2.43 | 132.8 | 5.99 | 17.2 | -21.5 | YES | 43.1 | 43.1 | 1.0000 |
| 3.0 | 3.63 | 139.9 | 4.22 | 10.1 | -22.6 | YES | 37.1 | 37.1 | 1.0000 |
| 4.0 | 4.83 | 145.5 | 3.44 | 4.5 | -23.9 | YES | 32.8 | 32.8 | 1.0000 |
| 5.0 | 6.04 | 149.6 | 3.13 | .4 | -24.3 | YES | 29.1 | 29.1 | 1.0000 |
| 6.0 | 7.25 | 153.1 | 2.91 | -3.1 | -25.6 | YES | 27.0 | 27.0 | 1.0000 |
| 7.0 | 8.45 | 156.1 | 2.70 | -6.1 | -27.0 | YES | 25.4 | 25.4 | 1.0000 |
| 8.0 | 9.66 | 158.6 | 2.57 | -8.6 | -28.7 | YES | 24.5 | 24.5 | 1.0000 |
| 9.0 | 10.87 | 160.6 | 2.57 | -10.6 | -29.9 | YES | 23.7 | 23.7 | 1.0000 |
| 10.0 | 12.07 | 162.2 | 2.64 | -12.2 | -22.6 | YES | 14.8 | 14.8 | .9878 |
| 11.0 | 13.28 | 163.4 | 2.77 | -13.4 | -23.4 | YES | 14.4 | 14.4 | .9862 |
| 12.0 | 14.48 | 164.6 | 2.89 | -14.6 | -24.2 | YES | 14.1 | 14.1 | .9851 |
| 13.0 | 15.69 | 165.7 | 3.02 | -15.7 | -25.1 | YES | 13.8 | 13.8 | .9840 |
| 14.0 | 16.90 | 166.7 | 3.14 | -16.7 | -26.0 | YES | 13.7 | 13.7 | .9836 |
| 15.0 | 18.10 | 167.7 | 3.27 | -17.7 | -26.3 | YES | 13.0 | 13.0 | .9807 |
| 16.0 | 19.31 | 169.8 | 3.45 | -19.8 | -27.6 | YES | 12.2 | 12.2 | .9778 |
| 17.0 | 20.51 | 171.8 | 3.63 | -21.8 | -28.6 | YES | 11.2 | 11.2 | .9595 |
| 18.0 | 21.72 | 173.7 | 3.82 | -23.7 | -29.8 | YES | 10.5 | 10.5 | .9428 |
| 19.0 | 22.92 | 175.1 | 4.01 | -25.1 | -30.2 | YES | 9.4 | 9.4 | .9187 |
| 20.0 | 24.13 | 176.4 | 4.19 | -26.4 | -23.6 | YES | 1.7 | 1.7 | .6047 |
| 21.0 | 25.33 | 177.6 | 4.38 | -27.6 | -30.4 | YES | 7.3 | 7.3 | .8692 |
| 22.0 | 26.54 | 178.7 | 4.56 | -28.7 | -32.1 | YES | 7.8 | 7.8 | .8802 |
| 23.0 | 27.74 | 177.8 | 4.79 | -27.8 | -31.6 | YES | 8.3 | 8.3 | .8919 |
| 24.0 | 28.94 | 177.4 | 5.05 | -27.4 | -32.7 | YES | 9.7 | 9.7 | .9237 |
| 25.0 | 30.15 | 177.4 | 5.35 | -27.4 | -33.1 | YES | 10.1 | 10.1 | .9333 |
| 26.0 | 31.35 | 177.5 | 5.71 | -27.5 | -33.1 | YES | 10.0 | 10.0 | .9312 |
| 27.0 | 32.55 | 177.7 | 6.12 | -27.7 | -33.5 | YES | 10.2 | 10.2 | .9365 |
| 28.0 | 33.82 | 168.7 | 3.09 | -18.7 | -20.3 | YES | 6.0 | 6.0 | .8406 |
| 29.0 | 34.95 | 178.6 | 7.18 | -28.6 | -30.6 | YES | 6.5 | 6.5 | .8504 |
| 30.0 | 36.15 | 184.7 | 7.60 | -34.7 | -34.9 | YES | 4.6 | 4.6 | .7712 |
| 31.0 | 37.34 | 187.1 | 7.94 | -37.1 | -34.6 | YES | 1.9 | 1.9 | .6189 |
| 32.0 | 38.64 | 186.3 | 5.25 | -36.3 | -35.6 | YES | 3.6 | 3.6 | .7223 |
| 33.0 | 39.84 | 185.7 | 5.92 | -35.7 | -37.3 | YES | 6.0 | 6.0 | .8387 |
| 34.0 | 41.04 | 185.5 | 6.85 | -35.5 | -38.0 | YES | 6.9 | 6.9 | .8597 |
| 35.0 | 42.27 | 191.9 | 2.95 | -41.9 | -40.4 | YES | 2.8 | 2.8 | .6804 |
| 36.0 | 43.47 | 192.8 | 3.05 | -42.8 | -41.0 | YES | 2.5 | 2.5 | .6613 |
| 37.0 | 44.68 | 193.6 | 3.15 | -43.6 | -42.4 | YES | 3.1 | 3.1 | .6935 |

ACTIVE PERFORMANCE PREDICTION
MEDITERRANEAN *INTER SOUND SPEED PROFILE, NUC TN 1006, P. 23

DIRECT PATH

| | | | | | | | | | | | |
|---|---|---|---|---|---|---|---|---|---|---|---|
| OUTP | 1.0 | U | ZX | 400.0 | U | ZTG | 1000.0 | U | FREQ | 2.0 | U |
| VWI | 15.0 | U | SALT | 35.0 | T | HS | 5.0 | C | ZBM | 6040. | U |
| ZONES | 2.0 | U | PHDX | 5.0 | T | PHDR | 5.0 | T | DELPX | 10.0 | U |
| MUB | -27.0 | T | MUV | -49.0 | T | ZC | 2000. | T | LAT | 35.0 | U |
| OUTR | 1.0 | U | MODE | 1.0 | U | SL | 135.0 | U | DELTH | 10.0 | U |
| TBP | 10.0 | U | PULSE | .10+00 | T | DI | 25.6 | C | BWS | 10.0 | T |
| NIN | -45.0 | T | NOUT | -60.6 | C | TVC | 12.0 | U | GDOP | 4.4 | C |
| RDN | -2.0 | T | CLIP | .0 | T | SIGMA | 6.0 | T | PFA | .100-02 | T |
| GO | .6000 | N | ALFA | .1265 | N | ZL | .00 | N | ZCJ | 0. | N |
| CX | 4968.13 | N | CT | 4973.07 | N | CL | .00 | N | CS | 4959.97 | N |
| TSUR | 61.6 | N | TAV | 59.9 | N | NOCZ | 2 | N | IRAP | 0 | N |

| | | | | | | | | | | | |
|---|---|---|---|---|---|---|---|---|---|---|---|
| LWA | 5.0 | U | | | | | | | | | |
| REFLS | 1.0 | T | | | | | | | | | |
| DELPR | 10.0 | U | | | | | | | | | |
| DUMP | .0 | T | | | | | | | | | |
| MPR | 2.0 | U | | | | | | | | | |
| BWR | 10.0 | U | | | | | | | | | |
| TGS | 15.0 | T | | | | | | | | | |
| SP | 5. | T | | | | | | | | | |
| PHIB | 10.20 | N | | | | | | | | | |
| CB | 5047.87 | N | | | | | | | | | |
| IAMOS | 3 | N | | | | | | | | | |

| RANGE (KYD) | TIME (SEC) | LOSS (DB) | ANGLE (DEG) | SIGNAL (DB) | REVERB (DB) | REV LIM | S/MN (DB) | EXCESS (DB) | PROB DETECT |
|---|---|---|---|---|---|---|---|---|---|
| 38.0 | 45.89 | 194.5 | 3.25 | -44.5 | -45.3 | YES | 4.9 | 4.9 | .7861 |
| 39.0 | 47.09 | 195.8 | 3.36 | -45.8 | -46.4 | YES | 4.6 | 4.6 | .7679 |

```
**********
* INPUTS,  RUN  2 *
**********
```

MODE 3, RUN

```
**********
* CALCULATIONS,  RUN  2 *
**********
```

BEAMX IS THE SIN(X)/X RESPONSE FUNCTION FOR A CONTINUOUS LINE ARRAY

BEAMR IS THE SIN(X)/X RESPONSE FUNCTION FOR A CONTINUOUS LINE ARRAY

THE LETTERS FOLLOWING THE NUMBERS IN THE HEADING ON THE PERFORMANCE PREDICTION PAGE SIGNIFY THE FOLLOWING,

| | |
|---|---|
| U | USER HAS SPECIFIED THIS INPUT VALUE ON THIS RUN |
| BLANK | SET BY USER ON A PREVIOUS RUN |
| T | TYPICAL VALUE SET IN ABSENCE OF USER SPECIFICATION |
| C | CALCULATED INTERNALLY BY PROGRAM (USER OPTION) |
| * | WRONG VALUE SPECIFIED BY USER (OUT OF RANGE OF ALLOWABLE VALUES. THE PRINTED VALUE IS A TYPICAL VALUE.) |
| N | NOT AN INPUT, CALCULATED INTERNALLY. |

REVERBERATION LEVELS AT TIMES CORRESPONDING TO 2-WAY
ACOUSTIC TRAVEL TIMES BETWEEN SOURCE AND TARGET.
( 2 PINGS -- TIME BETWEEN PINGS IS 10.00 SECONDS.)
THE SOUND PROPAGATES BETWEEN SOURCE AND TARGET BY

SURFACE BOUNCE -- BOUNCE 1

| TARGET RANGE KYD | TWO-WAY TIME SEC | BOTTOM REVERB DB | SURFACE REVERB DB | VOLUME REVERB DB | TOTAL REVERB DB | PING 1 REVERB DB | PING 2 REVERB DB |
|---|---|---|---|---|---|---|---|
| 39.0 | 47.09 | -72.2 | -50.6 | -48.8 | -46.4 | -46.6 | -59.7 |
| 40.0 | 48.30 | -72.7 | -65.4 | -50.7 | -50.1 | -50.5 | -60.6 |
| 41.0 | 49.50 | -73.4 | -64.9 | -51.9 | -51.2 | -51.7 | -61.4 |
| 42.0 | 50.71 | -74.0 | -64.2 | -54.6 | -53.4 | -54.1 | -61.5 |
| 43.0 | 51.91 | -74.8 | -63.4 | -56.1 | -52.1 | -55.3 | -54.8 |
| 44.0 | 53.12 | -75.6 | -62.6 | -57.7 | -54.2 | -56.4 | -58.2 |
| 45.0 | 54.32 | -76.4 | -62.7 | -58.7 | -55.3 | -57.2 | -59.9 |
| 46.0 | 55.53 | -77.4 | -64.3 | -59.7 | -56.2 | -58.4 | -60.2 |
| 47.0 | 56.73 | -78.4 | -65.9 | -60.6 | -55.4 | -59.4 | -57.6 |
| 48.0 | 57.94 | -79.4 | -67.5 | -61.4 | -57.0 | -60.4 | -59.8 |
| 49.0 | 59.14 | -80.6 | -68.5 | -62.1 | -57.5 | -61.2 | -59.9 |
| 50.0 | 60.34 | -81.8 | -69.0 | -62.5 | -57.6 | -61.6 | -59.7 |
| 51.0 | 61.61 | -83.2 | -69.5 | -52.2 | -51.4 | -52.1 | -59.5 |
| 52.0 | 62.75 | -84.6 | -69.9 | -57.6 | -55.2 | -57.3 | -59.3 |
| 53.0 | 63.95 | -86.2 | -70.3 | -59.9 | -56.3 | -59.5 | -59.0 |
| 54.0 | 65.16 | -88.0 | -70.8 | -60.6 | -57.3 | -60.2 | -60.4 |
| 55.0 | 66.36 | -90.0 | -69.4 | -56.2 | -54.8 | -56.0 | -61.1 |
| 56.0 | 67.56 | -92.4 | -68.0 | -60.2 | -57.4 | -59.6 | -61.4 |
| 57.0 | 68.76 | -95.4 | -67.3 | -60.7 | -58.6 | -59.9 | -64.6 |
| 58.0 | 69.97 | -99.4 | -66.7 | -60.8 | -58.8 | -59.8 | -65.5 |
| 59.0 | 71.17 | -300.0 | -66.0 | -60.7 | -58.8 | -59.6 | -66.7 |
| 60.0 | 72.37 | -300.0 | -65.4 | -60.6 | -58.8 | -59.3 | -68.2 |
| 61.0 | 73.57 | -300.0 | -64.8 | -60.4 | -58.7 | -59.1 | -68.9 |
| 62.0 | 74.76 | -300.0 | -64.3 | -61.8 | -59.4 | -59.9 | -69.6 |
| 63.0 | 75.96 | -300.0 | -63.7 | -64.5 | -60.6 | -61.1 | -70.2 |
| 64.0 | 77.16 | -300.0 | -63.1 | -65.5 | -60.7 | -61.2 | -70.8 |
| 65.0 | 78.46 | -300.0 | -67.3 | -66.6 | -63.2 | -63.9 | -71.4 |
| 66.0 | 79.66 | -300.0 | -70.3 | -67.0 | -64.5 | -65.4 | -72.0 |
| 67.0 | 80.86 | -300.0 | -71.7 | -67.4 | -65.1 | -66.0 | -72.6 |
| 68.0 | 81.94 | -300.0 | -72.7 | -69.6 | -66.7 | -67.9 | -73.1 |
| 69.0 | 83.14 | -300.0 | -73.4 | -70.3 | -67.4 | -68.5 | -73.7 |
| 70.0 | 84.33 | -300.0 | -73.7 | -71.4 | -68.2 | -69.4 | -74.3 |
| 71.0 | 85.52 | -300.0 | -74.3 | -72.0 | -69.4 | -70.0 | -78.4 |
| 72.0 | 86.72 | -300.0 | -75.0 | -72.5 | -70.1 | -70.6 | -79.8 |
| 73.0 | 87.91 | -300.0 | -75.6 | -73.1 | -71.0 | -71.2 | -86.6 |
| 74.0 | 89.10 | -300.0 | -76.3 | -73.6 | -71.7 | -71.7 | -97.1 |
| 75.0 | 90.29 | -300.0 | -77.0 | -74.1 | -72.3 | -72.3 | -97.7 |
| 76.0 | 91.48 | -300.0 | -77.7 | -74.7 | -72.9 | -72.9 | -300.0 |
| 77.0 | 92.67 | -300.0 | -78.4 | -75.2 | -73.5 | -73.5 | -300.0 |
| 78.0 | 93.86 | -300.0 | -79.2 | -75.7 | -74.1 | -74.1 | -300.0 |
| 79.0 | 95.19 | -300.0 | -80.0 | -83.0 | -78.3 | -78.3 | -300.0 |
| 80.0 | 96.38 | -300.0 | -80.8 | -86.0 | -79.6 | -79.6 | -300.0 |
| 81.0 | 97.57 | -300.0 | -112.2 | -86.5 | -86.5 | -86.5 | -300.0 |
| 82.0 | 98.76 | -300.0 | -300.0 | -87.0 | -87.0 | -87.0 | -300.0 |
| 83.0 | 100.00 | -300.0 | -300.0 | -97.5 | -97.5 | -97.5 | -300.0 |

ACTIVE PERFORMANCE PREDICTION
MEDITERRANEAN WINTER SOUND SPEED PROFILE, NUC TN 1006, P. 23

SURFACE BOUNCE -- BOUNCE 0

| | | | | | | | | | | | |
|---|---|---|---|---|---|---|---|---|---|---|---|
| OUTP | 1.0 | ZX | 400.0 | | ZTG | 1000.0 | | FREQ | 2.0 | LWA | 5.0 |
| VWI | 15.0 | SALT | 35.0 | T | HS | 5.0 | C | ZBM | 6040. | REFLS | 1.0 T |
| ZONES | 2.0 | PHDX | 5.0 | T | PHDR | 5.0 | T | DELPX | 10.0 | DELPR | 10.0 |
| MUB | -27.0 T | MUV | -49.0 | T | ZC | 2000. | T | LAT | 35.0 | DUMP | .0 T |
| OUTR | 1.0 | MODE | 3.0 | U | SL | 135.0 | | DELTH | 10.0 | MPR | 2.0 |
| TBP | 10.0 | PULSE | .10+00 | T | DI | 25.6 | C | BWS | 10.0 T | BWR | 10.0 |
| NIN | -45.0 T | NOUT | -60.6 | C | TVC | 12.0 | | GDOP | 4.4 C | TGS | 15.0 T |
| RDN | -2.0 T | CLIP | .0 | T | SIGMA | 6.0 | T | PFA | .100-02 T | SP | 5. T |
| GO | .0000 N | ALFA | .1265 | N | ZL | .00 | N | ZCJ | 0. N | PHIB | 10.20 N |
| CX | 4968.13 N | CT | 4973.07 | N | CL | .00 | N | CS | 4959.97 N | CB | 5047.87 N |
| TSUR | 61.6 N | TAV | 59.9 | N | NOCZ | 2 | N | IRAP | 0 N | IAMOS | 3 N |

| RANGE (KYD) | TIME (SEC) | LOSS (DB) | ANGLE (DEG) | SIGNAL (DB) | REVERB (DB) | REV LIM | S/MN (DB) | EXCESS (DB) | PROB DETECT |
|---|---|---|---|---|---|---|---|---|---|

SEE THE DIRECT PATH OUTPUTS (MODE=1) FOR FIRST-ZONE
PERFORMANCE PREDICTIONS FOR THIS SOUND-SPEED PROFILE.

ACTIVE PERFORMANCE PREDICTION
MEDITERRANEAN WINTER SOUND SPEED PROFILE, NUC TN 1006, P. 23

SURFACE BOUNCE -- BOUNCE 1

| | | | | | | | | | | | |
|---|---|---|---|---|---|---|---|---|---|---|---|
| OUTP | 1.0 | ZX | 400.0 | | ZTG | 1000.0 | | FREQ | 2.0 | LWA | 5.0 |
| VWI | 15.0 | SALT | 35.0 | T | HS | 5.0 | C | ZBM | 6040. | REFLS | 1.0 T |
| ZONES | 2.0 | PHDX | 5.0 | T | PHDR | 5.0 | T | DELPX | 10.0 | DELPR | 10.0 |
| MUB | -27.0 T | MUV | -49.0 | T | ZC | 2000. | T | LAT | 35.0 | DUMP | .0 T |
| OUTR | 1.0 | MODE | 3.0 | U | SL | 135.0 | | DELTH | 10.0 | MPR | 2.0 |
| TBP | 10.0 | PULSE | .10+00 | T | DI | 25.6 | C | BWS | 10.0 | T | BWR 10.0 |
| NIN | -45.0 T | NOUT | -60.6 | C | TVC | 12.0 | | GDOP | 4.4 | C | TGS 15.0 T |
| RDN | -2.0 T | CLIP | .0 | T | SIGMA | 6.0 | T | PFA | .100-02 | T | SP 5. T |
| GO | .0000 N | ALFA | .1265 | N | ZL | .00 | N | ZCJ | 0. | N | PHIB 10.20 N |
| CX | 4968.13 N | CT | 4973.07 | N | CL | .00 | N | CS | 4959.97 | N | CB 5047.87 N |
| TSUR | 61.6 N | TAV | 59.9 | N | NOCZ | 2 | N | IRAP | 0 | N | IAMOS 3 N |

| RANGE (KYD) | TIME (SEC) | LOSS (DB) | ANGLE (DEG) | SIGNAL (DB) | REVERB (DB) | REV LIM | S/MN (DB) | EXCESS (DB) | PROB DETECT |
|---|---|---|---|---|---|---|---|---|---|
| 39.0 | 47.09 | 195.8 | 3.36 | -45.8 | -46.4 | YES | 4.6 | 4.6 | .7679 |
| 40.0 | 48.30 | 197.6 | 3.48 | -47.6 | -50.1 | YES | 6.0 | 6.1 | .8419 |
| 41.0 | 49.50 | 199.2 | 3.59 | -49.2 | -51.2 | YES | 5.3 | 5.4 | .8105 |
| 42.0 | 50.71 | 200.7 | 3.71 | -50.7 | -53.4 | NO | 5.4 | 5.7 | .8255 |
| 43.0 | 51.91 | 202.1 | 3.83 | -52.1 | -52.1 | YES | 3.0 | 3.2 | .6993 |
| 44.0 | 53.12 | 203.2 | 3.95 | -53.2 | -54.2 | NO | 3.3 | 3.9 | .7328 |
| 45.0 | 54.32 | 204.0 | 4.05 | -54.0 | -55.3 | NO | 3.1 | 3.9 | .7357 |
| 46.0 | 55.53 | 204.9 | 4.16 | -54.9 | -56.2 | NO | 2.7 | 3.7 | .7258 |
| 47.0 | 56.73 | 205.7 | 4.27 | -55.7 | -55.4 | NO | 1.5 | 2.3 | .6451 |
| 48.0 | 57.94 | 206.5 | 4.38 | -56.5 | -57.0 | NO | 1.5 | 2.7 | .6730 |
| 49.0 | 59.14 | 207.3 | 4.48 | -57.3 | -57.5 | NO | .9 | 2.2 | .6416 |
| 50.0 | 60.34 | 207.7 | 4.59 | -57.7 | -57.6 | NO | .5 | 1.9 | .6196 |
| 51.0 | 61.61 | 200.5 | 3.34 | -50.5 | -51.4 | YES | 4.1 | 4.2 | .7504 |
| 52.0 | 62.75 | 206.5 | 4.85 | -56.5 | -55.2 | NO | .5 | 1.3 | .5801 |
| 53.0 | 63.95 | 206.5 | 5.01 | -56.5 | -56.3 | NO | 1.1 | 2.2 | .6365 |
| 54.0 | 65.16 | 206.5 | 5.18 | -56.5 | -57.3 | NO | 1.6 | 2.9 | .6852 |
| 55.0 | 66.36 | 206.6 | 5.37 | -56.6 | -54.8 | NO | .3 | 1.0 | .5604 |
| 56.0 | 67.56 | 206.7 | 5.57 | -56.7 | -57.4 | NO | 1.5 | 2.8 | .6780 |
| 57.0 | 68.76 | 206.8 | 5.80 | -56.8 | -58.6 | NO | 1.9 | 3.5 | .7135 |
| 58.0 | 69.97 | 206.9 | 6.05 | -56.9 | -58.8 | NO | 1.8 | 3.4 | .7105 |
| 59.0 | 71.17 | 207.1 | 6.32 | -57.1 | -58.8 | NO | 1.7 | 3.3 | .7037 |
| 60.0 | 72.37 | 207.3 | 6.62 | -57.3 | -58.8 | NO | 1.5 | 3.1 | .6937 |
| 61.0 | 73.57 | 207.5 | 6.95 | -57.5 | -58.7 | NO | 1.2 | 2.8 | .6747 |
| 62.0 | 74.76 | 209.9 | 7.26 | -59.9 | -59.4 | NO | -.9 | .8 | .5495 |
| 63.0 | 75.96 | 214.2 | 7.50 | -64.2 | -60.6 | NO | -4.9 | -3.1 | .3053 |
| 64.0 | 77.16 | 216.0 | 7.70 | -66.0 | -60.7 | NO | -6.6 | -4.8 | .2214 |
| 65.0 | 78.46 | 216.7 | 6.30 | -66.7 | -63.2 | NO | -6.8 | -4.9 | .2169 |
| 66.0 | 79.66 | 216.8 | 6.72 | -66.8 | -64.5 | NO | -6.7 | -4.7 | .2231 |
| 67.0 | 80.86 | 217.7 | 7.19 | -67.7 | -65.1 | NO | -7.6 | -5.6 | .1782 |
| 68.0 | 81.94 | 220.1 | 8.40 | -70.1 | -66.7 | NO | -9.8 | -7.8 | .1184 |
| 69.0 | 83.14 | 221.0 | 8.57 | -71.0 | -67.4 | NO | -10.7 | -8.7 | .0991 |
| 70.0 | 84.33 | 221.9 | 8.75 | -71.9 | -68.2 | NO | -11.5 | -9.5 | .0793 |
| 71.0 | 85.52 | 222.8 | 8.92 | -72.8 | -69.4 | NO | -12.4 | -10.4 | .0596 |
| 72.0 | 86.72 | 223.8 | 9.09 | -73.8 | -70.1 | NO | -13.3 | -11.3 | .0388 |
| 73.0 | 87.91 | 224.7 | 9.26 | -74.7 | -71.0 | NO | -14.2 | -12.2 | .0222 |
| 74.0 | 89.10 | 225.7 | 9.43 | -75.7 | -71.7 | NO | -15.1 | -13.1 | .0186 |
| 75.0 | 90.29 | 226.6 | 9.60 | -76.6 | -72.3 | NO | -16.1 | -14.1 | .0150 |

ACTIVE PERFORMANCE PREDICTION
MEDITERRANEAN WINTER SOUND SPEED PROFILE, NUC TN 1006, P. 23

SURFACE BOUNCE -- BOUNCE 1

| | | | | | | | | | | | |
|---|---|---|---|---|---|---|---|---|---|---|---|
| OUTP | 1.0 | ZX | 400.0 | | ZTG | 1000.0 | | FREQ | 2.0 | LWA | 5.0 |
| VWI | 15.0 | SALT | 35.0 | T | HS | 5.0 | C | ZBM | 6040. | REFLS | 1.0 T |
| ZONES | 2.0 | PHDX | 5.0 | T | PHDR | 5.0 | T | DELPX | 10.0 | DELPR | 10.0 |
| MUB | -27.0 T | MUV | -49.0 | T | ZC | 2000. | T | LAT | 35.0 | DUMP | .0 T |
| OUTR | 1.0 | MODE | 3.0 | U | SL | 135.0 | | DELTH | 10.0 | MPR | 2.0 |
| TBP | 10.0 | PULSE | .10+00 | T | DI | 25.6 | C | BWS | 10.0 T | BWR | 10.0 |
| NIN | -45.0 T | NOUT | -60.6 | C | TVC | 12.0 | | GDOP | 4.4 C | TGS | 15.0 T |
| RDN | -2.0 T | CLIP | .0 | T | SIGMA | 6.0 | T | PFA | .100-02 T | SP | 5. T |
| GO | .0000 N | ALFA | .1265 | N | ZL | .00 | N | ZCJ | 0. N | PHIB | 10.20 N |
| CX | 4968.13 N | CT | 4973.07 | N | CL | .00 | N | CS | 4959.97 N | CB | 5047.87 N |
| TSUR | 61.6 N | TAV | 59.9 | N | NOCZ | 2 | N | IRAP | 0 N | IAMOS | 3 N |

| RANGE (KYD) | TIME (SEC) | LOSS (DB) | ANGLE (DEG) | SIGNAL (DB) | REVERB (DB) | REV LIM | S/MN (DB) | EXCESS (DB) | PROB DETECT |
|---|---|---|---|---|---|---|---|---|---|
| 76.0 | 91.48 | 227.6 | 9.77 | -77.6 | -72.9 | NO | -17.0 | -15.0 | .0113 |
| 77.0 | 92.67 | 228.6 | 9.94 | -78.6 | -73.5 | NO | -18.0 | -16.0 | .0076 |
| 78.0 | 93.86 | 229.5 | 10.11 | -79.5 | -74.1 | NO | -19.0 | -17.0 | .0039 |
| 79.0 | 95.19 | 237.6 | 9.61 | -87.6 | -78.3 | NO | -27.0 | -25.0 | .0000 |
| 80.0 | 96.38 | 238.6 | 9.79 | -88.6 | -79.6 | NO | -28.0 | -26.0 | .0000 |
| 81.0 | 97.57 | 239.6 | 9.98 | -89.6 | -86.5 | NO | -29.0 | -27.0 | .0000 |
| 82.0 | 98.76 | 240.7 | 10.16 | -90.7 | -87.6 | NO | -30.1 | -28.1 | .0000 |
| 83.0 | 100.00 | 272.0 | -10.07 | -122.0 | -97.5 | NO | -61.4 | -59.4 | .0000 |

```
**********
* INPUTS,  RUN  3 *
**********

HEADER
WESTERN N. ATLANTIC WINTER SOUND SPEED PROFILE, NUC TN 1006, P. 47
  SSP 0 1488.0 10 1488.2 20 1488.6 30 1488.8 50 1488.8 75 1489.0 100 1489.2
* 125 1489.3 150 1489.6 200 1489.5 250 1485.5 300 1479.9 400 1477.2 500 1476.6
* 600 1476.6 700 1476.7 800 1477.2 900 1477.8 1000 1478.6 1100 1479.4
* 1200 1480.5 1300 1481.7 1400 1483.0 1500 1484.4 1750 1487.9 2000 1491.3
* 2500 1498.57 3000 1506.52 4000 1523.85
ZBM 17372
ZA 20, ZTG 300
PHDX=0, PHDR=0
OUTP 0
MODE=1,RUN

**********
* CALCULATIONS,  RUN  3 *
**********


BEAMX IS THE SIN(X)/X RESPONSE FUNCTION FOR A CONTINUOUS LINE ARRAY

BEAMR IS THE SIN(X)/X RESPONSE FUNCTION FOR A CONTINUOUS LINE ARRAY



THE LETTERS FOLLOWING THE NUMBERS IN THE HEADING ON THE
PERFORMANCE PREDICTION PAGE SIGNIFY THE FOLLOWING,

  U      USER HAS SPECIFIED THIS INPUT VALUE ON THIS RUN
BLANK    SET BY USER ON A PREVIOUS RUN
  T      TYPICAL VALUE SET IN ABSENCE OF USER SPECIFICATION
  C      CALCULATED INTERNALLY BY PROGRAM (USER OPTION)
  W      WRONG VALUE SPECIFIED BY USER (OUT OF RANGE OF ALLOW-
           ABLE VALUES.  THE PRINTED VALUE IS A TYPICAL VALUE.)
  N      NOT AN INPUT, CALCULATED INTERNALLY.
```

SOUND SPEED PROFILE AFTER EARTH CURVATURE CORRECTION AND CURVE FITTING

| LAYER NUMBER | DEPTH (FT) | SOUND SPEED (FT/SEC) | SSP SEGMENT PARAMETERS (JASA, VOL. 41, NO. 2, PP. 419-438) CA**2 | KA | ZA |
|---|---|---|---|---|---|
| 1 | .000 | 4881.824251 | .2214913+08 | .4066880-09 | -.1317770+05 |
| 2 | 65.566 | 4883.675617 | .2385609+08 | -.1383460-06 | .1074963+03 |
| 3 | 92.310 | 4884.191610 | .2386202+08 | -.1573519-07 | .2258650+03 |
| 4 | 164.148 | 4884.730599 | .2385417+08 | .3503356-08 | -.1129618+03 |
| 5 | 410.060 | 4886.415517 | .2388801+08 | -.7341937-08 | .6599851+03 |
| 6 | 495.840 | 4887.052483 | .2388441+08 | -.3073871-07 | .5350405+03 |
| MAX | 535.040 | 4887.1679002 | .2388441+08 | -.3073871-07 | .5350405+03 |
| 8 | 546.801 | 4887.157511 | .3582575+08 | -.5880864-12 | -.9214970+06 |
| 9 | 625.626 | 4887.018249 | .2388296+08 | -.2389725-06 | .6241136+03 |
| 10 | 652.959 | 4886.533793 | .2388232+08 | -.2760177-06 | .6279857+03 |
| 11 | 680.292 | 4885.110177 | .2399920+08 | -.3723707-07 | .2906778+03 |
| 12 | 964.329 | 4858.022883 | .2355957+08 | .3506278-06 | .1034561+04 |
| 13 | 984.849 | 4855.924476 | .2357178+08 | .8723283-06 | .1004841+04 |
| 14 | 998.522 | 4855.162433 | .3530054+08 | -.1369661-09 | -.5927139+05 |
| 15 | 1273.013 | 4847.816046 | .2348977+08 | .6197013-07 | .1362057+04 |
| 16 | 1327.706 | 4846.862134 | .2347903+08 | .8531808-08 | .1577096+04 |
| 17 | 1491.709 | 4845.666728 | .2347286+08 | .1632508-08 | .1937840+04 |
| MIN | 1937.840 | 4844.8794312 | .2347286+08 | .1632508-08 | .1937840+04 |
| 19 | 2952.988 | 4848.959949 | .2330293+08 | .3038165-09 | -.2462254+04 |
| 20 | 3281.020 | 4851.682678 | .2348170+08 | .1273930-08 | .1900813+04 |
| 21 | 3609.212 | 4854.825910 | .2334022+08 | .4814184-09 | -.8843195+03 |
| 22 | 4921.878 | 4870.859697 | .2255981+08 | .1485947-09 | -.1326012+05 |
| 23 | 5673.810 | 4881.516253 | .2595228+08 | -.1175741-09 | .3320168+05 |
| 24 | 6562.554 | 4894.250660 | .2252955+08 | .1243471-09 | -.1530363+05 |
| 25 | 9844.916 | 4944.954444 | .2169439+08 | .8038726-10 | -.2761407+05 |
| 26 | 11720.039 | 4977.532418 | .2959689+08 | -.9563049-10 | .5682859+05 |
| 27 | 13612.084 | 5011.165179 | .3792102+08 | -.5496851-10 | .1099431+06 |
| 28 | 17379.253 | 5077.355440 | .0000000 | .0000000 | .0000000 |

REVERBERATION LEVELS AT TIMES CORRESPONDING TO 2-WAY
ACOUSTIC TRAVEL TIMES BETWEEN SOURCE AND TARGET.
( 2 PINGS -- TIME BETWEEN PINGS IS 10.00 SECONDS.)
THE SOUND PROPAGATES BETWEEN SOURCE AND TARGET BY

SURFACE CHANNEL

| TARGET RANGE KYD | TWO-WAY TIME SEC | BOTTOM REVERB DB | SURFACE REVERB DB | VOLUME REVERB DB | TOTAL REVERB DB | PING 1 REVERB DB | PING 2 REVERB DB |
|---|---|---|---|---|---|---|---|
| 1.0 | 1.23 | -300.0 | -5.0 | .7 | 1.7 | 1.7 | -30.5 |
| 2.0 | 2.46 | -300.0 | -8.3 | -8.7 | -5.5 | -5.5 | -32.4 |
| 3.0 | 3.69 | -300.0 | -6.5 | -14.3 | -5.8 | -5.8 | -34.0 |
| 4.0 | 4.92 | -300.0 | -25.3 | -18.4 | -16.6 | -16.7 | -35.4 |
| 5.0 | 6.15 | -300.0 | -27.6 | -21.7 | -19.7 | -19.8 | -35.9 |
| 6.0 | 7.37 | -57.2 | -33.8 | -24.4 | -22.6 | -22.9 | -34.7 |
| 7.0 | 8.60 | -55.1 | -40.9 | -26.8 | -25.3 | -25.6 | -37.0 |
| 8.0 | 9.83 | -57.4 | -46.2 | -29.3 | -27.8 | -28.0 | -41.7 |
| 9.0 | 11.06 | -58.6 | -48.5 | -31.6 | -30.0 | -30.2 | -44.1 |
| 10.0 | 12.29 | -74.2 | -47.1 | -33.8 | -31.9 | -32.1 | -45.5 |
| 11.0 | 13.52 | -53.7 | -45.6 | -35.8 | -33.6 | -33.8 | -46.6 |
| 12.0 | 14.75 | -50.4 | -43.8 | -37.7 | -35.0 | -35.2 | -47.6 |
| 13.0 | 15.98 | -52.8 | -40.7 | -39.5 | -35.6 | -35.9 | -48.7 |
| 14.0 | 17.21 | -60.0 | -37.0 | -41.2 | -34.9 | -35.0 | -49.7 |
| 15.0 | 18.44 | -80.7 | -37.8 | -42.8 | -36.0 | -36.1 | -50.8 |
| 16.0 | 19.66 | -82.8 | -47.2 | -44.4 | -40.9 | -41.2 | -51.9 |
| 17.0 | 20.89 | -72.4 | -62.3 | -46.0 | -43.4 | -43.9 | -53.0 |
| 18.0 | 22.12 | -65.1 | -70.3 | -47.5 | -44.7 | -45.3 | -53.9 |
| 19.0 | 23.35 | -61.5 | -70.0 | -48.7 | -45.8 | -46.4 | -54.7 |
| 20.0 | 24.58 | -59.9 | -69.3 | -49.9 | -46.8 | -47.5 | -55.1 |
| 21.0 | 25.81 | -59.4 | -68.5 | -51.0 | -47.6 | -48.5 | -54.8 |
| 22.0 | 27.04 | -59.9 | -67.0 | -52.2 | -48.9 | -49.6 | -57.0 |
| 23.0 | 28.27 | -60.8 | -65.9 | -53.4 | -50.1 | -50.7 | -59.3 |
| 24.0 | 29.50 | -62.1 | -65.1 | -54.5 | -51.3 | -51.8 | -61.0 |
| 25.0 | 30.73 | -63.6 | -64.0 | -55.7 | -52.4 | -52.8 | -62.4 |
| 26.0 | 31.95 | -65.4 | -63.1 | -56.8 | -53.4 | -53.8 | -63.7 |
| 27.0 | 33.18 | -67.5 | -61.7 | -57.9 | -54.2 | -54.6 | -64.8 |
| 28.0 | 34.41 | -69.8 | -60.0 | -59.0 | -54.7 | -55.1 | -65.9 |
| 29.0 | 35.64 | -72.4 | -57.9 | -60.2 | -54.6 | -54.9 | -66.9 |
| 30.0 | 36.87 | -75.5 | -60.2 | -61.3 | -56.3 | -56.6 | -67.9 |
| 31.0 | 38.10 | -79.4 | -65.1 | -62.4 | -58.6 | -59.0 | -68.9 |
| 32.0 | 39.33 | -84.6 | -69.9 | -63.5 | -60.3 | -60.8 | -69.8 |
| 33.0 | 40.56 | -92.1 | -74.7 | -64.6 | -61.7 | -62.3 | -70.8 |
| 34.0 | 41.79 | -89.9 | -67.8 | -65.7 | -63.0 | -63.6 | -71.7 |
| 35.0 | 43.02 | -89.3 | -68.9 | -66.8 | -64.0 | -64.7 | -72.7 |
| 36.0 | 44.25 | -88.7 | -69.9 | -67.9 | -65.1 | -65.7 | -73.6 |
| 37.0 | 45.47 | -88.0 | -70.8 | -68.9 | -66.1 | -66.7 | -74.6 |
| 38.0 | 46.70 | -88.8 | -71.8 | -70.0 | -67.1 | -67.8 | -75.5 |
| 39.0 | 47.93 | -91.0 | -72.6 | -71.1 | -68.1 | -68.7 | -76.5 |
| 40.0 | 49.16 | -93.1 | -73.5 | -72.1 | -69.0 | -69.7 | -77.4 |
| 41.0 | 50.39 | -95.2 | -74.3 | -73.2 | -70.0 | -70.7 | -78.4 |
| 42.0 | 51.62 | -98.0 | -75.0 | -74.2 | -70.9 | -71.6 | -79.4 |
| 43.0 | 52.85 | -105.0 | -75.9 | -75.3 | -28.7 | -72.5 | -28.7 |
| 44.0 | 54.08 | -112.0 | -76.7 | -76.3 | -33.4 | -73.5 | -33.4 |
| 45.0 | 55.31 | -118.9 | -77.5 | -77.3 | -33.5 | -74.4 | -33.5 |

REVERBERATION LEVELS AT TIMES CORRESPONDING TO 2-WAY
ACOUSTIC TRAVEL TIMES BETWEEN SOURCE AND TARGET.
( 2 PINGS -- TIME BETWEEN PINGS IS 10.00 SECONDS.)
THE SOUND PROPAGATES BETWEEN SOURCE AND TARGET BY

SURFACE CHANNEL

| TARGET RANGE KYD | TWO-WAY TIME SEC | BOTTOM REVERB DB | SURFACE REVERB DB | VOLUME REVERB DB | TOTAL REVERB DB | PING 1 REVERB DB | PING 2 REVERB DB |
|---|---|---|---|---|---|---|---|
| 46.0 | 56.54 | -125.9 | -78.4 | -78.4 | -38.8 | -75.4 | -38.8 |
| 47.0 | 57.76 | -125.0 | -79.3 | -79.4 | -41.2 | -76.3 | -41.2 |
| 48.0 | 58.99 | -121.4 | -80.2 | -80.5 | -43.2 | -77.3 | -43.2 |
| 49.0 | 60.22 | -117.8 | -81.1 | -81.5 | -46.1 | -78.3 | -46.1 |
| 50.0 | 61.45 | -114.3 | -82.1 | -82.5 | -48.4 | -79.3 | -48.4 |
| 51.0 | 62.68 | -111.2 | -83.1 | -26.1 | -26.1 | -26.1 | -50.4 |
| 52.0 | 63.91 | -108.8 | -29.1 | -34.5 | -28.0 | -28.0 | -52.1 |
| 53.0 | 65.14 | -106.5 | -49.4 | -30.4 | -30.4 | -30.4 | -53.5 |
| 54.0 | 66.37 | -104.2 | -52.8 | -38.6 | -38.3 | -38.4 | -54.9 |
| 55.0 | 67.60 | -102.1 | -55.4 | -41.1 | -40.8 | -40.9 | -56.1 |
| 56.0 | 68.83 | -101.4 | -57.8 | -43.1 | -42.8 | -42.9 | -57.2 |
| 57.0 | 70.05 | -100.7 | -60.1 | -46.0 | -45.6 | -45.8 | -58.2 |
| 58.0 | 71.28 | -100.0 | -62.5 | -48.3 | -47.8 | -48.2 | -59.1 |
| 59.0 | 72.51 | -99.4 | -64.8 | -50.3 | -50.1 | -50.2 | -67.9 |
| 60.0 | 73.74 | -99.4 | -67.1 | -52.0 | -51.9 | -51.9 | -73.8 |
| 61.0 | 74.97 | -99.3 | -69.3 | -53.4 | -53.3 | -53.3 | -76.1 |
| 62.0 | 76.20 | -99.2 | -71.3 | -54.8 | -54.7 | -54.7 | -81.0 |
| 63.0 | 77.43 | -99.2 | -73.1 | -56.0 | -55.9 | -55.9 | -83.0 |
| 64.0 | 78.66 | -99.5 | -74.7 | -57.1 | -57.1 | -57.1 | -84.9 |
| 65.0 | 79.89 | -99.7 | -76.0 | -58.2 | -58.1 | -58.1 | -87.2 |
| 66.0 | 81.12 | -100.0 | -77.0 | -59.1 | -59.0 | -59.0 | -89.1 |
| 67.0 | 82.35 | -100.3 | -83.4 | -67.9 | -67.7 | -67.8 | -91.0 |
| 68.0 | 83.57 | -100.8 | -85.7 | -73.8 | -73.5 | -73.5 | -103.5 |
| 69.0 | 84.80 | -101.2 | -88.0 | -76.0 | -75.7 | -75.8 | -104.4 |
| 70.0 | 86.03 | -101.7 | -90.3 | -81.3 | -80.7 | -80.7 | -105.2 |
| 71.0 | 87.26 | -102.3 | -92.5 | -83.2 | -82.7 | -82.7 | -106.1 |
| 72.0 | 88.49 | -102.8 | -94.8 | -85.2 | -84.6 | -84.7 | -108.6 |
| 73.0 | 89.72 | -103.4 | -108.8 | -87.1 | -87.0 | -87.0 | -109.4 |
| 74.0 | 90.95 | -104.1 | -109.9 | -89.0 | -88.8 | -88.9 | -110.3 |
| 75.0 | 92.18 | -104.7 | -110.9 | -91.0 | -90.7 | -90.8 | -111.2 |
| 76.0 | 93.41 | -105.4 | -111.9 | -109.8 | -102.9 | -103.4 | -112.1 |
| 77.0 | 94.64 | -106.2 | -112.9 | -110.8 | -103.7 | -104.3 | -113.1 |
| 78.0 | 95.86 | -106.9 | -114.0 | -111.9 | -104.6 | -105.1 | -114.1 |
| 79.0 | 97.09 | -107.7 | -115.0 | -112.9 | -105.5 | -106.0 | -115.2 |
| 80.0 | 98.32 | -108.5 | -300.0 | -300.0 | -107.8 | -108.5 | -116.3 |

ACTIVE PERFORMANCE PREDICTION
WESTERN N. ATLANTIC WINTER SOUND SPEED PROFILE, NUC TN 1006, P. 47

SURFACE CHANNEL

| | | | | | | | | | | | |
|---|---|---|---|---|---|---|---|---|---|---|---|
| OUTP | .0 | U | ZX | 20.0 | U | ZTG | 300.0 | U | FREQ | 2.0 | LRA | 5.0 | |
| VMI | 15.0 | | SALT | 35.0 | T | HS | 5.0 | C | ZBM | 17372. | U | REFLS | 1.0 | T |
| ZONES | 2.0 | | PHDX | .0 | U | PHDR | .0 | U | DELPX | 10.0 | | DELPR | 10.0 | |
| MUB | -27.0 | T | MUV | -49.0 | T | ZC | 2000. | T | LAT | 35.0 | | DUMP | .0 | T |
| OUTR | 1.0 | | MODE | 1.0 | U | SL | 135.0 | | DELTH | 10.0 | | MPR | 2.0 | |
| TBP | 10.0 | | PULSE | .10+00 | T | DI | 25.6 | C | BWS | 10.0 | T | BWR | 10.0 | |
| NIN | -45.0 | T | NOUT | -60.6 | C | TVC | 12.0 | | GDOP | 4.4 | C | TGS | 15.0 | T |
| RDN | -2.0 | T | CLIP | .0 | T | SIGMA | 6.0 | T | PFA | .100-02 | T | SP | 5. | T |
| GO | .0107 | N | ALFA | .1283 | N | ZL | 492.13 | N | ZCJ | 6152. | N | PHIB | 15.93 | N |
| CX | 4882.39 | N | CT | 4885.53 | N | CL | 4887.14 | N | CS | 4861.89 | N | CB | 5077.36 | N |
| TSUR | 49.0 | N | TAV | 36.4 | N | NOCZ | 0 | N | IRAP | 0 | N | IAMOS | 1 | N |

| RANGE (KYD) | TIME (SEC) | LOSS (DB) | ANGLE (DEG) | SIGNAL (DB) | REVERB (DB) | REV LIM | S/MN (DB) | EXCESS (DB) | PROB DETECT |
|---|---|---|---|---|---|---|---|---|---|
| 1.0 | 1.23 | 120.6 | .00 | 29.4 | 1.7 | YES | 32.1 | 32.1 | 1.0000 |
| 2.0 | 2.46 | 133.2 | .00 | 16.8 | -5.5 | YES | 26.7 | 26.7 | 1.0000 |
| 3.0 | 3.69 | 140.8 | .00 | 9.2 | -5.8 | YES | 19.4 | 19.4 | 1.0000 |
| 4.0 | 4.92 | 146.4 | .00 | 3.6 | -16.6 | YES | 24.7 | 24.7 | 1.0000 |
| 5.0 | 6.15 | 150.9 | .00 | -.9 | -19.7 | YES | 23.2 | 23.2 | 1.0000 |
| 6.0 | 7.37 | 154.8 | .00 | -4.8 | -22.6 | YES | 22.3 | 22.3 | 1.0000 |
| 7.0 | 8.60 | 158.3 | .00 | -8.3 | -25.3 | YES | 21.4 | 21.4 | 1.0000 |
| 8.0 | 9.83 | 161.6 | .00 | -11.6 | -27.8 | YES | 20.7 | 20.7 | 1.0000 |
| 9.0 | 11.06 | 164.5 | .00 | -14.5 | -30.0 | YES | 19.9 | 19.9 | 1.0000 |
| 10.0 | 12.29 | 167.3 | .00 | -17.3 | -31.9 | YES | 19.1 | 19.1 | 1.0000 |
| 11.0 | 13.52 | 169.8 | .00 | -19.8 | -33.6 | YES | 18.2 | 18.2 | 1.0000 |
| 12.0 | 14.75 | 172.3 | .00 | -22.3 | -35.0 | YES | 17.1 | 17.1 | .9966 |
| 13.0 | 15.98 | 174.6 | .00 | -24.6 | -35.6 | YES | 15.5 | 15.5 | .9903 |
| 14.0 | 17.21 | 176.8 | .00 | -26.8 | -34.9 | YES | 12.5 | 12.5 | .9789 |
| 15.0 | 18.44 | 178.9 | .00 | -28.9 | -36.0 | YES | 11.5 | 11.5 | .9652 |
| 16.0 | 19.66 | 180.9 | .00 | -30.9 | -40.9 | YES | 14.3 | 14.3 | .9857 |
| 17.0 | 20.89 | 182.8 | .00 | -32.8 | -43.4 | YES | 14.8 | 14.8 | .9879 |
| 18.0 | 22.12 | 184.2 | .00 | -34.2 | -44.7 | YES | 14.7 | 14.7 | .9872 |
| 19.0 | 23.35 | 185.7 | .00 | -35.7 | -45.8 | YES | 14.2 | 14.2 | .9855 |
| 20.0 | 24.58 | 187.1 | .00 | -37.1 | -46.8 | YES | 13.7 | 13.7 | .9834 |
| 21.0 | 25.81 | 188.5 | .00 | -38.5 | -47.6 | YES | 13.0 | 13.0 | .9809 |
| 22.0 | 27.04 | 189.8 | .00 | -39.8 | -48.9 | YES | 12.7 | 12.7 | .9799 |
| 23.0 | 28.27 | 191.2 | .00 | -41.2 | -50.1 | YES | 12.4 | 12.4 | .9787 |
| 24.0 | 29.50 | 192.5 | .00 | -42.5 | -51.3 | YES | 12.0 | 12.1 | .9773 |
| 25.0 | 30.73 | 193.9 | .00 | -43.9 | -52.4 | YES | 11.4 | 11.7 | .9690 |
| 26.0 | 31.95 | 195.2 | .00 | -45.2 | -53.4 | NO | 10.8 | 11.2 | .9584 |
| 27.0 | 33.18 | 196.5 | .00 | -46.5 | -54.2 | NO | 10.1 | 10.6 | .9444 |
| 28.0 | 34.41 | 197.7 | .00 | -47.7 | -54.7 | NO | 9.1 | 9.7 | .9244 |
| 29.0 | 35.64 | 199.0 | .00 | -49.0 | -54.6 | NO | 7.8 | 8.4 | .8941 |
| 30.0 | 36.87 | 200.3 | .00 | -50.3 | -56.3 | NO | 7.4 | 8.4 | .8956 |
| 31.0 | 38.10 | 201.5 | .00 | -51.5 | -58.6 | NO | 7.1 | 8.7 | .9018 |
| 32.0 | 39.33 | 202.8 | .00 | -52.8 | -60.3 | NO | 6.4 | 8.3 | .8919 |
| 33.0 | 40.56 | 204.0 | .00 | -54.0 | -61.7 | NO | 5.6 | 7.5 | .8739 |
| 34.0 | 41.79 | 205.2 | .00 | -55.2 | -63.0 | NO | 4.6 | 6.6 | .8526 |
| 35.0 | 43.02 | 206.4 | .00 | -56.4 | -64.0 | NO | 3.5 | 5.5 | .8157 |
| 36.0 | 44.25 | 207.7 | .00 | -57.7 | -65.1 | NO | 2.4 | 4.4 | .7620 |
| 37.0 | 45.47 | 208.9 | .00 | -58.9 | -66.1 | NO | 1.3 | 3.3 | .7071 |

ACTIVE PERFORMANCE PREDICTION
WESTERN N. ATLANTIC WINTER SOUND SPEED PROFILE, NUC TN 1006, P. 47

SURFACE CHANNEL

| | | | | | | | | | | | |
|---|---|---|---|---|---|---|---|---|---|---|---|
| OUTP | .0 | U | ZX | 20.0 | U | ZTG | 300.0 | U | FREQ | 2.0 | | LWA | 5.0 | |
| VWI | 15.0 | | SALT | 35.0 | T | HS | 5.0 | C | ZBM | 17372. | U | REFLS | 1.0 | T |
| ZONES | 2.0 | | PHDX | .0 | U | PHDR | .0 | U | DELPX | 10.0 | | DELPR | 10.0 | |
| MUB | -27.0 | T | MUV | -49.0 | T | ZC | 2000. | T | LAT | 35.0 | | DUMP | .0 | T |
| OUTR | 1.0 | | MODE | 1.0 | U | SL | 135.0 | | DELTH | 10.0 | | MPR | 2.0 | |
| TBP | 10.0 | | PULSE | .10+00 | T | DI | 25.6 | C | BWS | 10.0 | T | BWR | 10.0 | |
| NIN | -45.0 | T | NOUT | -60.6 | C | TVC | 12.0 | | GDOP | 4.4 | C | TGS | 15.0 | T |
| RDN | -2.0 | T | CLIP | .0 | T | SIGMA | 6.0 | T | PFA | .100-02 | T | SP | 5. | T |
| GO | .0107 | N | ALFA | .1283 | N | ZL | 492.13 | N | ZCJ | 6152. | N | PHIB | 15.93 | N |
| CX | 4882.39 | N | CT | 4885.53 | N | CL | 4887.14 | N | CS | 4881.89 | N | CB | 5077.36 | N |
| TSUR | 49.0 | N | TAV | 36.4 | N | NOCZ | 0 | N | IRAP | 0 | N | IAMOS | 1 | N |

| RANGE (KYD) | TIME (SEC) | LOSS (DB) | ANGLE (DEG) | SIGNAL (DB) | REVERB (DB) | REV LIM | S/MN (DB) | EXCESS (DB) | PROB DETECT |
|---|---|---|---|---|---|---|---|---|---|
| 38.0 | 46.70 | 210.1 | .00 | -60.1 | -67.1 | NO | .2 | 2.2 | .6412 |
| 39.0 | 47.93 | 211.3 | .00 | -61.3 | -68.1 | NO | -.9 | 1.1 | .5698 |
| 40.0 | 49.16 | 212.4 | .00 | -62.4 | -69.0 | NO | -2.0 | -.0 | .4981 |
| 41.0 | 50.39 | 213.6 | .00 | -63.6 | -70.0 | NO | -3.2 | -1.2 | .4259 |
| 42.0 | 51.62 | 214.8 | .00 | -64.8 | -70.9 | NO | -4.3 | -2.3 | .3536 |
| 43.0 | 52.85 | 216.0 | .00 | -66.0 | -28.7 | YES | -32.9 | -32.9 | .0000 |
| 44.0 | 54.08 | 217.1 | .00 | -67.1 | -33.4 | YES | -29.3 | -29.3 | .0000 |
| 45.0 | 55.31 | 218.3 | .00 | -68.3 | -33.5 | YES | -30.4 | -30.4 | .0000 |
| 46.0 | 56.54 | 219.5 | .00 | -69.5 | -38.8 | YES | -26.3 | -26.3 | .0000 |
| 47.0 | 57.76 | 220.6 | .00 | -70.6 | -41.2 | YES | -25.1 | -25.1 | .0000 |
| 48.0 | 58.99 | 221.8 | .00 | -71.8 | -43.2 | YES | -24.3 | -24.3 | .0000 |
| 49.0 | 60.22 | 222.9 | .00 | -72.9 | -46.1 | YES | -22.8 | -22.8 | .0000 |
| 50.0 | 61.45 | 224.1 | .00 | -74.1 | -48.4 | YES | -21.8 | -21.8 | .0000 |
| 51.0 | 62.68 | 225.2 | .00 | -75.2 | -26.1 | YES | -44.7 | -44.7 | .0000 |
| 52.0 | 63.91 | 226.3 | .00 | -76.3 | -28.0 | YES | -43.9 | -43.9 | .0000 |
| 53.0 | 65.14 | 227.5 | .00 | -77.5 | -30.4 | YES | -42.7 | -42.7 | .0000 |
| 54.0 | 66.37 | 228.6 | .00 | -78.6 | -38.3 | YES | -35.9 | -35.9 | .0000 |
| 55.0 | 67.60 | 229.7 | .00 | -79.7 | -40.8 | YES | -34.6 | -34.6 | .0000 |
| 56.0 | 68.83 | 230.8 | .00 | -80.8 | -42.8 | YES | -33.8 | -33.8 | .0000 |
| 57.0 | 70.05 | 232.0 | .00 | -82.0 | -45.6 | YES | -32.3 | -32.3 | .0000 |
| 58.0 | 71.28 | 233.1 | .00 | -83.1 | -47.8 | YES | -31.4 | -31.4 | .0000 |
| 59.0 | 72.51 | 234.2 | .00 | -84.2 | -50.1 | YES | -30.6 | -30.6 | .0000 |
| 60.0 | 73.74 | 235.3 | .00 | -85.3 | -51.9 | YES | -30.4 | -30.2 | .0000 |
| 61.0 | 74.97 | 236.4 | .00 | -86.4 | -53.3 | NO | -30.5 | -30.1 | .0000 |
| 62.0 | 76.20 | 237.5 | .00 | -87.5 | -54.7 | NO | -30.7 | -30.1 | .0000 |
| 63.0 | 77.43 | 238.6 | .00 | -88.6 | -55.9 | NO | -31.1 | -30.2 | .0000 |
| 64.0 | 78.66 | 239.7 | .00 | -89.7 | -57.1 | NO | -31.7 | -30.5 | .0000 |
| 65.0 | 79.89 | 240.8 | .00 | -90.8 | -58.1 | NO | -32.4 | -30.9 | .0000 |
| 66.0 | 81.12 | 241.9 | .00 | -91.9 | -59.0 | NO | -33.1 | -31.5 | .0000 |
| 67.0 | 82.35 | 243.0 | .00 | -93.0 | -67.7 | NO | -32.7 | -30.7 | .0000 |
| 68.0 | 83.57 | 244.1 | .00 | -94.1 | -73.5 | NO | -33.6 | -31.6 | .0000 |
| 69.0 | 84.80 | 245.2 | .00 | -95.2 | -75.7 | NO | -34.6 | -32.6 | .0000 |
| 70.0 | 86.03 | 246.3 | .00 | -96.3 | -80.7 | NO | -35.7 | -33.7 | .0000 |
| 71.0 | 87.26 | 247.4 | .00 | -97.4 | -82.7 | NO | -36.8 | -34.8 | .0000 |
| 72.0 | 88.49 | 248.5 | .00 | -98.5 | -84.6 | NO | -37.9 | -35.9 | .0000 |
| 73.0 | 89.72 | 249.6 | .00 | -99.6 | -87.0 | NO | -39.0 | -37.0 | .0000 |
| 74.0 | 90.95 | 250.7 | .00 | -100.7 | -88.8 | NO | -40.0 | -38.0 | .0000 |

ACTIVE PERFORMANCE PREDICTION
WESTERN N. ATLANTIC WINTER SOUND SPEED PROFILE, NUC TN 1006, P. 47

SURFACE CHANNEL

| | | | | | | | | | | | | | | | |
|---|---|---|---|---|---|---|---|---|---|---|---|---|---|---|---|
| OUTP | .0 | U | ZX | 20.0 | U | ZTG | 300.0 | U | FREQ | 2.0 | | LWA | 5.0 | | |
| VWI | 15.0 | | SALT | 35.0 | T | HS | 5.0 | C | ZBM | 17372. | U | REFLS | 1.0 | T |
| ZONES | 2.0 | | PHDX | .0 | U | PHDR | .0 | U | DELPX | 10.0 | | DELPR | 10.0 | | |
| MUB | -27.0 | T | MUV | -49.0 | T | ZC | 2000. | T | LAT | 35.0 | | DUMP | .0 | T | |
| OUTR | 1.0 | | MODE | 1.0 | U | SL | 135.0 | | DELTH | 10.0 | | MPR | 2.0 | | |
| TBP | 10.0 | | PULSE | .10+00 | T | DI | 25.6 | C | BWS | 10.0 | T | BWR | 10.0 | | |
| NIN | -45.0 | T | NOUT | -60.6 | C | TVC | 12.0 | | GDOP | 4.4 | C | TGS | 15.0 | T | |
| RDN | -2.0 | T | CLIP | .0 | T | SIGMA | 6.0 | T | PFA | .100-02 | T | SP | 5. | T | |
| GD | .0107 | N | ALFA | .1283 | N | ZL | 492.13 | N | ZCJ | 6152. | N | PHIB | 15.93 | N | |
| CX | 4882.39 | N | CT | 4885.53 | N | CL | 4887.14 | N | CS | 4881.89 | N | CB | 5077.36 | N | |
| TSUR | 49.0 | N | TAV | 36.4 | N | NOCZ | 0 | N | IRAP | 0 | N | IAMOS | 1 | N | |

| RANGE (KYD) | TIME (SEC) | LOSS (DB) | ANGLE (DEG) | SIGNAL (DB) | REVERB (DB) | REV LIM | S/MN (DB) | EXCESS (DB) | PROB DETECT |
|---|---|---|---|---|---|---|---|---|---|
| 75.0 | 92.18 | 251.8 | .00 | -101.8 | -90.7 | NO | -41.1 | -39.1 | .0000 |
| 76.0 | 93.41 | 252.8 | .00 | -102.8 | -102.9 | NO | -42.2 | -40.2 | .0000 |
| 77.0 | 94.64 | 253.9 | .00 | -103.9 | -103.7 | NO | -43.3 | -41.3 | .0000 |
| 78.0 | 95.86 | 255.0 | .00 | -105.0 | -104.6 | NO | -44.4 | -42.4 | .0000 |
| 79.0 | 97.09 | 256.1 | .00 | -106.1 | -105.5 | NO | -45.4 | -43.4 | .0000 |
| 80.0 | 98.32 | 257.1 | .00 | -107.1 | -107.8 | NO | -46.5 | -44.5 | .0000 |

```
**********
* INPUTS,  RUN  4 *
**********

PHDX=40, PHDR=40
MODE=2,RUN

**********
* CALCULATIONS,  RUN  4 *
**********

 BEAMX IS THE SIN(X)/X RESPONSE FUNCTION FOR A CONTINUOUS LINE ARRAY

 BEAMR IS THE SIN(X)/X RESPONSE FUNCTION FOR A CONTINUOUS LINE ARRAY


 THE LETTERS FOLLOWING THE NUMBERS IN THE HEADING ON THE
 PERFORMANCE PREDICTION PAGE SIGNIFY THE FOLLOWING,

   U      USER HAS SPECIFIED THIS INPUT VALUE ON THIS RUN
 BLANK    SET BY USER ON A PREVIOUS RUN
   T      TYPICAL VALUE SET IN ABSENCE OF USER SPECIFICATION
   C      CALCULATED INTERNALLY BY PROGRAM (USER OPTION)
   W      WRONG VALUE SPECIFIED BY USER (OUT OF RANGE OF ALLOW-
            ABLE VALUES.  THE PRINTED VALUE IS A TYPICAL VALUE.)
   N      NOT AN INPUT, CALCULATED INTERNALLY.
```

REVERBERATION LEVELS AT TIMES CORRESPONDING TO 2-WAY
ACOUSTIC TRAVEL TIMES BETWEEN SOURCE AND TARGET.
( 2 PINGS -- TIME BETWEEN PINGS IS 10.00 SECONDS.)
THE SOUND PROPAGATES BETWEEN SOURCE AND TARGET BY

BOTTOM BOUNCE -- BOUNCE 1

| TARGET RANGE KYD | TWO-WAY TIME SEC | BOTTOM REVERB DB | SURFACE REVERB DB | VOLUME REVERB DB | TOTAL REVERB DB | PING 1 REVERB DB | PING 2 REVERB DB |
|---|---|---|---|---|---|---|---|
| 1.0 | 14.11 | -52.4 | -49.4 | -85.2 | -31.7 | -47.6 | -31.9 |
| 2.0 | 14.30 | -62.1 | -47.3 | -83.6 | -32.7 | -47.1 | -32.9 |
| 3.0 | 14.52 | -71.8 | -44.9 | -83.0 | -33.7 | -44.9 | -34.0 |
| 4.0 | 14.82 | -77.5 | -42.5 | -82.1 | -34.8 | -42.5 | -35.6 |
| 5.0 | 15.31 | -76.6 | -43.7 | -80.3 | -37.1 | -43.7 | -38.2 |
| 6.0 | 15.80 | -76.1 | -44.9 | -78.2 | -39.3 | -44.8 | -40.8 |
| 7.0 | 16.36 | -73.0 | -46.8 | -80.0 | -42.0 | -46.8 | -43.7 |
| 8.0 | 17.07 | -49.8 | -53.6 | -82.1 | -44.9 | -48.3 | -47.5 |
| 9.0 | 17.77 | -47.0 | -60.4 | -84.5 | -46.7 | -46.8 | -61.2 |
| 10.0 | 18.52 | -46.7 | -64.8 | -75.8 | -46.7 | -46.7 | -73.6 |
| 11.0 | 19.36 | -47.6 | -52.2 | -62.4 | -46.2 | -46.2 | -66.8 |
| 12.0 | 20.21 | -49.8 | -39.7 | -48.9 | -38.8 | -38.8 | -58.3 |
| 13.0 | 21.08 | -52.4 | -28.0 | -46.3 | -27.9 | -28.0 | -49.6 |
| 14.0 | 22.03 | -55.8 | -29.1 | -46.5 | -28.9 | -29.0 | -45.7 |
| 15.0 | 22.97 | -59.7 | -30.1 | -47.1 | -29.9 | -30.0 | -46.4 |
| 16.0 | 23.93 | -63.8 | -31.2 | -50.1 | -31.0 | -31.1 | -47.0 |
| 17.0 | 24.94 | -68.5 | -36.3 | -54.4 | -35.9 | -36.2 | -47.7 |
| 18.0 | 25.95 | -73.4 | -41.7 | -59.4 | -40.7 | -41.6 | -48.3 |
| 19.0 | 26.97 | -78.4 | -47.0 | -68.7 | -45.7 | -47.0 | -51.8 |
| 20.0 | 28.03 | -79.3 | -68.0 | -74.9 | -55.0 | -66.9 | -55.3 |
| 21.0 | 29.09 | -69.5 | -93.2 | -96.2 | -58.5 | -69.5 | -58.8 |
| 22.0 | 30.27 | -57.7 | -97.6 | -104.3 | -56.5 | -57.7 | -62.6 |
| 23.0 | 31.23 | -48.1 | -96.8 | -104.8 | -48.1 | -48.1 | -68.2 |
| 24.0 | 32.32 | -45.9 | -95.9 | -99.2 | -45.9 | -45.9 | -73.0 |
| 25.0 | 33.42 | -46.7 | -83.9 | -80.5 | -46.7 | -46.7 | -75.1 |
| 26.0 | 34.52 | -47.4 | -67.8 | -80.0 | -47.4 | -47.4 | -77.2 |
| 27.0 | 35.64 | -48.2 | -67.6 | -79.2 | -48.1 | -48.1 | -79.6 |
| 28.0 | 36.75 | -51.2 | -67.4 | -78.8 | -51.0 | -51.0 | -82.1 |
| 29.0 | 37.87 | -55.1 | -67.2 | -79.7 | -54.8 | -54.8 | -84.7 |
| 30.0 | 39.01 | -59.0 | -68.6 | -80.7 | -58.6 | -58.6 | -87.5 |
| 31.0 | 40.14 | -63.0 | -70.1 | -82.0 | -62.2 | -62.2 | -90.1 |
| 32.0 | 41.28 | -72.0 | -71.5 | -83.7 | -68.5 | -68.6 | -86.1 |
| 33.0 | 42.42 | -90.3 | -73.6 | -85.6 | -72.9 | -73.2 | -84.7 |
| 34.0 | 43.57 | -108.6 | -75.7 | -87.5 | -74.9 | -75.4 | -84.8 |
| 35.0 | 44.71 | -126.9 | -77.9 | -89.8 | -76.8 | -77.6 | -84.7 |
| 36.0 | 45.87 | -145.3 | -80.4 | -92.2 | -78.8 | -80.1 | -84.7 |
| 37.0 | 47.02 | -137.3 | -83.0 | -94.7 | -80.6 | -82.7 | -84.7 |
| 38.0 | 48.18 | -123.6 | -85.7 | -97.5 | -82.6 | -85.4 | -85.8 |
| 39.0 | 49.34 | -109.9 | -88.7 | -100.3 | -84.5 | -88.4 | -86.8 |
| 40.0 | 50.50 | -96.2 | -91.7 | -103.3 | -85.8 | -90.2 | -87.8 |
| 41.0 | 51.66 | -85.0 | -94.9 | -106.5 | -83.2 | -84.6 | -88.8 |
| 42.0 | 52.83 | -84.9 | -98.4 | -109.7 | -28.4 | -84.7 | -28.4 |
| 43.0 | 53.99 | -84.8 | -101.8 | -113.2 | -34.7 | -84.7 | -34.7 |
| 44.0 | 55.16 | -84.7 | -105.5 | -116.4 | -31.2 | -84.7 | -31.2 |
| 45.0 | 56.33 | -84.6 | -109.1 | -119.6 | -38.5 | -84.6 | -38.5 |

REVERBERATION LEVELS AT TIMES CORRESPONDING TO 2-WAY
ACOUSTIC TRAVEL TIMES BETWEEN SOURCE AND TARGET.
( 2 PINGS -- TIME BETWEEN PINGS IS 10.00 SECONDS.)
THE SOUND PROPAGATES BETWEEN SOURCE AND TARGET BY

BOTTOM BOUNCE -- BOUNCE 1

| TARGET RANGE KYD | TWO-WAY TIME SEC | BOTTOM REVERB DB | SURFACE REVERB DB | VOLUME REVERB DB | TOTAL REVERB DB | PING 1 REVERB DB | PING 2 REVERB DB |
|---|---|---|---|---|---|---|---|
| 46.0 | 57.51 | -85.2 | -112.4 | -122.1 | -40.9 | -85.2 | -40.9 |
| 47.0 | 58.68 | -86.2 | -115.2 | -124.0 | -42.9 | -86.2 | -42.9 |
| 48.0 | 59.86 | -87.2 | -117.1 | -125.6 | -45.6 | -87.2 | -45.6 |
| 49.0 | 61.03 | -88.3 | -118.7 | -126.8 | -47.9 | -88.3 | -47.9 |
| 50.0 | 62.21 | -89.3 | -120.0 | -128.0 | -49.8 | -89.3 | -49.8 |
| 51.0 | 63.38 | -90.8 | -121.3 | -33.0 | -33.0 | -33.0 | -51.6 |
| 52.0 | 64.56 | -92.4 | -81.8 | -36.0 | -35.9 | -36.0 | -53.0 |
| 53.0 | 65.74 | -93.9 | -80.0 | -36.9 | -36.8 | -36.9 | -54.3 |
| 54.0 | 66.92 | -95.4 | -78.9 | -39.8 | -39.7 | -39.8 | -55.5 |
| 55.0 | 68.09 | -97.1 | -79.0 | -41.9 | -41.8 | -41.9 | -56.6 |
| 56.0 | 69.27 | -99.0 | -79.1 | -44.2 | -44.0 | -44.2 | -57.7 |
| 57.0 | 70.45 | -100.8 | -82.5 | -46.8 | -46.5 | -46.8 | -58.6 |
| 58.0 | 71.63 | -102.7 | -84.5 | -48.9 | -48.5 | -48.9 | -59.5 |
| 59.0 | 72.81 | -104.6 | -86.3 | -50.8 | -50.8 | -50.8 | -72.4 |
| 60.0 | 73.99 | -106.8 | -88.1 | -52.3 | -52.3 | -52.3 | -74.6 |
| 61.0 | 75.17 | -108.9 | -89.6 | -53.7 | -53.6 | -53.7 | -76.7 |
| 62.0 | 76.35 | -111.1 | -91.7 | -54.9 | -54.9 | -54.9 | -81.8 |

ACTIVE PERFORMANCE PREDICTION
WESTERN N. ATLANTIC WINTER SOUND SPEED PROFILE, NUC TN 1006, P. 47

BOTTOM BOUNCE -- BOUNCE 1

| | | | | | | | | | | | |
|---|---|---|---|---|---|---|---|---|---|---|---|
| OUTP | .0 | ZX | 20.0 | | ZTG | 300.0 | | FREQ | 2.0 | LWA | 5.0 | |
| VWI | 15.0 | SALT | 35.0 | T | HS | 5.0 | C | ZBM | 17372. | REFLS | 1.0 | T |
| ZONES | 2.0 | PHDX | 40.0 | U | PHDR | 40.0 | U | DELPX | 10.0 | DELPR | 10.0 | |
| MUB | -27.0 | T | MUV | -49.0 | T | ZC | 2000. | T | LAT | 35.0 | DUMP | .0 | T |
| OUTR | 1.0 | | MODE | 2.0 | U | SL | 135.0 | | DELTH | 10.0 | MPR | 2.0 | |
| TBP | 10.0 | | PULSE | .10+00 | T | DI | 25.6 | C | BWS | 10.0 | T | BWR | 10.0 | |
| NIN | -45.0 | T | NOUT | -60.6 | C | TVC | 12.0 | | GDOP | 4.4 | C | TGS | 15.0 | T |
| RDN | -2.0 | T | CLIP | .0 | T | SIGMA | 6.0 | T | PFA | .100-02 | T | SP | 5. | T |
| GO | .0107 | N | ALFA | .1277 | N | ZL | 492.13 | N | ZCJ | 6152. | N | PHIB | 15.93 | N |
| CX | 4882.39 | N | CT | 4885.53 | N | CL | 4887.14 | N | CS | 4881.89 | N | CB | 5077.36 | N |
| TSUR | 49.0 | N | TAV | 36.4 | N | NOCZ | 0 | N | IRAP | 0 | N | IAMOS | 1 | N |

| RANGE (KYD) | TIME (SEC) | LOSS (DB) | ANGLE (DEG) | SIGNAL (DB) | REVERB (DB) | REV LIM | S/MN (DB) | EXCESS (DB) | PROB DETECT |
|---|---|---|---|---|---|---|---|---|---|
| 1.0 | 14.11 | 223.7 | 85.20 | -73.7 | -31.7 | YES | -37.6 | -37.6 | .0000 |
| 2.0 | 14.30 | 225.1 | 80.43 | -75.1 | -32.7 | YES | -37.9 | -37.9 | .0000 |
| 3.0 | 14.52 | 237.6 | -75.67 | -87.6 | -33.7 | YES | -49.5 | -49.5 | .0000 |
| 4.0 | 14.82 | 219.0 | 71.16 | -69.0 | -34.8 | YES | -29.8 | -29.8 | .0000 |
| 5.0 | 15.31 | 218.8 | 67.06 | -68.8 | -37.1 | YES | -27.3 | -27.3 | .0000 |
| 6.0 | 15.80 | 264.1 | 62.97 | -114.1 | -39.3 | YES | -70.4 | -70.4 | .0000 |
| 7.0 | 16.36 | 213.0 | 59.15 | -63.0 | -42.0 | YES | -16.7 | -16.7 | .0049 |
| 8.0 | 17.07 | 208.9 | 55.89 | -58.9 | -44.9 | YES | -9.9 | -9.9 | .0711 |
| 9.0 | 17.77 | 223.0 | 52.63 | -73.0 | -46.7 | YES | -22.4 | -22.4 | .0000 |
| 10.0 | 18.52 | 213.9 | 49.62 | -63.9 | -46.7 | YES | -13.3 | -13.3 | .0182 |
| 11.0 | 19.36 | 197.0 | 47.12 | -47.0 | -46.2 | YES | 3.3 | 3.3 | .7034 |
| 12.0 | 20.21 | 189.1 | 44.61 | -39.1 | -38.8 | YES | 4.0 | 4.0 | .7411 |
| 13.0 | 21.08 | 185.7 | 42.28 | -35.7 | -27.9 | YES | -3.3 | -3.3 | .2940 |
| 14.0 | 22.03 | 185.1 | 40.37 | -35.1 | -28.9 | YES | -1.8 | -1.8 | .3863 |
| 15.0 | 22.97 | 186.2 | 38.47 | -36.2 | -29.9 | YES | -1.8 | -1.8 | .3843 |
| 16.0 | 23.93 | 188.8 | 36.64 | -38.8 | -31.0 | YES | -3.4 | -3.4 | .2903 |
| 17.0 | 24.94 | 192.4 | 35.19 | -42.4 | -35.9 | YES | -2.1 | -2.1 | .3686 |
| 18.0 | 25.95 | 197.4 | 33.74 | -47.4 | -40.7 | YES | -2.3 | -2.3 | .3531 |
| 19.0 | 26.97 | 204.3 | 32.30 | -54.3 | -45.7 | YES | -4.5 | -4.5 | .2333 |
| 20.0 | 28.03 | 212.2 | 31.17 | -62.2 | -55.0 | NO | -5.2 | -4.5 | .2326 |
| 21.0 | 29.09 | 224.2 | 30.06 | -74.2 | -58.5 | NO | -15.5 | -14.0 | .0154 |
| 22.0 | 30.27 | 248.2 | 29.34 | -98.2 | -56.5 | NO | -40.5 | -39.4 | .0000 |
| 23.0 | 31.23 | 242.1 | 28.01 | -92.1 | -48.1 | YES | -40.2 | -40.2 | .0000 |
| 24.0 | 32.32 | 229.6 | 27.15 | -79.6 | -45.9 | YES | -29.7 | -29.7 | .0000 |
| 25.0 | 33.42 | 224.3 | 26.28 | -74.3 | -46.7 | YES | -23.7 | -23.7 | .0000 |
| 26.0 | 34.52 | 222.0 | 25.50 | -72.0 | -47.4 | YES | -20.7 | -20.7 | .0000 |
| 27.0 | 35.64 | 221.2 | 24.82 | -71.2 | -48.1 | YES | -19.3 | -19.3 | .0000 |
| 28.0 | 36.75 | 221.2 | 24.14 | -71.2 | -51.0 | YES | -16.8 | -16.8 | .0048 |
| 29.0 | 37.87 | 221.8 | 23.49 | -71.8 | -54.8 | NO | -14.9 | -14.2 | .0144 |
| 30.0 | 39.01 | 222.8 | 22.95 | -72.8 | -58.6 | NO | -14.2 | -12.6 | .0208 |
| 31.0 | 40.14 | 224.2 | 22.40 | -74.2 | -62.2 | NO | -14.5 | -12.6 | .0208 |
| 32.0 | 41.28 | 225.9 | 21.87 | -75.9 | -68.5 | NO | -15.5 | -13.5 | .0174 |
| 33.0 | 42.42 | 227.7 | 21.43 | -77.7 | -72.9 | NO | -17.2 | -15.2 | .0109 |
| 34.0 | 43.57 | 229.8 | 20.99 | -79.8 | -74.9 | NO | -19.2 | -17.2 | .0030 |
| 35.0 | 44.71 | 232.1 | 20.56 | -82.1 | -76.8 | NO | -21.5 | -19.5 | .0000 |
| 36.0 | 45.87 | 234.5 | 20.20 | -84.5 | -78.8 | NO | -23.9 | -21.9 | .0000 |
| 37.0 | 47.02 | 237.1 | 19.83 | -87.1 | -80.6 | NO | -26.4 | -24.4 | .0000 |

ACTIVE PERFORMANCE PREDICTION
WESTERN N. ATLANTIC WINTER SOUND SPEED PROFILE, NUC TN 1006, P. 47

BOTTOM BOUNCE -- BOUNCE 1

| | | | | | | | | | | | |
|---|---|---|---|---|---|---|---|---|---|---|---|
| OUTP | .0 | ZX | 20.0 | | ZTG | 300.0 | | FREQ | 2.0 | LWA | 5.0 |
| VWI | 15.0 | SALT | 35.0 | T | HS | 5.0 | C | ZBM | 17372. | REFLS | 1.0 T |
| ZONES | 2.0 | PHDX | 40.0 | U | PHDR | 40.0 | U | DELPX | 10.0 | DELPR | 10.0 |
| MUB | -27.0 T | MUV | -49.0 | T | ZC | 2000. | T | LAT | 35.0 | DUMP | .0 T |
| OUTR | 1.0 | MODE | 2.0 | U | SL | 135.0 | | DELTH | 10.0 | MPR | 2.0 |
| TBP | 10.0 | PULSE | .10+00T | | DI | 25.6 | C | BWS | 10.0 T | BWR | 10.0 |
| NIN | -45.0 T | NOUT | -60.6 | C | TVC | 12.0 | | GDOP | 4.4 C | TGS | 15.0 T |
| RDN | -2.0 T | CLIP | .0 | T | SIGMA | 6.0 | T | PFA | .100-02T | SP | 5. T |
| GO | .0107 N | ALFA | .1277 | N | ZL | 492.13 | N | ZCJ | 6152. N | PHIB | 15.93 N |
| CX | 4882.39 N | CT | 4885.53 | N | CL | 4887.14 | N | CS | 4881.89 N | CB | 5077.36 N |
| TSUR | 49.0 N | TAV | 36.4 | N | NOCZ | 0 | N | IRAP | 0 N | IAMOS | 1 N |

| RANGE (KYD) | TIME (SEC) | LOSS (DB) | ANGLE (DEG) | SIGNAL (DB) | REVERB (DB) | REV LIM | S/MN (DB) | EXCESS (DB) | PROB DETECT |
|---|---|---|---|---|---|---|---|---|---|
| 38.0 | 48.18 | 239.9 | 19.49 | -89.9 | -82.6 | NO | -29.2 | -27.2 | .0000 |
| 39.0 | 49.34 | 242.7 | 19.19 | -92.7 | -84.5 | NO | -32.1 | -30.1 | .0000 |
| 40.0 | 50.50 | 245.9 | 18.89 | -95.9 | -85.8 | NO | -35.2 | -33.2 | .0000 |
| 41.0 | 51.66 | 249.2 | 18.62 | -99.2 | -83.2 | NO | -38.5 | -36.5 | .0000 |
| 42.0 | 52.83 | 252.6 | 18.37 | -102.6 | -28.4 | YES | -69.8 | -69.8 | .0000 |
| 43.0 | 53.99 | 256.6 | 18.12 | -106.6 | -34.7 | YES | -67.4 | -67.4 | .0000 |
| 44.0 | 55.16 | 260.6 | 17.91 | -110.6 | -31.2 | YES | -75.0 | -75.0 | .0000 |
| 45.0 | 56.33 | 265.3 | 17.70 | -115.3 | -38.5 | YES | -72.4 | -72.4 | .0000 |
| 46.0 | 57.51 | 268.3 | -17.53 | -118.3 | -40.9 | YES | -73.1 | -73.1 | .0000 |
| 47.0 | 58.68 | 269.6 | -17.35 | -119.6 | -42.9 | YES | -72.5 | -72.5 | .0000 |
| 48.0 | 59.86 | 270.9 | -17.19 | -120.9 | -45.6 | YES | -71.2 | -71.2 | .0000 |
| 49.0 | 61.03 | 272.2 | -17.03 | -122.2 | -47.9 | YES | -70.4 | -70.4 | .0000 |
| 50.0 | 62.21 | 273.5 | -16.90 | -123.5 | -49.8 | YES | -70.1 | -70.1 | .0000 |
| 51.0 | 63.38 | 274.8 | -16.77 | -124.8 | -33.0 | YES | -87.4 | -87.4 | .0000 |
| 52.0 | 64.56 | 276.2 | -16.65 | -126.2 | -35.9 | YES | -85.9 | -85.9 | .0000 |
| 53.0 | 65.74 | 277.6 | -16.55 | -127.6 | -36.8 | YES | -86.4 | -86.4 | .0000 |
| 54.0 | 66.92 | 279.0 | -16.45 | -129.0 | -39.7 | YES | -84.9 | -84.9 | .0000 |
| 55.0 | 68.09 | 280.4 | -16.37 | -130.4 | -41.8 | YES | -84.4 | -84.4 | .0000 |
| 56.0 | 69.27 | 281.9 | -16.29 | -131.9 | -44.0 | YES | -83.8 | -83.8 | .0000 |
| 57.0 | 70.45 | 283.5 | -16.22 | -133.5 | -46.5 | YES | -83.0 | -83.0 | .0000 |
| 58.0 | 71.63 | 285.1 | -16.16 | -135.1 | -48.5 | YES | -82.8 | -82.8 | .0000 |
| 59.0 | 72.81 | 285.9 | 16.10 | -135.9 | -50.8 | YES | -81.8 | -81.8 | .0000 |
| 60.0 | 73.99 | 286.7 | 16.06 | -136.7 | -52.3 | YES | -81.4 | -81.2 | .0000 |
| 61.0 | 75.17 | 287.8 | 16.02 | -137.8 | -53.6 | NO | -81.7 | -81.3 | .0000 |
| 62.0 | 76.35 | 289.5 | 15.99 | -139.5 | -54.9 | NO | -82.5 | -81.8 | .0000 |

```
**********************
* INPUTS,  RUN  5 *
**********************

PHDX=5, PHDR=5
MODE=3,RUN

**************************
* CALCULATIONS,  RUN  5 *
**************************

 BEAMX IS THE SIN(X)/X RESPONSE FUNCTION FOR A CONTINUOUS LINE ARRAY

 BEAMR IS THE SIN(X)/X RESPONSE FUNCTION FOR A CONTINUOUS LINE ARRAY
```

THE LETTERS FOLLOWING THE NUMBERS IN THE HEADING ON THE PERFORMANCE PREDICTION PAGE SIGNIFY THE FOLLOWING,

| | |
|---|---|
| U | USER HAS SPECIFIED THIS INPUT VALUE ON THIS RUN |
| BLANK | SET BY USER ON A PREVIOUS RUN |
| T | TYPICAL VALUE SET IN ABSENCE OF USER SPECIFICATION |
| C | CALCULATED INTERNALLY BY PROGRAM (USER OPTION) |
| W | WRONG VALUE SPECIFIED BY USER (OUT OF RANGE OF ALLOWABLE VALUES. THE PRINTED VALUE IS A TYPICAL VALUE.) |
| N | NOT AN INPUT, CALCULATED INTERNALLY. |

REVERBERATION LEVELS AT TIMES CORRESPONDING TO 2-WAY
ACOUSTIC TRAVEL TIMES BETWEEN SOURCE AND TARGET.
( 2 PINGS -- TIME BETWEEN PINGS IS 10.00 SECONDS.)
THE SOUND PROPAGATES BETWEEN SOURCE AND TARGET BY

CONVERGENCE ZONE -- ZONE 1

| TARGET RANGE KYD | TWO-WAY TIME SEC | BOTTOM REVERB DB | SURFACE REVERB DB | VOLUME REVERB DB | TOTAL REVERB DB | PING 1 REVERB DB | PING 2 REVERB DB |
|---|---|---|---|---|---|---|---|
| 51.0 | 63.08 | -88.2 | -89.2 | -31.7 | -31.7 | -31.7 | -50.8 |
| 52.0 | 64.29 | -88.9 | -35.6 | -35.4 | -32.4 | -32.5 | -52.4 |
| 53.0 | 65.55 | -89.7 | -41.4 | -36.2 | -35.0 | -35.1 | -53.9 |
| 54.0 | 66.72 | -90.3 | -44.2 | -39.4 | -38.1 | -38.2 | -55.2 |
| 55.0 | 67.93 | -91.2 | -47.6 | -41.7 | -40.6 | -40.7 | -56.4 |
| 56.0 | 69.14 | -92.3 | -50.5 | -43.8 | -42.8 | -42.9 | -57.5 |
| 57.0 | 70.44 | -93.5 | -55.3 | -46.7 | -45.9 | -46.2 | -58.5 |
| 58.0 | 71.67 | -94.6 | -58.5 | -49.0 | -48.2 | -48.5 | -59.5 |
| 59.0 | 72.90 | -95.9 | -61.4 | -50.9 | -50.5 | -50.6 | -72.3 |
| 60.0 | 74.12 | -97.4 | -64.2 | -52.5 | -52.2 | -52.2 | -74.5 |
| 61.0 | 75.35 | -98.8 | -67.0 | -53.9 | -53.6 | -53.7 | -79.3 |
| 62.0 | 76.58 | -100.3 | -69.8 | -55.2 | -55.0 | -55.0 | -81.7 |
| 63.0 | 77.81 | -101.9 | -72.7 | -56.4 | -56.3 | -56.3 | -83.7 |
| 64.0 | 79.03 | -103.7 | -75.6 | -57.5 | -57.4 | -57.4 | -86.0 |
| 65.0 | 80.26 | -105.4 | -78.3 | -58.4 | -58.4 | -58.4 | -88.0 |
| 66.0 | 81.49 | -107.2 | -81.0 | -59.4 | -59.3 | -59.3 | -89.9 |
| 67.0 | 82.72 | -109.2 | -83.5 | -72.2 | -71.9 | -71.9 | -101.3 |
| 68.0 | 83.94 | -111.3 | -86.0 | -74.5 | -74.2 | -74.2 | -111.0 |
| 69.0 | 85.17 | -113.4 | -88.5 | -76.7 | -76.4 | -76.4 | -112.1 |

REVERBERATION LEVELS AT TIMES CORRESPONDING TO 2-WAY
ACOUSTIC TRAVEL TIMES BETWEEN SOURCE AND TARGET.
( 2 PINGS -- TIME BETWEEN PINGS IS 10.00 SECONDS.)
THE SOUND PROPAGATES BETWEEN SOURCE AND TARGET BY

CONVERGENCE ZONE -- ZONE 2

| TARGET RANGE KYD | TWO-WAY TIME SEC | BOTTOM REVERB DB | SURFACE REVERB DB | VOLUME REVERB DB | TOTAL REVERB DB | PING 1 REVERB DB | PING 2 REVERB DB |
|---|---|---|---|---|---|---|---|
| 103.0 | 127.39 | -300.0 | -300.0 | -62.8 | -62.6 | -62.8 | -75.2 |
| 104.0 | 128.62 | -300.0 | -68.0 | -67.1 | -64.2 | -64.5 | -76.3 |
| 105.0 | 129.82 | -300.0 | -72.0 | -67.4 | -65.9 | -66.1 | -78.3 |
| 106.0 | 131.04 | -300.0 | -74.2 | -69.3 | -67.8 | -68.1 | -79.8 |
| 107.0 | 132.26 | -300.0 | -75.8 | -70.8 | -69.3 | -69.6 | -81.1 |
| 108.0 | 133.47 | -300.0 | -77.3 | -72.2 | -70.7 | -71.0 | -82.3 |
| 109.0 | 134.68 | -300.0 | -79.4 | -73.5 | -72.1 | -72.5 | -83.4 |
| 110.0 | 135.89 | -300.0 | -81.0 | -74.6 | -73.4 | -73.7 | -84.5 |
| 111.0 | 137.10 | -300.0 | -82.6 | -75.7 | -74.6 | -74.9 | -85.6 |
| 112.0 | 138.30 | -300.0 | -84.2 | -76.7 | -75.7 | -76.0 | -86.5 |
| 113.0 | 139.66 | -300.0 | -86.5 | -78.6 | -77.5 | -78.0 | -87.4 |
| 114.0 | 140.89 | -300.0 | -89.2 | -80.1 | -79.1 | -79.6 | -88.3 |
| 115.0 | 142.12 | -300.0 | -91.0 | -81.4 | -80.3 | -80.9 | -89.2 |
| 116.0 | 143.34 | -300.0 | -92.6 | -82.5 | -81.5 | -82.1 | -90.0 |
| 117.0 | 144.57 | -300.0 | -94.2 | -83.7 | -82.6 | -83.3 | -90.8 |
| 118.0 | 145.80 | -300.0 | -95.8 | -84.8 | -83.7 | -84.4 | -91.6 |
| 119.0 | 147.03 | -300.0 | -97.4 | -85.8 | -84.7 | -85.5 | -92.3 |
| 120.0 | 148.25 | -300.0 | -98.9 | -86.7 | -85.6 | -86.4 | -93.1 |
| 121.0 | 149.48 | -300.0 | -100.3 | -87.5 | -86.4 | -87.3 | -93.7 |
| 122.0 | 150.71 | -300.0 | -101.9 | -88.4 | -87.3 | -88.2 | -94.4 |
| 123.0 | 151.94 | -300.0 | -103.4 | -89.2 | -88.1 | -89.1 | -95.0 |
| 124.0 | 153.16 | -300.0 | -105.0 | -90.0 | -88.9 | -89.9 | -95.7 |
| 125.0 | 154.39 | -300.0 | -106.5 | -90.8 | -90.5 | -90.7 | -103.4 |
| 126.0 | 155.62 | -300.0 | -108.1 | -91.6 | -91.4 | -91.5 | -107.2 |
| 127.0 | 156.85 | -300.0 | -109.7 | -92.3 | -92.1 | -92.2 | -108.5 |
| 128.0 | 158.07 | -300.0 | -111.2 | -93.0 | -92.9 | -93.0 | -109.8 |
| 129.0 | 159.30 | -300.0 | -112.7 | -93.7 | -93.6 | -93.6 | -111.0 |
| 130.0 | 160.53 | -300.0 | -114.2 | -94.3 | -94.2 | -94.3 | -112.3 |
| 131.0 | 161.76 | -300.0 | -115.6 | -95.0 | -94.9 | -94.9 | -113.5 |
| 132.0 | 162.98 | -300.0 | -117.0 | -95.6 | -95.5 | -95.6 | -114.8 |
| 133.0 | 164.21 | -300.0 | -118.4 | -103.4 | -103.1 | -103.3 | -116.1 |
| 134.0 | 165.44 | -300.0 | -119.9 | -107.3 | -106.9 | -107.1 | -122.8 |
| 135.0 | 166.67 | -300.0 | -121.3 | -108.5 | -108.2 | -108.3 | -124.0 |
| 136.0 | 167.89 | -300.0 | -122.6 | -109.8 | -109.5 | -109.6 | -125.2 |
| 137.0 | 169.12 | -300.0 | -124.0 | -111.1 | -110.7 | -110.8 | -127.0 |
| 138.0 | 170.35 | -300.0 | -125.4 | -112.3 | -112.0 | -112.1 | -128.2 |
| 139.0 | 171.57 | -300.0 | -126.8 | -113.6 | -113.3 | -113.4 | -129.7 |
| 140.0 | 172.80 | -300.0 | -128.1 | -114.8 | -114.6 | -114.6 | -300.0 |
| 141.0 | 174.03 | -300.0 | -129.5 | -116.1 | -115.9 | -115.9 | -300.0 |

ACTIVE PERFORMANCE PREDICTION
WESTERN N. ATLANTIC WINTER SOUND SPEED PROFILE, NUC TN 1006, P. 47

CONVERGENCE ZONE -- ZONE 1

| | | | | | | | | | | | |
|---|---|---|---|---|---|---|---|---|---|---|---|
| OUTP | .0 | ZX | 20.0 | | ZTG | 300.0 | | FREQ | 2.0 | | LWA | 5.0 | |
| VMI | 15.0 | SALT | 35.0 | T | HS | 5.0 | C | ZBM | 17372. | | REFLS | 1.0 | T |
| ZONES | 2.0 | PHDX | 5.0 | U | PHDR | 5.0 | U | DELPX | 10.0 | | DELPR | 10.0 | |
| MUB | -27.0 | T MUV | -49.0 | T | ZC | 2000. | T | LAT | 35.0 | | DUMP | .0 | T |
| OUTR | 1.0 | MODE | 3.0 | U | SL | 135.0 | | DELTH | 10.0 | | MPR | 2.0 | |
| TBP | 10.0 | PULSE | .10+00 | T | DI | 25.6 | C | BWS | 10.0 | T | BWR | 10.0 | |
| NIN | -45.0 | T NOUT | -60.6 | C | TVC | 12.0 | | GDOP | 4.4 | C | TGS | 15.0 | T |
| RDN | -2.0 | T CLIP | .0 | T | SIGMA | 6.0 | T | PFA | .100-02 | T | SP | 5. | T |
| GD | .0107 | N ALFA | .1277 | N | ZL | 492.13 | N | ZCJ | 6152. | N | PHIB | 15.93 | N |
| CX | 4882.39 | N CT | 4885.53 | N | CL | 4887.14 | N | CS | 4881.89 | N | CB | 5077.36 | N |
| TSUR | 49.0 | N TAV | 36.4 | N | NOCZ | 0 | N | IRAP | 0 | N | IAMOS | 1 | N |

| RANGE (KYD) | TIME (SEC) | LOSS (DB) | ANGLE (DEG) | SIGNAL (DB) | REVERB (DB) | REV LIM | S/MN (DB) | EXCESS (DB) | PROB DETECT |
|---|---|---|---|---|---|---|---|---|---|
| 51.0 | 63.08 | 180.1 | 3.98 | -30.1 | -31.7 | YES | 6.0 | 6.0 | .8385 |
| 52.0 | 64.29 | 186.6 | 7.78 | -36.6 | -32.4 | YES | .2 | .2 | .5158 |
| 53.0 | 65.55 | 189.8 | 4.76 | -39.8 | -35.0 | YES | -.4 | -.4 | .4746 |
| 54.0 | 66.72 | 195.1 | 9.70 | -45.1 | -38.1 | YES | -2.6 | -2.6 | .3338 |
| 55.0 | 67.93 | 198.9 | 10.52 | -48.9 | -40.6 | YES | -4.1 | -4.1 | .2572 |
| 56.0 | 69.14 | 203.4 | 11.30 | -53.4 | -42.8 | YES | -6.4 | -6.4 | .1512 |
| 57.0 | 70.44 | 207.2 | 3.50 | -57.2 | -45.9 | YES | -7.2 | -7.2 | .1316 |
| 58.0 | 71.67 | 209.6 | 3.43 | -59.6 | -48.2 | YES | -7.6 | -7.6 | .1229 |
| 59.0 | 72.90 | 211.8 | 3.35 | -61.8 | -50.5 | YES | -7.9 | -7.8 | .1186 |
| 60.0 | 74.12 | 213.8 | 3.27 | -63.8 | -52.2 | YES | -8.6 | -8.5 | .1040 |
| 61.0 | 75.35 | 215.6 | 3.19 | -65.6 | -53.6 | NO | -9.5 | -9.1 | .0896 |
| 62.0 | 76.58 | 217.4 | 3.11 | -67.4 | -55.0 | NO | -10.4 | -9.7 | .0760 |
| 63.0 | 77.81 | 219.0 | 3.03 | -69.0 | -56.3 | NO | -11.3 | -10.3 | .0612 |
| 64.0 | 79.03 | 220.5 | 2.95 | -70.5 | -57.4 | NO | -12.4 | -11.1 | .0444 |
| 65.0 | 80.26 | 222.0 | 2.87 | -72.0 | -58.4 | NO | -13.4 | -11.9 | .0255 |
| 66.0 | 81.49 | 223.4 | 2.79 | -73.4 | -59.3 | NO | -14.5 | -12.8 | .0199 |
| 67.0 | 82.72 | 224.8 | 2.72 | -74.8 | -71.9 | NO | -14.2 | -12.2 | .0221 |
| 68.0 | 83.94 | 226.0 | 2.64 | -76.0 | -74.2 | NO | -15.5 | -13.5 | .0173 |
| 69.0 | 85.17 | 227.3 | 2.56 | -77.3 | -76.4 | NO | -16.7 | -14.7 | .0127 |

ACTIVE PERFORMANCE PREDICTION
WESTERN N. ATLANTIC WINTER SOUND SPEED PROFILE, NUC TN 1006, P. 47

CONVERGENCE ZONE -- ZONE 2

| | | | | | | | | | | | |
|---|---|---|---|---|---|---|---|---|---|---|---|
| OUTP | .0 | ZX | 20.0 | | ZTG | 300.0 | | FREQ | 2.0 | LWA | 5.0 |
| VWI | 15.0 | SALT | 35.0 | T | HS | 5.0 | C | ZBM | 17372. | REFLS | 1.0 T |
| ZONES | 2.0 | PHDX | 5.0 | U | PHDR | 5.0 | U | DELPX | 10.0 | DELPR | 10.0 |
| MUB | -27.0 T | MUV | -49.0 | T | ZC | 2000. | T | LAT | 35.0 | DUMP | .0 T |
| OUTR | 1.0 | MODE | 3.0 | U | SL | 135.0 | | DELTH | 10.0 | MPR | 2.0 |
| TBP | 10.0 | PULSE | .10+00 | T | DI | 25.6 | C | BWS | 10.0 T | BWR | 10.0 |
| NIN | -45.0 T | NOUT | -60.6 | C | TVC | 12.0 | | GDOP | 4.4 C | TGS | 15.0 T |
| RDN | -2.0 T | CLIP | .0 | T | SIGMA | 6.0 | T | PFA | .100-02 T | SP | 5. T |
| GO | .0107 N | ALFA | .1277 | N | ZL | 492.13 | N | ZCJ | 6152. N | PHIB | 15.93 N |
| CX | 4882.39 N | CT | 4885.53 | N | CL | 4887.14 | N | CS | 4881.89 N | CB | 5077.36 N |
| TSUR | 49.0 N | TAV | 36.4 | N | NOCZ | 0 | N | IRAP | 0 N | IAMOS | 1 N |

| RANGE (KYD) | TIME (SEC) | LOSS (DB) | ANGLE (DEG) | SIGNAL (DB) | REVERB (DB) | REV LIM | S/MN (DB) | EXCESS (DB) | PROB DETECT |
|---|---|---|---|---|---|---|---|---|---|
| 103.0 | 127.39 | 213.7 | 4.35 | -63.7 | -62.6 | NO | -4.0 | -2.0 | .3708 |
| 104.0 | 128.62 | 219.1 | 3.97 | -69.1 | -64.2 | NO | -9.1 | -7.1 | .1345 |
| 105.0 | 129.82 | 222.6 | 7.89 | -72.6 | -65.9 | NO | -12.4 | -10.4 | .0603 |
| 106.0 | 131.04 | 224.9 | 8.43 | -74.9 | -67.8 | NO | -14.6 | -12.6 | .0208 |
| 107.0 | 132.26 | 227.1 | 8.94 | -77.1 | -69.3 | NO | -16.7 | -14.7 | .0128 |
| 108.0 | 133.47 | 229.7 | 9.42 | -79.7 | -70.7 | NO | -19.2 | -17.2 | .0029 |
| 109.0 | 134.68 | 232.1 | 9.86 | -82.1 | -72.1 | NO | -21.6 | -19.6 | .0000 |
| 110.0 | 135.89 | 234.2 | 10.28 | -84.2 | -73.4 | NO | -23.7 | -21.7 | .0000 |
| 111.0 | 137.10 | 236.3 | 10.70 | -86.3 | -74.6 | NO | -25.7 | -23.7 | .0000 |
| 112.0 | 138.30 | 238.4 | 11.10 | -88.4 | -75.7 | NO | -27.8 | -25.8 | .0000 |
| 113.0 | 139.66 | 240.6 | 3.62 | -90.6 | -77.5 | NO | -30.0 | -28.0 | .0000 |
| 114.0 | 140.89 | 242.1 | 3.59 | -92.1 | -79.1 | NO | -31.5 | -29.5 | .0000 |
| 115.0 | 142.12 | 243.6 | 3.55 | -93.6 | -80.3 | NO | -33.0 | -31.0 | .0000 |
| 116.0 | 143.34 | 244.9 | 3.51 | -94.9 | -81.5 | NO | -34.3 | -32.3 | .0000 |
| 117.0 | 144.57 | 246.2 | 3.47 | -96.2 | -82.6 | NO | -35.6 | -33.6 | .0000 |
| 118.0 | 145.80 | 247.5 | 3.43 | -97.5 | -83.7 | NO | -36.9 | -34.9 | .0000 |
| 119.0 | 147.03 | 248.7 | 3.40 | -98.7 | -84.7 | NO | -38.1 | -36.1 | .0000 |
| 120.0 | 148.25 | 249.8 | 3.36 | -99.8 | -85.6 | NO | -39.2 | -37.2 | .0000 |
| 121.0 | 149.48 | 250.9 | 3.32 | -100.9 | -86.4 | NO | -40.3 | -38.3 | .0000 |
| 122.0 | 150.71 | 252.0 | 3.28 | -102.0 | -87.3 | NO | -41.4 | -39.4 | .0000 |
| 123.0 | 151.94 | 253.1 | 3.25 | -103.1 | -88.1 | NO | -42.4 | -40.4 | .0000 |
| 124.0 | 153.16 | 254.1 | 3.21 | -104.1 | -88.9 | NO | -43.4 | -41.4 | .0000 |
| 125.0 | 154.39 | 255.1 | 3.17 | -105.1 | -90.5 | NO | -44.4 | -42.4 | .0000 |
| 126.0 | 155.62 | 256.0 | 3.13 | -106.0 | -91.4 | NO | -45.4 | -43.4 | .0000 |
| 127.0 | 156.85 | 256.9 | 3.09 | -106.9 | -92.1 | NO | -46.3 | -44.3 | .0000 |
| 128.0 | 158.07 | 257.8 | 3.06 | -107.8 | -92.9 | NO | -47.2 | -45.2 | .0000 |
| 129.0 | 159.30 | 258.7 | 3.02 | -108.7 | -93.6 | NO | -48.1 | -46.1 | .0000 |
| 130.0 | 160.53 | 259.6 | 2.98 | -109.6 | -94.2 | NO | -49.0 | -47.0 | .0000 |
| 131.0 | 161.76 | 260.5 | 2.94 | -110.5 | -94.9 | NO | -49.8 | -47.8 | .0000 |
| 132.0 | 162.98 | 261.3 | 2.90 | -111.3 | -95.5 | NO | -50.7 | -48.7 | .0000 |
| 133.0 | 164.21 | 262.1 | 2.87 | -112.1 | -103.1 | NO | -51.5 | -49.5 | .0000 |
| 134.0 | 165.44 | 262.9 | 2.83 | -112.9 | -106.9 | NO | -52.3 | -50.3 | .0000 |
| 135.0 | 166.67 | 263.7 | 2.79 | -113.7 | -108.2 | NO | -53.1 | -51.1 | .0000 |
| 136.0 | 167.89 | 264.5 | 2.75 | -114.5 | -109.5 | NO | -53.8 | -51.8 | .0000 |
| 137.0 | 169.12 | 265.2 | 2.71 | -115.2 | -110.7 | NO | -54.6 | -52.6 | .0000 |
| 138.0 | 170.35 | 266.0 | 2.68 | -116.0 | -112.0 | NO | -55.4 | -53.4 | .0000 |
| 139.0 | 171.57 | 266.7 | 2.64 | -116.7 | -113.3 | NO | -56.1 | -54.1 | .0000 |

ACTIVE PERFORMANCE PREDICTION
WESTERN N. ATLANTIC WINTER SOUND SPEED PROFILE, NUC TN 1006, P. 47

CONVERGENCE ZONE -- ZONE 2

| | | | | | | | | | | | | | | | |
|---|---|---|---|---|---|---|---|---|---|---|---|---|---|---|---|
| OUTP | .0 | | ZX | 20.0 | | ZTG | 300.0 | | FREQ | 2.0 | | LWA | 5.0 | | |
| VWI | 15.0 | | SALT | 35.0 | T | HS | 5.0 | C | ZBM | 17372. | | REFLS | 1.0 | T |
| ZONES | 2.0 | | PHDX | 5.0 | U | PHDR | 5.0 | U | DELPX | 10.0 | | DELPR | 10.0 | |
| MUB | -27.0 | T | MUV | -49.0 | T | ZC | 2000. | T | LAT | 35.0 | | DUMP | .0 | T |
| OUTR | 1.0 | | MODE | 3.0 | U | SL | 135.0 | | DELTH | 10.0 | | MPR | 2.0 | |
| TBP | 10.0 | | PULSE | .10+00 | T | DI | 25.6 | C | BWS | 10.0 | T | BWR | 10.0 | |
| NIN | -45.0 | T | NOUT | -60.6 | C | TVC | 12.0 | | GDOP | 4.4 | C | TGS | 15.0 | T |
| RDN | -2.0 | T | CLIP | .0 | T | SIGMA | 6.0 | T | PFA | .100-02 | T | SP | 5. | T |
| GO | .0107 | N | ALFA | .1277 | N | ZL | 492.13 | N | ZCJ | 6152. | N | PHIB | 15.93 | N |
| CX | 4882.39 | N | CT | 4885.53 | N | CL | 4887.14 | N | CS | 4881.89 | N | CB | 5077.36 | N |
| TSUR | 49.0 | N | TAV | 36.4 | N | NOCZ | 0 | N | IRAP | 0 | N | IAMOS | 1 | N |

| RANGE (KYD) | TIME (SEC) | LOSS (DB) | ANGLE (DEG) | SIGNAL (DB) | REVERB (DB) | REV LIM | S/MN (DB) | EXCESS (DB) | PROB DETECT |
|---|---|---|---|---|---|---|---|---|---|
| 140.0 | 172.80 | 267.5 | 2.60 | -117.5 | -114.6 | NO | -56.8 | -54.8 | .0000 |
| 141.0 | 174.03 | 268.2 | 2.56 | -118.2 | -115.9 | NO | -57.6 | -55.6 | .0000 |

```
*********************
* INPUTS, RUN  6 *
*********************

 END

@FIN
```

## INITIAL DISTRIBUTION LIST

1 Assistant Secretary of the Navy (R&D)
2 Director of Defense (R&E)
- Library
- WSEG

8 Chief of Naval Operations
- NOP-095
- NOP-098T
- NOP-32
- NOP-322
- NOP-966 (Systems Analysis Division)
- NOP-981
- NOP-981G
- NOP-981H

3 Chief of Naval Material
- NMAT-03L
- NMAT-031
- NMAT-033

3 Naval Air Systems Command
- NAIR-370
- NAIR-5330
- NAIR-604

3 Naval Electronic Systems Command
- EPO-3
- PME-124
- PME-124TA

9 Naval Sea Systems Command
- SEA-03B
- SEA-06G
- SEA-060
- SEA-09G3
- SEA-06H
- SEA-661
- SEA-09G32
- PMS-395-11
- PMS-395-23

3 Office of Naval Research
- ONR 102-OS
- ONR 221
- ONR 468

1 Naval Ship Engineering Center (NSEC-6034)
1 Air Development Squadron ONE/VX-1
3 Antisubmarine Warfare Systems Project Office
  ASW-13
  ASW-14
  ASW-15
1 ASW Tactical School, Atlantic (Library)
1 Atlantic Fleet
1 Commander, Naval Surface Force
1 Cruiser-Destroyer Force, Pacific (code 425)
1 Destroyer Development Group TWO (Dick McKee)
1 Destroyer Development Group, Atlantic (Scientific Advisory Team)
1 Fleet ASW School
1 Fleet Numerical Weather Central
1 Fleet Sonar School
1 Naval Air Development Center (Library)
1 Naval Civil Engineering Laboratory
2 Naval Coastal Systems Laboratory
  Library
  Tom Watson
1 Naval Electronics Laboratory
1 Naval Missile Center (Library)
3 Naval Oceanographic Office
  Donald Gearson
  *037-B*
  Library: Code 3330-bd
5 Naval Surface Weapons Center
  Library
  Code 050
  Code 221
  Code 730
  Code 880
1 Naval Personnel and Training Research Laboratory (Library) San Diego
1 Naval Postgraduate School (Library)
5 Naval Research Laboratory
  Library
  Code 8000
  Code 8100
  Code 8400
  Code 8700
1 Naval Ship Research and Development Center
  Annapolis Division (Library)
1 David W. Taylor Naval Ship Research and Development Center, Bethesda
1 Naval Training Equipment Center (Code 02)
1 Naval Underwater Systems Center, New London Laboratory (Library)
1 Naval Underwater Systems Center, Newport Laboratory (Library)
1 Naval War College

1 Naval Weapons Center (Code 753)
1 Navy Underwater Sound Reference Laboratory (Library)
1 Operational Test and Evaluation Force, Atlantic
1 Operational Test and Evaluation Force, Pacific
1 Operational Test and Evaluation Force, Test and Evaluation Detachment, New London
1 Pacific Fleet (Code 93)
1 Submarine Development Group ONE
1 Submarine Development Group TWO
1 Submarine Flotilla ONE
1 Submarine Forces, Atlantic
1 Submarine Forces, Naval Submarine Base, New London
1 Submarine Forces, Pacific
1 Training Command, Atlantic
1 Training Command, Pacific
12 Defense Documentation Center
1 Armed Forces Staff College (Administrative Command)
1 National Academy of Sciences, National Research Council, Committee on Undersea Warfare (Executive Secretary)
1 Applied Physics Laboratory, University of Washington
1 Applied Research Laboratory, University of Texas
1 Marine Physical Laboratory, University of California, Scripps Institution of Oceanography
1 Applied Research Laboratory, Pennsylvania State University
1 AFSPCOMMCEN/SUR, San Antonio, TX 78243
1 UK Scientific Mission (Miss A. P. King) (UNCL/A only)
1 P. Graycar, University of Florida (UNCL/A only)

**Center Distribution:**

| | |
|---|---|
| 00 | 30 (36) |
| 01 | 35 (2) |
| 02 | 40 (2) |
| 03 | 45 (2) |
| | 65 |
| 05 | 6501 |
| 11 | 6562 (25) |
| 14 (2) | 6565 (2) |
| 15 | 90 |
| 25 | 96 |